
Reports

3-1-1979

A Two-Dimensional Hydrodynamic and Biogeochemical Water Quality Model and It's Application to the Lower James River

H. S. Chen
Virginia Institute of Marine Science

R. J. Lukens
Virginia Institute of Marine Science

C. S. Fang
Virginia Institute of Marine Science

Follow this and additional works at: <https://scholarworks.wm.edu/reports>

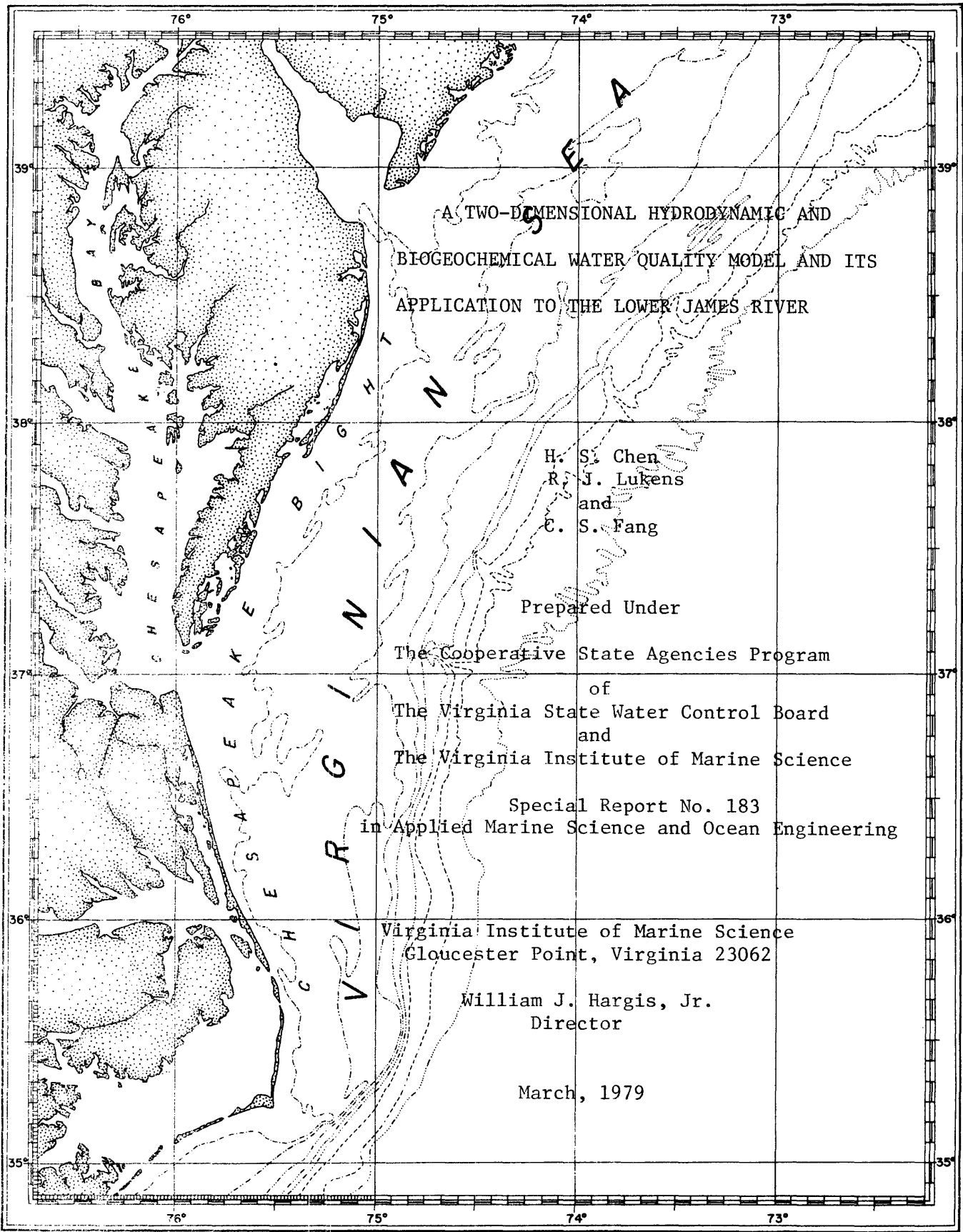
 Part of the [Marine Biology Commons](#)

Recommended Citation

Chen, H. S., Lukens, R. J., & Fang, C. S. (1979) A Two-Dimensional Hydrodynamic and Biogeochemical Water Quality Model and It's Application to the Lower James River. Special Reports in Applied Marine Science and Ocean Engineering (SRAMSOE) No. 183. Virginia Institute of Marine Science, College of William and Mary. <https://doi.org/10.21220/V5V45D>

This Report is brought to you for free and open access by W&M ScholarWorks. It has been accepted for inclusion in Reports by an authorized administrator of W&M ScholarWorks. For more information, please contact scholarworks@wm.edu.

21110
102



A TWO-DIMENSIONAL HYDRODYNAMIC AND
BIOGEOCHEMICAL WATER QUALITY MODEL AND ITS
APPLICATION TO THE LOWER JAMES RIVER

H. S. Chen
R. J. Lukens
and
C. S. Fang

Prepared Under

The Cooperative State Agencies Program

of

The Virginia State Water Control Board

and

The Virginia Institute of Marine Science

Special Report No. 183
in Applied Marine Science and Ocean Engineering

Virginia Institute of Marine Science
Gloucester Point, Virginia 23062

William J. Hargis, Jr.
Director

March, 1979

A TWO-DIMENSIONAL HYDRODYNAMIC AND BIOGEOCHEMICAL
WATER QUALITY MODEL AND ITS APPLICATION TO THE
LOWER JAMES RIVER

by

H. S. Chen
R. J. Lukens
and
C. S. Fang

PREPARED UNDER
THE COOPERATIVE STATE AGENCIES PROGRAM
OF
THE VIRGINIA STATE WATER CONTROL BOARD
AND THE VIRGINIA INSTITUTE OF MARINE SCIENCE

Project Officers

Dale Jones
Raymond Bowles

Virginia State Water Control Board

Special Report No. 183
in Applied Marine Science and
Ocean Engineering

Virginia Institute of Marine Science
Gloucester Point, Virginia 23062

William J. Hargis, Jr.
Director

March, 1979

TABLE OF CONTENTS

	Page
List of Tables.....	iii
List of Figures.....	v
Acknowledgements.....	vi
Abstract.....	vii
1. Introduction.....	1
2. Mathematical Formulation of a Biogeochemical Water Quality Model.....	4
2.1 Hydrodynamic Transport Processes.....	4
2.2 Water Quality Transport and Biochemical Reaction Processes.....	11
3. Variational Statement and Finite Element Numerical Approximation.....	21
3.1 Galerkin's Variational Statement.....	21
3.2 Finite Element Approximation and Linear Triangular Element.....	23
3.3 Time Integration.....	32
3.4 Treatment of Boundary Condition.....	35
4. Some Computational Aspects.....	38
4.1 Verification by Studying Simple Problem.....	40
5. Application to the Lower James River.....	46
5.1 Finite Element Network of the River.....	46
5.2 Hydrodynamic Model.....	51
5.3 Biogeochemical Water Quality Model.....	51
5.4 Sensitivity.....	68
5.5 Water Quality Discussion.....	112
6. Conclusion.....	117
References.....	118
Appendix A. Summary of Water Quality Data.....	121

LIST OF TABLES

	Page
4.1 Convergence of $\frac{C}{C_0}$ With Respect to Δt at Point 24.....	45
5.1a Some Tide Data of Lower James River.....	52
5.1b Tidal Input for the Lower James River Hydrodynamic Model.....	53
5.2a Municipal and Industrial Waste Loads of Lower James River, 1976.....	70
5.2b Point Sources for the Lower James River Water Quality Model...	72
5.3a Total Non-point Sources of Wastes Over a Period of 61 Days from June 17 - Aug. 16, 1976.....	74
5.3b Daily Non-point Sources for the Lower James River Water Quality Model.....	77
5.4 Values of Boundary Condition for Biogeochemical Water Quality Model.....	79
5.5 Calibrated Values for Hydrodynamic and Biogeochemical Water Quality Parameters.....	91
5.6a Sensitivity of Salinity Distribution to the Change of Various Parameters.....	103
5.6b Sensitivity of Coliform Bacteria Distribution to the Change of Various Parameters.....	103
5.6c Sensitivity of Chlorophyll 'a' Distribution to the Change of Various Parameters.....	104
5.6d Sensitivity of Organic-N Distribution to the Change of Various Parameters.....	105
5.6e Sensitivity of Ammonia-N Distribution to the Change of Various Parameters.....	106
5.6f Sensitivity of Nitrite-Nitrate-N Distribution to the Change of Various Parameters.....	107
5.6g Sensitivity of Organic-P Distribution to the Change of Various Parameters.....	108
5.6h Sensitivity of Inorganic-P Distribution to the Change of Various Parameters.....	109

LIST OF FIGURES

	Page
2.1 Definition sketch of the Cartesian Coordinate System.....	5
2.2 Schematic diagram showing the inter-reactions of the ten constituents.....	13
3.1 Domain and triangular elements.....	25
3.2 Definition sketch of boundary normal.....	36
4.1 Finite element grid of rectangular channel.....	41
4.2 Comparison of concentration propagation of analytical solution and numerical solution without decay.....	42
4.3 Comparison of concentration propagation of analytical solution and FEM numerical solution with decay.....	43
4.4 Time history of concentration of analytical solution and FEM numerical solution.....	44
5.1 Tidewater Virginia showing the area of the lower James River.....	47
5.1a Finite element network of lower James River showing nodal positions and some field survey stations.....	48
5.1b Finite element network of lower James River showing element locations.....	49
5.1c Nodal depths in meters of lower James River.....	50
5.2 Time history of water elevation and flow velocity at node.....	54-
a&b	55
5.3 Calculated results of water elevation and flow circulation	
A,a- within a tidal cycle.....	56-
F,f	67
5.4 Locations of point waste sources.....	69
5.5 Basins of non-point waste sources.....	73
5.6 Meaning of symbols for Figures 5.6a through 5.6j.....	80
5.6 Calibrated results of biogeochemical water quality and the	81-
a-j field data at several locations along lower James River.....	90
5.7 Tidal averaged distribution of different constituents in the	92-
a-k lower James River.....	102

List of Tables (Cont'd)

	Page
5.6i Sensitivity of CBOD Distribution to the Change of Various Parameters.....	110
5.6j Sensitivity of DO Deficit Distribution to the Change of Various Parameters.....	111
5.7 General Pattern of Immediate Change of Biogeochemical Water Quality Components Subject to the Change in Components and in Parameters.....	113
A.1 Biogeochemical Water Quality of Two Slack Water Runs.....	122

ACKNOWLEDGEMENT

This report is jointly supported by the Virginia State Water Control Board (SWCB) and the Virginia Institute of Marine Science (VIMS) through the Cooperative State Agencies (CSA) program. This research is a parallel effort undertaken by the CSA program and the 208 Hampton Roads program of the U. S. Environmental Protection Agency, in addition to the benefits derived from the hydrodynamic model which is developed for the Federal Insurance Administration, Department of Housing and Urban Development for the flooding study of the Chesapeake Bay.

Appreciation is expressed to Messrs. Dale Jones, Raymond Bowles and M. D. Phillips of the SWCB for their review of this report.

A great number of individuals in the Department of Physical Oceanography and Hydraulics and the Department of Estuarine Processes were involved in the field study and sample analysis. Many thanks are due to them. Particular thanks are due to Dr. John D. Wang for his generous supply of his CAFE computer program. Discussions with Drs. Paul V. Hyer and Bruce Neilson of VIMS have been helpful. Appreciation is also extended to Mr. Bernard Hsieh for preparing some of the figures and tables. Finally, special thanks should go to Ms. Shirley Crossley for her patient typing of this report.

ABSTRACT

A TWO-DIMENSIONAL HYDRODYNAMIC AND BIOGEOCHEMICAL WATER QUALITY MODEL AND ITS APPLICATION TO THE LOWER JAMES RIVER

This report presents a two-dimensional real-time mathematical model. The model combines hydrodynamic and biogeochemical water quality systems to predict flow circulation, water elevation and water quality response in a natural water body such as river, estuary or sea.

The hydrodynamic system is based on the vertically averaged two-dimensional continuity and momentum equations.

The biogeochemical system is based on the vertically averaged two-dimensional conservation of mass equation. The system consists of ten coupled sub-systems corresponding to ten constituents; namely, salinity, coliform bacteria, phytoplankton, organic nitrogen, ammonia nitrogen, nitrite-nitrate nitrogen, organic phosphorous, inorganic phosphorous, carbonaceous biochemical oxygen demand and dissolved oxygen deficit. Where these sub-systems are coupled, Michaelis-Menten and first order reaction kinetics in reaction processes are assumed.

The model uses Glerkin's weighted residual finite element numerical scheme, and is applied to study of lower James River.

1. INTRODUCTION

An intelligent management of water quality in a natural water body is becoming increasingly important to ensure a healthy environment and efficient use of water resources under the stress of rapid increase of municipal, industrial and agricultural wastes. The problem of waste treatment management is reflected in Section 208 of the Federal Water Pollution Control Act Amendments of 1972, which was created to provide guidelines for the development and implementation of area wide waste treatment management plans. The waste management plans include not only the point sources of pollution from effluents of industrial and municipal waste water treatment facilities, but also the non-point sources of pollution from urban and non-urban storm runoff. The crucial engineering decision is to determine the degree of waste treatment required to maintain the use of the water resources. This includes the prediction of the water quality response of the natural water body to the waste discharges from waste treatment facilities and urban and non-urban runoff.

Within the last decade, due to the difficulty of simulating biochemical reaction processes in physical models, mathematical models have been used increasingly to predict water quality in natural waters. The mathematical models of aquatic ecosystems are generally classified into three types; namely biodemographic model, bioenergetic model and biogeochemical model. (Najarian and Harleman 1976, Harleman 1977). Most water quality engineering models employ the biogeochemical approach, which is based on the conservation of mass, to determine the water quality distribution. One-dimensional mathematical modelings of some specific ecosystems have been extensively investigated by many investigators such as Thomann (1974), O'Connor, et al (1975) and Najarian and

Harleman (1976), just to name a few. Two-dimensional models have also been approached by several investigators such as Chen and Orlob (1971), Leendertse and Liu (1974) and Brandes and Masch (1975). Although each makes progress on water quality calculation, each is limited to some extent in application, either due to the absence of hydrodynamic descriptions, or due to the limitation to some specific ecosystem, or due to the unfavorable computational cost.

When wastes are discharged to a natural water body, they are in general subject to the coupled influence of hydrodynamic transport processes and biochemical reaction processes. The former, mainly depending on flow circulation, includes advection, mixing, and dispersion of the constituents of the wastes, while the latter, which leads to production or decay or transformation of the constituents through biochemical interaction, depends on both the biochemical characteristics of the constituents of the wastes and the hydrodynamic behavior of the water body. In this report, the water quality modeling is intent to incorporate water circulation to an aquatic ecosystem which consists of ten constituents. These are salinity, coliform bacteria, phytoplankton, organic nitrogen, ammonia nitrogen, nitrite nitrate nitrogen, organic phosphorous, inorganic phosphorus, carbonaceous biochemical oxygen demand and dissolved oxygen deficit. In Chapter 2 the two-dimensional depth-integrated mathematical model for the aquatic ecosystem is formulated based on the principle of conservation of mass and momentum for fluid motion. The model portrays hydrodynamic transport processes and biochemical water quality reaction processes in natural waters. The interaction processes among the water quality constituents assumes either Michaelis-Menten reaction kinetics or

first order reaction kinetics. In Chapter 3 Galerkin's weighted residual finite element techniques, incorporated with both a forward difference scheme for the hydrodynamic system and a half-station central difference for the water quality system in time, is described as it is employed for the solution. In Chapter 4 the model is used to calculate the concentration distribution of the water quality in a rectangular channel. The numerical result is compared with the exact analytic solution. Some computational aspects are also discussed. In Chapter 5 the model is applied to the lower James River, a fairly complex estuarine river dominated by tidal effects. The calibration and the sensitivity are also studied. The calibrated results and field observations are presented and discussed. In Chapter 6 a few short conclusions are made concerning the model. In Appendix A the field data from two slack water runs are illustrated.

2. MATHEMATICAL FORMULATION OF A BIOGEOCHEMICAL WATER QUALITY MODEL

In this chapter a real-time two-dimensional depth-integrated mathematical model of an aquatic ecosystem is formulated. The model depicts hydrodynamic transport and biochemical reaction processes to determine water elevation, circulation, and concentration distributions of the constituents of water quality in a natural water body such as a river, lake, estuary or sea which is subject to hydrodynamic forcing and waste loads.

2.1 Hydrodynamic transport processes⁺

The model describing the hydrodynamic transport processes employed the principles of conservations of mass and momentum for fluid motion to determine water elevation and circulation. If a water domain of shallow depth and great horizontal extent is dealt with, the pressure distribution can be assumed to be hydrostatic. Therefore, the two-dimensional depth integrated hydrodynamic equations in a Cartesian coordinate system (x,y,z) as shown in Figure 2.1, with the Boussinesq approximation can be written (Phillips 1966, Connor and Wang, 1974, Nihoul 1975).

$$\frac{\partial H}{\partial t} + \frac{\partial q_x}{\partial x} + \frac{\partial q_y}{\partial y} = Q \quad (2.1)$$

$$\begin{aligned} \frac{\partial q_x}{\partial t} + \frac{\partial H^{-1} q_x^2}{\partial x} + \frac{\partial H^{-1} q_x q_y}{\partial y} - f q_y = - \frac{H}{\rho_0} \frac{\partial}{\partial x} (p^s + \rho g \eta) \\ + \frac{\partial T_{xx}}{\partial x} + \frac{\partial T_{yx}}{\partial y} + \frac{1}{\rho_0} (\tau_x^s - \tau_x^b) \end{aligned} \quad (2.2a)$$

⁺Material in this section (2.1-2.1.4) is not different in essence from Chen (1978) who developed a storm surge model for ocean-bay coastal waters. It is included here for completeness.

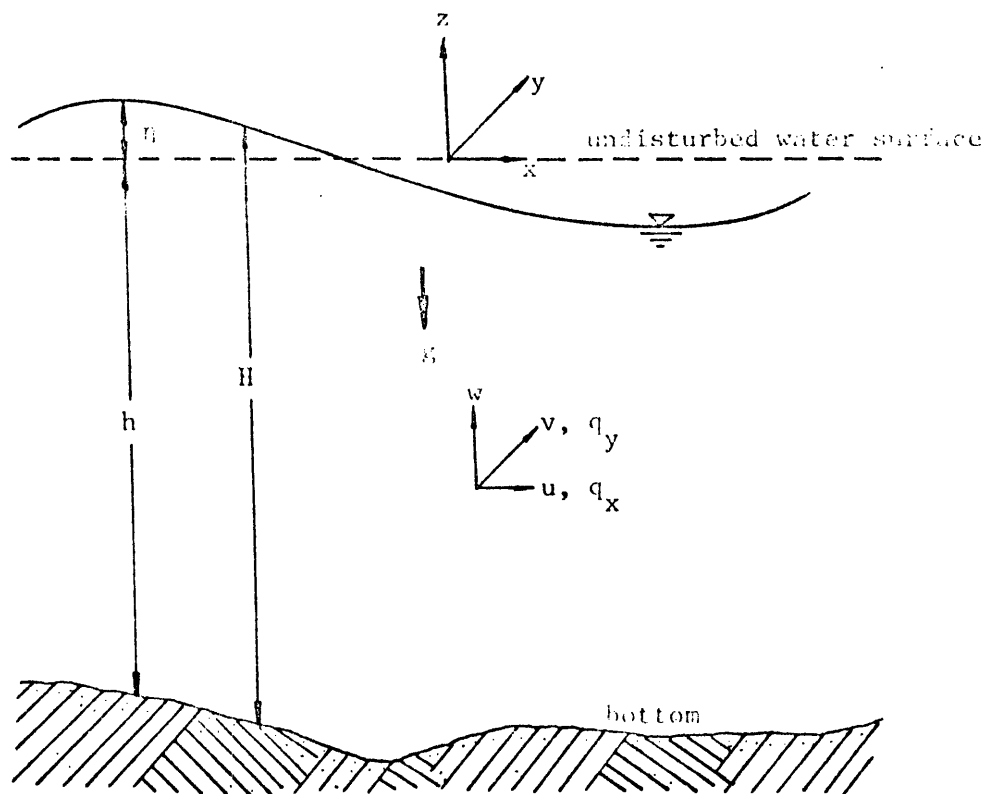


Figure 2.1. Definition sketch of the Cartesian Coordinate System.

$$\frac{\partial q_y}{\partial t} + \frac{\partial H^{-1} q_y q_x}{\partial x} + \frac{\partial H^{-1} q_y^2}{\partial y} + f q_x = - \frac{H}{\rho_0} \frac{\partial}{\partial y} (p^s + \rho g \eta) + \frac{\partial T_{xy}}{\partial x} + \frac{\partial T_{yy}}{\partial y} + \frac{1}{\rho_0} (\tau_y^s - \tau_x^b) \quad (2.2b)$$

where $H(x,y,t) = h(x,y) + \eta(x,y,t)$ (2.3)

$$q_x(x,y,t) = \int_{-h}^{\eta} u(x,y,z,t) dz, \quad q_y(x,y,t) = \int_{-h}^{\eta} v(x,y,z,t) dz \quad (2.4)$$

$$\rho(x,y,t) = \rho_0 + \Delta\rho(x,y,t) \quad (2.5)$$

The symbols used in equations (2.1) through (2.5) are defined as follows:

t = time variable

H = total water depth

h = undisturbed water depth

η = water surface elevation above undisturbed water surface

$\{u,v\}$ = water velocity components in x and y directions respectively

$\{q_x, q_y\} = \{q_i\}$ = water transport components in x and y directions respectively; $i = x, y$.

Q = rate of adding water mass per unit area

f = Coriolis coefficient = $2\Omega \sin\phi$

$\rho, \rho_0, \Delta\rho$ = water density, constant mean density, density deviation

p^s = atmospheric pressure

g = gravitation acceleration

$$\begin{pmatrix} T_{xx} & T_{xy} \\ T_{yx} & T_{yy} \end{pmatrix} = (T_{ij}) = \text{internal stress tensor; } i, j = x, y$$

$\{\tau_x^s, \tau_y^s\} = \{\tau_i^s\}$ = wind stress components in x and y directions respectively; $i = x, y$

$\{\tau_x^b, \tau_y^b\} = \{\tau_i^b\}$ = bottom friction components in x and y directions respectively; $i = x, y$

Equation (2.1) states that the total rate of change of mass per unit area is equal to the rate of adding mass per unit area, in consequence of the principle of conservation of mass. While equations (2.2a and b), which follow from the principle of conservation of momentum, include terms representing from left to right the inertial term, convective term, Coriolis term, pressure terms, internal stress terms, free surface (wind) stress term and bottom friction term. Water depth is still a function of position.

Among the variables in equations (2.1), (2.2a) and (2.2b), p^s and τ_i^s are the forcing functions from the storm. τ_{ij} and τ_i^b are assumed functions of H and q_i . Hence, equations (2.1) through (2.2b) constitute a set of three simultaneous partial differential equations for three unknowns; H (or η), q_x and q_y .

2.1.1 Wind Stress

The wind stress on the water surface is too complicated to be accurately estimated due to the complicated nature of the turbulent wind field and the deformable water surface. Nevertheless, it is now widely accepted that the wind stress is related to the wind velocity through the following expression proposed by Van Dorn (1953).

$$\tau_i^s = c_a \rho_a U_{10} U_{10i} \quad ; \quad i = x, y \quad (2.6)$$

where c_a = wind drag coefficient

ρ_a = air density

$\{U_{10i}\} = \{U_{10x}, U_{10y}\}$ = x and y components of wind velocity at 10-meters above undisturbed water surface

$U_{10} = \sqrt{U_{10x}^2 + U_{10y}^2}$ = wind speed at 10-meters above undisturbed water surface

The wind drag coefficient c_a is in general a function of wind speed

$$c_a = \begin{cases} c_o & ; U_{10} \leq U_{cr} \\ c_o + c_1 \left(1 - \frac{U_{cr}}{U_{10}}\right)^2 & ; U_{10} \geq U_{cr} \end{cases} \quad (2.7)$$

The values of the coefficients c_o and c_1 and the critical wind speed U_{cr} suggested by different investigators are respectively:

	Van Dorn (1953)	Wilson (1960) and Reid and Bodine (1968)
c_o	1.2E-3	1.1E-3
c_1	2.2E-3	2.5E-3
U_{cr} (m/s)	5.6	7.2

Note that other investigators have used other forms for c_a , such as Heaps (1969), Wu (1969), Whitaker (1973) and Wang and Connor (1975). All of these expressions of c_a are consistent with the present state of knowledge, but equation (2.7) works well in this study.

2.1.2 Bottom Friction

Bottom friction is another important factor, particularly in shallow water. Although several investigators (Heap 1969; Durance 1974) have attempted to represent the bottom friction by a linear relation to the water transport, it is now commonly accepted that a quadratic relation to the mean water velocity must be used.

$$\tau_1^b = c_f \rho_o H^{-2} \sqrt{q_x^2 + q_y^2} q_1 \quad (2.8)$$

where c_f is the coefficient of bottom friction. c_f is in general a

function of Reynolds number and bottom roughness, and its order of magnitude may range from 0.001 to 0.1.

2.1.3 Internal Stress

Internal stress originally arises from the eddy and molecular viscosities and the non-uniformity of flow velocity through water depth in the depth integrated approach. Physically, it represents the energy dissipation in the fluid and it also serves as a means to control short wave noise generated in numerical processes. In order to obtain a closed formulation, we assume that internal stress is related to mean flow velocity;

$$T_{ij} = \epsilon_{ij} \frac{H}{2} \left(\frac{\partial H^{-1} q_i}{\partial j} + \frac{\partial H^{-1} q_j}{\partial i} \right) \quad i, j = x, y \quad (2.9)$$

where ϵ_{ij} may be interpreted as "eddy viscosity" coefficient. Although ϵ_{ij} may depend on the mean flow, water depth and flow history, the dependence of ϵ_{ij} on the flow conditions is unknown. The value of ϵ_{ij} is therefore mainly determined from experience and by trial. An estimate of ϵ_{ij} is suggested by Wang and Connor (1975) by comparing the internal stress term with the pressure term

$$\epsilon \sim a g \frac{\eta^*}{U^*} \Delta s^*$$

where a is constant and ranges from 0.1 ~ 0.01. η^* is the typical free surface displacement, U^* the typical mean flow velocity and Δs^* the typical spatial grid size.

2.1.4 Initial and Boundary Conditions

In order to complete the mathematic formulation of the

hydrodynamic transport problem, the initial and boundary conditions should be properly prescribed.

The initial conditions specify free surface elevation and water transport in the entire water domain at the initial time

$$\begin{aligned} \eta(x,y,t) &= \eta_0(x,y) \quad \text{or} \quad H(x,y,0) = H_0(x,y) \\ q_i(x,y,t) &= q_{i0}(x,y); \quad i = x,y \quad \begin{array}{l} \text{for all } (x,y) \\ \text{at } t=0 \end{array} \end{aligned} \quad (2.10)$$

The boundary conditions encountered in the problem normally are of two types. They are the land boundaries at the water-land interface and the open (water) boundary at the artificial termination of the computational grid system. For an enclosed water body, such as a lake, only the land boundary needs to be considered. For an open coastal area, such as the lower James River, both types of boundaries must be considered.

Before specifying the boundary conditions, we define at the boundaries the normal and tangential water transports

$$\begin{aligned} q_n &= \alpha_{nx}q_x + \alpha_{ny}q_y \\ q_s &= -\alpha_{ny}q_x + \alpha_{nx}q_y \end{aligned} \quad (2.11)$$

where n is the unit normal vector outward from the water domain, s the unit tangential vector along the boundary, and the direction cosines

$$\begin{aligned} \alpha_{nx} &= \cos(n,x) \\ \alpha_{ny} &= \cos(n,y) \end{aligned} \quad (2.12)$$

consequently

$$\begin{aligned} q_x &= \alpha_{nx}q_n - \alpha_{ny}q_s \\ q_y &= \alpha_{nx}q_s + \alpha_{ny}q_n \end{aligned} \quad (2.13)$$

Define the x and y components of force measures due to internal stress

$$\begin{aligned} T_x &= \alpha_{nx} T_{xx} + \alpha_{ny} T_{yx} \\ T_y &= \alpha_{nx} T_{xy} + \alpha_{ny} T_{yy} \end{aligned} \quad (2.14)$$

At the land boundary a fixed vertical solid wall is assumed, and the normal water transport is specified to be zero.

$$q_n = q_n^* = 0 \quad (2.15)$$

where the superscript * denotes (and hereafter except when noted) a prescribed value.

At the open boundary the water surface elevation is

$$\eta = \eta^* \quad (2.16)$$

in which η^* is either the astronomical tide or the measured field data.

The boundary conditions which specify the x and y component of force measures are written

$$\begin{aligned} T_x &= T_x^* \\ T_y &= T_y^* \end{aligned} \quad (2.17)$$

In this study T_x^* and T_y^* are assumed to be of second order significance and are imposed to be zero in the calculation.

2.2 Water Quality Transport and Biochemical Reaction Processes

The water quality modelling is an attempt to deal with an aquatic ecosystem which consists of ten coupled sub-systems, corresponding to the ten constituents; namely, salinity, coliform bacteria, phytoplankton (represented by chlorophyll 'a'), organic nitrogen, ammonia nitrogen,

nitrite nitrate nitrogen, organic phosphorous, inorganic phosphorus, carbonaceous biochemical oxygen demand, and dissolved oxygen deficit. Salinity and coliform bacteria are considered as two independent subsystems, while the other eight constituents are coupled together through biochemical transformation processes. The interactions for the ten constituents are illustrated in figure 2.2. The model is formulated by employing a sequence of ten conservation of mass equations for ten water quality constituents. If C_i denotes the concentration of the i -th constituent, the two-dimensional depth integrated conservation of mass equation for the i -th constituent can be written

$$\frac{\partial HC_i}{\partial t} + \frac{\partial q_x C_i}{\partial x} + \frac{\partial q_y C_i}{\partial y} = \frac{\partial}{\partial x} \epsilon_{xi} H \frac{\partial C_i}{\partial x} + \frac{\partial}{\partial y} \epsilon_{yi} H \frac{\partial C_i}{\partial y} + HR_{Ii} + HR_{Ei} \quad (2.18)$$

here $i=1,2,3,\dots,9,0$ corresponding to the ten constituents. Therefore equation (2.18) actually contains a set of ten equations for ten unknowns C_i . (ϵ_{xi} , ϵ_{yi}) are the dispersion coefficients in x and y directions respectively. R_{Ii} stands for the internal generation (or decay) of substance C_i through physical and biochemical reaction processes, and R_{Ei} stands for the external additions to (or withdrawals from) the ecosystem.

In equation (2.18) the terms reading from left to right represent the inertial term, convective terms, diffusive terms, internal generation term, and external addition term respectively. The dispersion coefficients generally depend on the internal stresses of the flow and the non-uniformity of the concentration distribution of the substance through water depth. Here they are assumed to be related to the mean flow

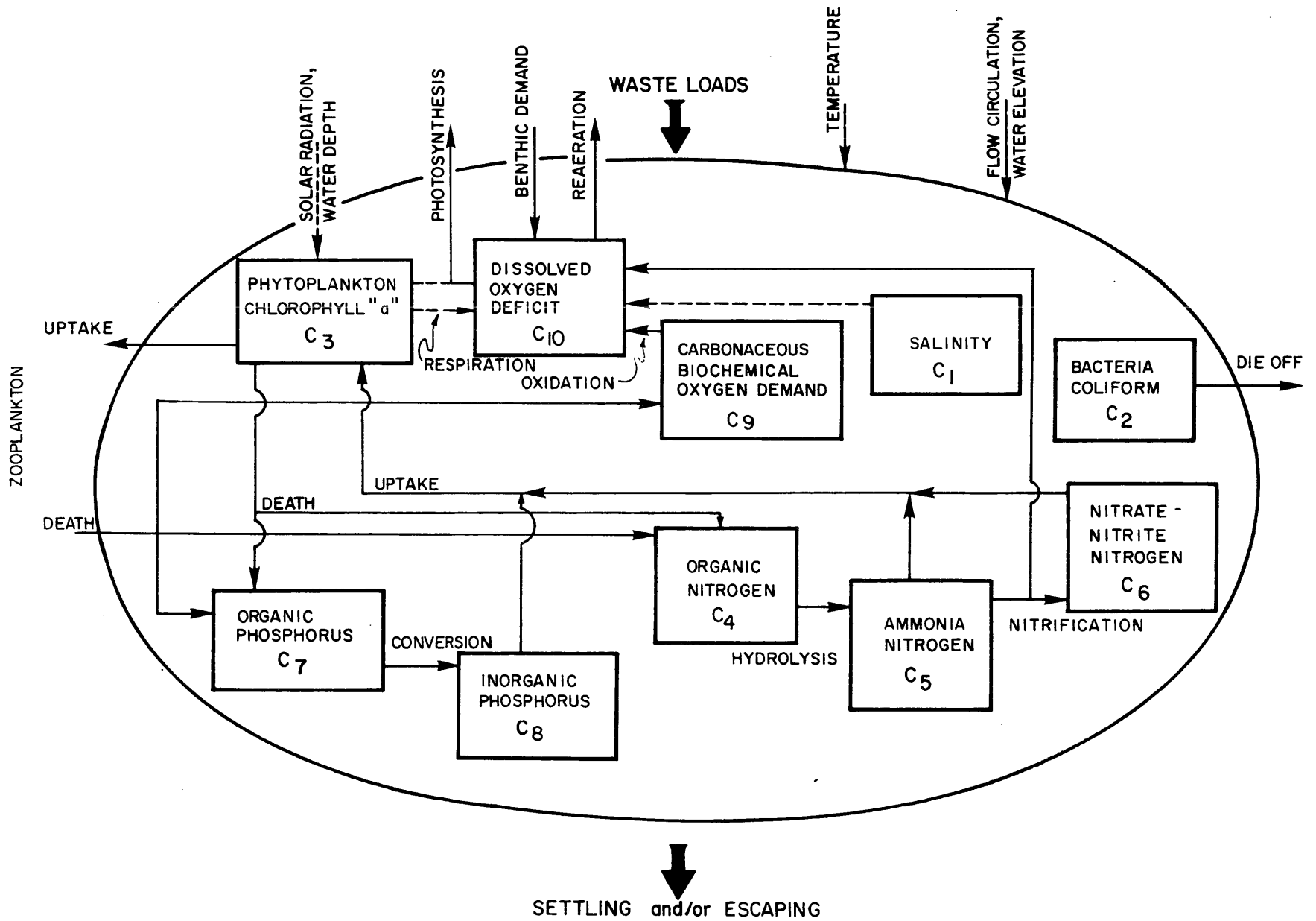


Figure 2.2. Schematic diagram showing the inter-reactions of the ten constituents.

$$(\epsilon_{xi}^*, \epsilon_{yi}^*) = (\epsilon_{xi}^* H^{-\frac{1}{6}} q_x, \epsilon_{yi}^* H^{-\frac{1}{6}} q_y) + (\epsilon_{xi}^{**}, \epsilon_{yi}^{**}) \quad (2.19)$$

here $(\epsilon_{xi}^*, \epsilon_{yi}^*)$ are regarded as constants, and $(\epsilon_{xi}^{**}, \epsilon_{yi}^{**})$ are introduced to meet the increase of diffusivity in natural water body by local effects due to meteorology and marine traffic. ρR_{Ei} is the time rate of external addition (or withdrawal) of mass of substance C_i and is assumed to be of the form

$$HR_{Ei} = -k_{si} HC_i + L_i \quad (2.20)$$

where the first term in equation (2.20) is the settling or escaping term and k_{si} is the settling or escaping rate. The second term L_i is the external waste loads from point and non-point sources. ρR_{Ii} stands for the time rate of internal generation (or decay) of mass of substance C_i through physical and biochemical reaction processes. The rates of reaction processes in this study are assumed to be one of the following two types: Michaelis-Menten reaction kinetics (Dugdale 1976, Parsons, Takahashi and Hargrave 1977) for nutrient uptake by primary producers, and first order reaction kinetics (Harleman 1970) for the others. According to each specific constituent R_{Ii} is assumed as follows:

(i=1) Salinity C_1

$$R_{I1} = 0 \quad (2.21)$$

Equation (2.21) indicates that there is no internal source of salinity except at the ocean boundary and from the external source.

(i=2) Coliform Bacteria C_2

$$R_{I2} = -k_2 C_2, \text{ where } k_2 = k_2^* (1.040)^{T-20} \quad (2.22)$$

where the exponential temperature dependence of the die-off rate k_2 is adopted. k_2^* is the die-off rate at temperature 20°C and T is temperature of water in centigrade degrees.

(i=3) Chlorophyll 'a' C_3

$$R_{I3} = (G-D-Z)C_3 \quad (2.23)$$

where G stands for the growth rate, D the endogenous respiration rate, and Z the grazing rate by zooplankton. For the growth rate, it is in general affected by temperature, light, and supply of nutrients, and is assumed to be the linear temperature dependence incorporating both with vertical extinction of solar radiation and self-shading effect and with the Michaelis-Menten effects for nutrients. Therefore

$$G = k_g^* T \left(\frac{e}{k_e H} \left(1 - e^{-\frac{I_o}{I_s}} \right) \right) \left(\frac{C_5 + C_6}{C_5 + C_6 + k_{mn}} \right) \left(\frac{C_8}{C_8 + k_{mp}} \right) \quad (2.24)$$

where k_g^* is the growth rate coefficient, k_{mn} and k_{mp} are the inorganic nitrogen and inorganic phosphorous Michaelis constants respectively. The constant $e = 2.71828$. $\frac{I_o}{I_s}$ is the solar radiation and is assumed to be a sine curve in daytime and zero in night time.

$$I_o = \begin{cases} I_s \sin \left(\frac{\pi(t-t^*)}{12} \right) > 0 & \text{for daytime} \\ 0 & \text{otherwise for night time} \end{cases} \quad (2.25)$$

in which time t is in hours and t^* refers to sunrise time. The light extinction coefficient of water column, k_e , is incorporated nonlinearly with chlorophyll as (Thomann, DiToro, and O'Connor 1974)

$$k_e = k_e^* + 0.008 C_3 + 0.054 C_3^{0.67} \quad (2.26)$$

in which k_e^* is the extinction coefficient at zero phytoplankton concentration.

The endogenous respiration rate is assumed

$$D = \frac{k_r^* T}{k_e^* H} \quad (2.27)$$

in which k_r^* is the respiration rate. For the grazing rate by zooplankton, Z , it in general depends solely on the concentration of herbivorous zooplankton biomass. Since zooplankton is disregarded in this study because of lack of field data, it is assumed that

$$Z = \frac{k_z^* T}{k_e^* H} \quad (2.28)$$

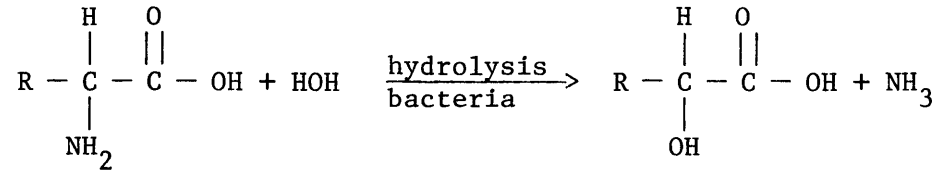
where k_z^* is the grazing coefficient.

(i=4) Organic Nitrogen (Org-N) C_4

$$R_{I4} = r_n (D + 0.4Z)C_3 - k_4 C_4, \quad k_4 = k_4^* T \quad (2.29)$$

where r_n is the ratio of nitrogen to chlorophyll and k_4^* the coefficient of the hydrolysis of organic nitrogen. Therefore, the first term in equation (2.29) represents sources due to death of phytoplankton and zooplankton, here it is assumed that 40% of chlorophyll 'a' uptaken by zooplankton becomes wastes (and death) of zooplankton and re-enter to the assumed aquatic ecosystem. The second term represents a sink term due to hydrolysis of organic nitrogen to ammonia nitrogen. The process of hydrolysis is also known as ammonification. It is carried out mainly by Saprophytic bacteria and is temperature dependent. The chemical formula of the hydrolysis of α -amino acid can be described as

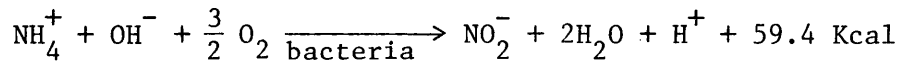
(Najarin and Harleman 1975)



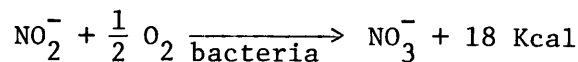
(i=5) Ammonia Nitrogen (NH₃-N) C₅

$$R_{I5} = - \left[1 - \frac{C_6}{C_6 + K_{mn}} \right] r_n GC_3 + k_4 C_4 - k_5 C_5, \quad k_5 = k_5^* T \quad (2.30)$$

where k_5^* is the coefficient of the nitrification. In equation (2.30), the first term represents the uptake of ammonia nitrogen by phytoplankton and $\left(1 - \frac{C_6}{C_6 + K_{mn}} \right)$ is ammonia preference by phytoplankton, the second term the source produced by the forward feeding hydrolysis reaction of org-N to NH₃-N, and the third term the oxidation of NH₃-N due to nitrification. The process of nitrification is a bacterially mediated biochemical reaction. It involves two stages, each requiring the presence of specific bacteria. In the first stage NH₃-N is oxidized to NO₂-N by bacteria of the genus Nitrosomonas as follows (O'Connor, et al., 1975):



In the second stage, nitrite NO₂-N is subsequently oxidized to nitrate by bacteria of the genus Nitrobacter as follows:



Note that the stoichiometric analysis indicates that the reaction of the first stage requires 3.43 grams of oxygen utilization for each gram of NH₃-N oxidized to NO₂-N, and that of the second stage requires 1.14 grams of oxygen utilization for each gram of NO₂-N to NO₃-N. Therefore the total oxygen utilization in the entire nitrification process is 4.57 grams of oxygen per gram of NH₃-N oxidized to NO₃-N. This oxygen conversion factor, 4.57, is used later, without regard to two separate

stages, in the conservation of mass equation for dissolved oxygen deficit.

(i=6) Nitrite-Nitrate Nitrogen (NO₂-N and NO₃-N) C₆

$$R_{I6} = - \left(\frac{C_6}{C_6 + k_{mn}} \right) r_n GC_3 + k_5 C_5, \quad (2.31)$$

where the expression in parenthesis is an assumed nitrite-nitrate preference by phytoplankton. The first term in equation (2.31) is a sink term representing the utilization of nitrite-nitrate nitrogen by phytoplankton. The second term is a source term representing the production of nitrite-nitrate nitrogen by nitrification.

(i=7) Organic Phosphorus (Org-P) C₇

$$R_{I7} = r_p (D + 0.4Z) C_3 - k_7 C_7, \quad k_7 = k_7^* T \quad (2.32)$$

where r_p is the rate of phosphorus to chlorophyll, and k_7^* the coefficient of conversion of org-P to inorg-P. The first term in equation (2.32) is the production of org-P by the death of phytoplankton and the waste of zooplankton. The second term is a sink term by converting org-P to inorg-P.

(i=8) Inorganic Phosphorus (Inorg-P) C₈

$$R_{I8} = -r_p GC_3 + k_7 C_7 \quad (2.33)$$

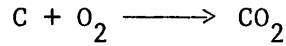
where the first term represents the uptake by phytoplankton, the second term a feeding source due to the conversion of org-P to inorg-P.

(i=9) Carbonaceous Biochemical Oxygen Demand (CBOD) C₉

$$R_{I9} = 2.67 r_c (0.4Z) C_3 - k_9 C_9, \quad k_9 = k_9^* \cdot (1.047)^{T-20} \quad (2.34)$$

where r_c is the ratio of carbon to chlorophyll and k_9^* the coefficient of

CBOD oxidation. The first term represents the production source contributed by the wastes of zooplankton, the conversion factor, 2.67 is obtained from the fact that the complete oxidation reaction of each gram of carbon (atomic weight = 12) from carbonaceous substances requires 2.67 grams of oxygen (molecular weight = 32).



The second term is a sink term representing the oxidation.

(i=0) Dissolved Oxygen Deficit (DO deficit) C_o

$$R_{I0} = k_9 C_9 + 4.57 k_5 C_5 - a_p G C_3 + a_r D C_3 + b_o - k_o C_o \quad (2.35)$$

$$a_p = 2.67 r_c k_{op}$$

$$a_r = 2.67 r_c / k_{or}$$

$$k_o = k_o^* \sqrt{\frac{q_x^2 + q_y^2}{H}} \cdot (1.024)^{T-20} + k_o^{**} \quad (2.36)$$

where k_{op} is the photosynthetic quotient and k_{or} the respiratory quotient. They are dimensionless parameters to indicate the relative amounts of oxygen and carbon involved in the processes of photosynthesis and respiration (Strickland 1960). The term b_o represents the benthic DO demand. The coefficients k_o^* and k_o^{**} are the reaeration coefficient constants. Equation (2.36) (modified from Isaacs (1969)) is used in this study, although various formulas by various authors for reaeration coefficients have been developed (Nemerow, 1974). k_o^{**} is included to meet the increase of reaeration due to local effects of meteorology and marine traffic.

The first term in equation (2.35) is the feeding source subject

to oxidation and the second term a source due to the oxygen utilization by nitrification. The oxygen conversion factor, 4.57, has been already explained in the section (i=5). The third and fourth terms represent respectively the sink and source due to photosynthesis and respiration of phytoplankton. The fifth term is a source due to the benthic oxygen demand and the last term a sink representing reaeration.

2.2.1 Initial and Boundary Conditions

The initial conditions specify concentration of each constituent in the entire water body at the initial time

$$C_i(x,y,t) = C_{i0}(x,y) \quad \text{for all } (x,y) \quad (2.37)$$

where $i = 1,2,3,\dots,9,0$, and $C_{i0}(x,y)$ are prescribed.

The boundary conditions encountered in the water quality problem generally are of three types; concentration, dispersive flux, and total flux. They are respectively, at a boundary point (x,y)

$$(i) \quad C_i(x,y,t) = C_i^*(x,y,t) \quad (2.38)$$

$$(ii) \quad \left(\epsilon_x H \frac{\partial C_i}{\partial x}, \epsilon_y H \frac{\partial C_i}{\partial y} \right) = (F_{Dx}^*, F_{Dy}^*) \quad (2.39)$$

$$(iii) \quad \left(q_x C_i - \epsilon_x H \frac{\partial C_i}{\partial x}, q_y C_i - \epsilon_y H \frac{\partial C_i}{\partial y} \right) = (F_{Tx}^*, F_{Ty}^*) \quad (2.40)$$

where (F_{Dx}^*, F_{Dy}^*) and (F_{Tx}^*, F_{Ty}^*) are the dispersive flux vector and the total flux vector respectively. The choice of the boundary condition depends on the individual case.

Similar to equations (2.11) and (2.12), the normal water quality flux is expressed, F_{Dn}^* and F_{Tn}^*

$$F_{Dn}^* = \alpha_{nx} F_{Dx}^* + \alpha_{ny} F_{Dy}^* \quad (2.41)$$

$$F_{Tn}^* = \alpha_{nx} F_{Tx}^* + \alpha_{ny} F_{Ty}^*$$

3. VARIATIONAL STATEMENT AND FINITE ELEMENT NUMERICAL APPROXIMATION⁺

The system of governing equations (2.1), (2.2a and b) with proper initial and boundary conditions defines a complete mathematical formulation of the biogeochemical water quality problem. It is an initial boundary value problem (I.B.V.P.) consisting of thirteen nonlinear equations for thirteen unknowns η , q_x , q_y , and C_i ($i=1,2,3,\dots,9,0$), and is too complicated to be solved by analytical means. In this study a finite element scheme is used for the numerical solution. For practical and economic reasons, there is no intention to solve the I.B.V.P. simultaneously and nonlinearly. Instead it is linearized by invoking the values at the previous time step and then solving each equation successively.

3.1 Galerkin's Variational Statement

The Galerkin's weighted residual finite element numerical scheme is employed in this work. The variational statements for the hydrodynamic and the water quality systems, equations (2.1), (2.2a and b) and (2.18) with the proper boundary conditions can be obtained by invoking Stokes' theorem as follows:

$$\iint_A \left(\frac{\partial H}{\partial t} + \frac{\partial q_x}{\partial x} + \frac{\partial q_y}{\partial y} - Q \right) \delta H \, dA = 0 \quad (3.1)$$

$$\iint_A \left\{ \left(\frac{\partial q_x}{\partial t} + \frac{\partial H^{-1} q_x^2}{\partial x} + \frac{\partial H^{-1} q_y q_x}{\partial y} - f q_y + \frac{H}{\rho_o} \frac{\partial}{\partial x} (p^s + \rho g \eta) - \frac{\tau_x^s - \tau_x^b}{\rho_o} \right) \delta q_x + \tau_{xx} \frac{\partial \delta q_x}{\partial x} + \tau_{yx} \frac{\partial \delta q_x}{\partial y} \right\} dA - \int_{\partial A} \tau_x^* \delta q_x \, dL = 0 \quad (3.2a)$$

⁺Material, except the water quality part, in this chapter is not different in essence from Chen (1978)

$$\iint_A \left\{ \left(\frac{\partial q_y}{\partial t} + \frac{\partial H^{-1} q_x q_y}{\partial x} + \frac{\partial H^{-1} q_y^2}{\partial t} + f q_x + \frac{H}{\rho_o} \frac{\partial}{\partial y} (p^s + \rho g \eta) - \frac{\tau_y^s - \tau_y^b}{\rho_o} \right) \delta q_y + T_{xy} \frac{\partial \delta q_y}{\partial x} + T_{yy} \frac{\partial \delta q_y}{\partial y} \right\} dA - \int_{\partial A} T_y^* \delta q_y dL = 0 \quad (3.2b)$$

$$\iint_A \left\{ \left(H \frac{\partial C_i}{\partial t} + q_x \frac{\partial C_i}{\partial x} + q_y \frac{\partial C_i}{\partial y} + Q C_i - H R_{Ii} - H R_{Ei} \right) \delta C_i + \epsilon_{xi} H \frac{\partial C_i}{\partial x} \frac{\partial \delta C_i}{\partial x} + \epsilon_{yi} H \frac{\partial C_i}{\partial y} \frac{\partial \delta C_i}{\partial y} \right\} dA - \int_{\partial A} F_{Dn}^* \delta C_i dL = 0 \quad (3.3)$$

where A is the water domain of interest, ∂A is the boundary curve of the domain A. dA and dL are associated with area and line integrals. δH , δq_x , δq_y and δC_i are the weighting functions. Note that equation (2.1) has been used in obtaining equation (3.3). Note also that the second order derivatives contained in the internal stress terms in equations (2.2a and b) and in diffusivity term in equation (2.18) have been reduced to a first order derivative in equations (3.2a and b) and (3.3). In this situation, a linear interpolation function is also an admissible function and can be used for approximation. However, a linear interpolation function chosen to describe a large domain A will lose accuracy in general. Therefore, the entire domain A will be divided into finite elements, and an approximate solution within each element will be sought by using a simple linear interpolation function with unknown nodal variables H , q_x , q_y and C_i .

3.2 Finite Element Approximation and Linear Triangular Element

In this study the entire water domain of interest is divided into small triangular elements, each with three nodes. Within each element, the field variables H , q_x , q_y , and C_i are approximated by a linear interpolation (shape) function N_j^e ($j=1,2,3$ corresponding to three nodes) with unknowns being the nodal variables H_j^e , q_{xj}^e , q_{yj}^e and C_{ij}^e at the element nodal point, i.e., in the "e" element

$$H^e = N_1^e H_1^e + N_2^e H_2^e + N_3^e H_3^e = \{N^e\}^T \{H^e\} = \{H^e\}^T \{N^e\} \quad (3.4)$$

$$q_x^e = N_1^e q_{x1}^e + N_2^e q_{x2}^e + N_3^e q_{x3}^e = \{N^e\}^T \{q_x^e\} = \{q_x^e\}^T \{N^e\} \quad (3.5a)$$

$$q_y^e = N_1^e q_{y1}^e + N_2^e q_{y2}^e + N_3^e q_{y3}^e = \{N^e\}^T \{q_y^e\} = \{q_y^e\}^T \{N^e\} \quad (3.5b)$$

$$C_i^e = N_1^e C_{i1}^e + N_2^e C_{i2}^e + N_3^e C_{i3}^e = \{N^e\}^T \{C_i^e\} = \{C_i^e\}^T \{N^e\} \quad (3.6)$$

In the preceding, the transposes of arrays $\{H^e\}$, $\{q_x^e\}$, $\{q_y^e\}$ and $\{C_i^e\}$ are respectively

$$\{H^e\}^T = \{H_1^e, H_2^e, H_3^e\} \quad (3.7)$$

$$\{q_x^e\}^T = \{q_{x1}^e, q_{x2}^e, q_{x3}^e\} \quad (3.8a)$$

$$\{q_y^e\}^T = \{q_{y1}^e, q_{y2}^e, q_{y3}^e\} \quad (3.8b)$$

$$\{C_i^e\} = \{C_{i1}^e, C_{i2}^e, C_{i3}^e\} \quad (3.9)$$

With the numerical subscripts referring to the nodes, $\{N^e\}^T$ is the row vector

$$\{N^e\}^T = \{N_1^e, N_2^e, N_3^e\} \quad (3.10)$$

with

$$N_j^e = (a_j + b_j x + c_j y) / 2\Delta^e \quad ; \quad j = 1, 2, 3 \quad (3.11a)$$

$$a_1 = x_2^e y_3^e - x_3^e y_2^e \quad (3.11b)$$

$$b_1 = y_2^e - y_3^e \quad (3.11c)$$

$$c_1 = x_3^e - x_2^e \quad (3.11d)$$

(equations for $a_2, a_3, b_2, b_3, c_2, c_3$ are cyclic permutations on $1, 2, 3$)

and $\Delta^e =$ the area of the element $e = \frac{1}{2} \begin{vmatrix} 1 & x_1^e & y_1^e \\ 1 & x_2^e & y_2^e \\ 1 & x_3^e & y_3^e \end{vmatrix} \quad (3.11e)$

where (x_j^e, y_j^e) are the coordinates of the element nodal point j as shown in figure 3.1. The interpolation functions N_j^e are linear functions of the coordinate. It is obvious that each interpolation function N_j^e is a pyramid, being unity at one node and going linearly to zero at surrounding nodes. These linear interpolation functions are employed to approximate the solution for each three nodal triangular elements in the domain A.

3.2.2 Evaluation of the Variational Statements

The interpolation functions given by equations (3.4) through (3.10) are used to evaluate the integral equations (3.1), (3.2a and b), and (3.3). In the following calculation of the integrals, we shall omit, for brevity, the symbols dA in all area integrals and dL in all line integral, and also omit, when not ambiguous, the superscript e .

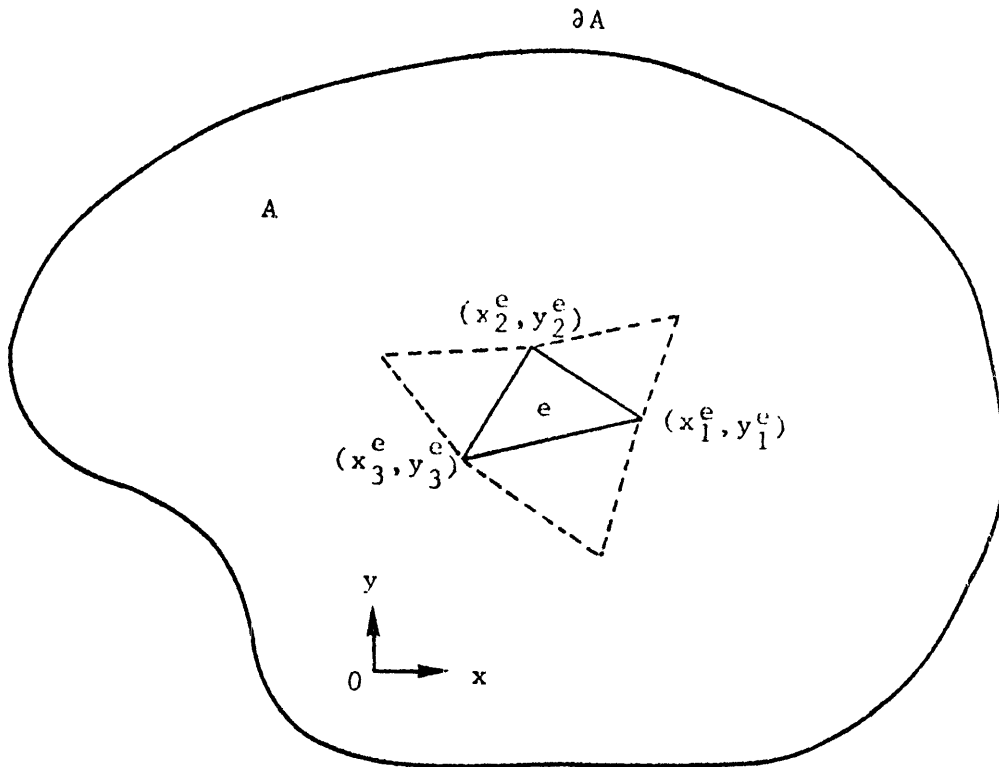


Figure 3.1. Domain and triangular elements

The calculation of each integral of equation (3.1) is sequently obtained to be

$$\begin{aligned} \iint_A \frac{\partial H}{\partial t} \delta H &= \sum_{e \in A} \iint_e \frac{\partial H}{\partial t} \delta H = \sum_{e \in A} \{\delta H\}^T \iint_e \{N\} \{N\}^T \frac{\partial \{H\}}{\partial t} \\ &= \sum_{e \in A} \{\delta H\}^T (M_h^e) \frac{\partial \{H\}}{\partial t} \end{aligned} \quad (3.12a)$$

$$\begin{aligned} \iint_A \frac{\partial q_x}{\partial x} \delta H &= \sum_{e \in A} \iint_e \frac{\partial q_x}{\partial x} \delta H = \sum_{e \in A} \{\delta H\}^T \iint_e \{N\} \frac{\partial \{N\}^T}{\partial x} \{q_x\} \\ &= \sum_{e \in A} \{\delta H\}^T (G_x^e) \{q_x\} \end{aligned} \quad (3.12b)$$

$$\begin{aligned} \iint_A \frac{\partial q_y}{\partial y} \delta H &= \sum_{e \in A} \iint_e \frac{\partial q_y}{\partial y} \delta H = \sum_{e \in A} \{\delta H\}^T \iint_e \{N\} \frac{\partial \{N\}^T}{\partial y} \{q_y\} \\ &= \sum_{e \in A} \{\delta H\}^T (G_y^e) \{q_y\} \end{aligned} \quad (3.12c)$$

$$\begin{aligned} \iint_A Q \delta H &= \sum_{e \in A} \iint_e Q \delta H = \sum_{e \in A} \{\delta H\}^T \iint_e \{N\} \{N\}^T \{Q\} \\ &= \sum_{e \in A} \{\delta H\}^T (M_h^e) \{Q\} \end{aligned} \quad (3.12d)$$

where the matrices

$$(M_h^e) = \iint_e \{N\} \{N\}^T = \frac{\Delta}{12} \begin{pmatrix} 2 & 1 & 1 \\ 1 & 2 & 1 \\ 1 & 1 & 2 \end{pmatrix} \quad (3.13a)$$

$$(G_x^e) = \iint_e \{N\} \frac{\partial \{N\}^T}{\partial x} = \frac{1}{6} \begin{pmatrix} b_1 & b_2 & b_3 \\ b_1 & b_2 & b_3 \\ b_1 & b_2 & b_3 \end{pmatrix} \quad (3.13b)$$

$$\{G_y^e\} = \iint_e \{N\} \frac{\partial \{N\}^T}{\partial y} = \frac{1}{6} \begin{pmatrix} c_1 & c_2 & c_3 \\ c_1 & c_2 & c_3 \\ c_1 & c_2 & c_3 \end{pmatrix} \quad (3.13c)$$

Equation (3.1) is then reduced to

$$\sum_{e \in A} \{\delta H\}^T \left\{ (M_h) \frac{\partial \{H\}}{\partial t} + (G_x) \{q_x\} + (G_y) \{q_y\} - (M_h) \{Q\} \right\} = 0 \quad (3.14)$$

Next we define the global vector arrays as follows

$$\{\delta H\} = \text{union of all } \{\delta H^e\} \quad ; \quad (3.15a)$$

$$\{H\} = \text{union of all } \{H^e\} \quad (3.15b)$$

$$\{\delta q\} = \text{union of all } \{\delta q_x^e\} \text{ and } \{\delta q_y^e\} \quad (3.15c)$$

$$\{q\} = \text{union of all } \{q_x^e\} \text{ and } \{q_y^e\} \quad ; \quad e \in A \quad (3.15d)$$

Then equation (3.14) can be assembled into a simple equation in matrix form

$$\{\delta H\}^T \left\{ (M_h) \frac{\partial \{H\}}{\partial t} + (G_h) \{q\} + \{R_h\} \right\} = 0 \quad (3.16)$$

where the global matrices (M_h) , (G_h) and $\{R_h\}$ are known from the assemblage of the element matrices (M_h^e) , (G_x^e) and $\{G_y^e\}$, and $(M_h^e) \{Q^e\}$ respectively. Since the element of $\{\delta H\}$ determines the test function, which is an arbitrary function, the terms within the brackets must vanish; i.e.

$$(M_h) \frac{\partial \{H\}}{\partial t} + (G_h) \{q\} + \{R_h\} = 0 \quad (3.17)$$

Note that (M_h) is symmetric. Equation (3.17) represents a set of first order differential equations in time.

The calculation of each integral of equation (3.2a and b) in element e is given as follows:

For equation (3.2a)

$$\iint_e \frac{\partial q_x}{\partial t} \delta q_x = \{\delta q_x\}^T (M_h) \frac{\partial \{q_x\}}{\partial t}$$

Defining $c_{ij} = H^{-1} q_i q_j$; $i, j = x, y$

$$\iint_e \frac{\partial H^{-1} q_x^2}{\partial x} \delta q_x \cong \{\delta q_x\}^T (G_x) \{c_{xx}\}$$

$$\iint_e \frac{\partial H^{-1} q_y q_x}{\partial y} \delta q_y = \{\delta q_x\}^T (G_y) \{c_{yx}\}$$

$$\iint_e f q_y \delta q_x = \{\delta q_x\}^T f (M_h) \{q_y\}$$

$$\iint_e \frac{H}{\rho_o} \frac{\partial p^s}{\partial x} \delta q_x = \{\delta q_x\} (M_h) \{H\} \frac{(b_1 p_1 + b_2 p_2 + b_3 p_3)}{2 \rho_o \Delta}$$

$$\iint_e gH \frac{\partial \eta}{\partial x} \delta q_x = \{\delta q_x\}^T (M_h) \{H\} \frac{g(b_1 \eta_1 + b_2 \eta_2 + b_3 \eta_3)}{2 \Delta}$$

$$\text{Defining } (M_{3\gamma}) = \iint_e \{N\} \{N\}^T \{\gamma\} \{N\}^T$$

$$= \frac{\Delta}{60} \begin{pmatrix} 2\bar{\gamma} + 4\gamma_1 & 2\bar{\gamma} - \gamma_3 & 2\bar{\gamma} - \gamma_2 \\ 2\bar{\gamma} - \gamma_3 & 2\bar{\gamma} + 4\gamma_2 & 2\bar{\gamma} - \gamma_1 \\ 2\bar{\gamma} - \gamma_2 & 2\bar{\gamma} - \gamma_1 & 2\bar{\gamma} + 4\gamma_3 \end{pmatrix}$$

$$\text{and } \bar{\gamma} = \gamma_1 + \gamma_2 + \gamma_3$$

(3.18)

$$\iint_e \frac{gH\Delta\rho}{\rho_o} \frac{\partial \eta}{\partial x} \delta q_x \cong \{\delta q_x\}^T \frac{g(b_1 \eta_1 + b_2 \eta_2 + b_3 \eta_3)}{2 \rho_o \Delta} (M_{3\Delta\rho}) \{H\}$$

$$\iint_e \frac{gH\eta}{\rho_o} \frac{\partial \Delta\rho}{\partial x} \delta q_x \cong \{\delta q_x\}^T \frac{g(b_1 \Delta\rho_1 + b_2 \Delta\rho_2 + b_3 \Delta\rho_3)}{2 \rho_o \Delta} (M_{3\eta}) \{H\}$$

$$\iint_e \frac{\tau_x^s}{\rho_o} \delta q_x = \{\delta q_x\}^T \frac{1}{\rho_o} (M_h) \{\tau_x^s\}$$

$$\iint_e \frac{\tau_x^b}{\rho_o} \delta q_x = \{\delta q_x\}^T \frac{1}{\rho_o} (M_h) \{\tau_x^b\}$$

Defining $\bar{H} = (H_1 + H_2 + H_3)$ as in equation (3.18) and flow velocities $(u, v) = H^{-1}(q_x, q_y)$

$$\iint_e T_{xx} \frac{\partial \delta q_x}{\partial x} = \{\delta q_x\}^T \frac{\epsilon_{xx} \bar{H}}{12\Delta} (M_{bb}) \{u\} \quad ;$$

$$\text{where } (M_{bb}) = \begin{pmatrix} b_1^2 & b_1 b_2 & b_1 b_3 \\ b_2 b_1 & b_2^2 & b_2 b_3 \\ b_3 b_1 & b_3 b_2 & b_3^2 \end{pmatrix}$$

$$\iint_e T_{yx} \frac{\partial \delta q_x}{\partial y} = \{\delta q_x\}^T \frac{\epsilon_{yx} \bar{H}}{24\Delta} \left\{ (M_{cb}) \{v\} + (M_{cc}) \{u\} \right\} \quad ;$$

$$\text{where } (M_{cb}) = \begin{pmatrix} c_1 b_1 & c_1 b_2 & c_1 b_3 \\ c_2 b_1 & c_2 b_2 & c_2 b_3 \\ c_3 b_1 & c_3 b_2 & c_3 b_3 \end{pmatrix}$$

$$\text{and } (M_{cc}) = \begin{pmatrix} c_1^2 & c_1 c_2 & c_1 c_3 \\ c_2 c_1 & c_2^2 & c_2 c_3 \\ c_3 c_1 & c_3 c_2 & c_3^2 \end{pmatrix}$$

$$\int_{\partial e} \mathbf{T}_x^* \delta \mathbf{q}_x = \{\delta \mathbf{q}_x\}^T \int_{\partial e} \{\mathbf{N}\} \{\mathbf{N}\}^T \{\mathbf{T}_x^*\} = \{\delta \mathbf{q}_x\}^T \frac{L^e}{6} \begin{pmatrix} 2 & 1 \\ 1 & 2 \end{pmatrix} \{\mathbf{T}_x^*\}$$

For equation (3.2b)

$$\iint_e \frac{\partial q_y}{\partial t} \delta q_y = \{\delta q_y\}^T (M_h) \frac{\partial \{q_y\}}{\partial t}$$

$$\iint_e \frac{\partial H^{-1} q_x q_y}{\partial x} \delta q_y \cong \{\delta q_y\}^T (G_x) \{c_{xy}\}$$

$$\iint_e \frac{\partial H^{-1} q_y^2}{\partial y} \delta q_y \cong \{\delta q_y\}^T (G_y) \{c_{yy}\}$$

$$\iint_e f q_x \delta q_y = \{\delta q_y\}^T f (M_h) \{q_x\}$$

$$\iint_e \frac{H}{\rho_o} \frac{\partial p^s}{\partial y} \delta q_y = \{\delta q_y\}^T (M_h) \{H\} \frac{(c_1 p_1 + c_2 p_2 + c_3 p_3)}{2 \rho_o \Delta}$$

$$\iint_e g H \frac{\partial \eta}{\partial y} \delta q_y = \{\delta q_y\}^T (M_h) \{H\} \frac{g(c_1 \eta_1 + c_2 \eta_2 + c_3 \eta_3)}{2 \Delta}$$

$$\iint_e \frac{g H \Delta \rho}{\rho_o} \frac{\partial \eta}{\partial y} \delta q_y \cong \{\delta q_y\}^T \frac{g(c_1 \eta_1 + c_2 \eta_2 + c_3 \eta_3)}{2 \rho_o \Delta} (M_{3\Delta\rho}) \{H\}$$

$$\iint_e \frac{g H \eta}{\rho_o} \frac{\partial \Delta \rho}{\partial y} \delta q_y \cong \{\delta q_y\}^T \frac{g(c_1 \Delta \rho_1 + c_2 \Delta \rho_2 + c_3 \Delta \rho_3)}{2 \rho_o \Delta} (M_{3\eta}) \{H\}$$

$$\iint_e \frac{\tau_y^s}{\rho_o} \delta q_y = \{\delta q_y\}^T \frac{1}{\rho_o} (M_h) \{\tau_y^s\}$$

$$\begin{aligned}
\iint_e \frac{\tau_y^b}{\rho_o} \delta q_y &\cong \{\delta q_y\}^T \frac{1}{\rho_o} (M_h) \{\tau_y^b\} \\
\iint_e T_{xy} \frac{\partial \delta q_y}{\partial x} &\cong \{\delta q_y\}^T \frac{\epsilon_{xy} \bar{H}}{24\Delta} \left\{ (M_{cb})^T \{u\} + (M_{bb}) \{v\} \right\} \\
\iint_e T_{yy} \frac{\partial \delta q_y}{\partial y} &\cong \{\delta q_y\}^T \frac{\epsilon_{yy} \bar{H}}{12\Delta} (M_{cc}) \{v\} \\
\int_{\partial e} T_y^* \delta q_y &= \{\delta q_y\}^T \frac{L^e}{6} \begin{pmatrix} 2 & 1 \\ 1 & 2 \end{pmatrix} \{T_y^*\}
\end{aligned}$$

Now all the integrals are substituted into equations (3.2a and b) and assemblage is performed, the resultant equation can be represented by the matrix form

$$(M_m) \frac{\partial \{q\}}{\partial t} + (G_m) \{q\} + (K_m) \{\eta\} + \{R_m\} = 0 \quad (3.19)$$

where the matrices (M_m) , (G_m) , (K_m) and $\{R_m\}$ are obtained through the assemblage of all the element in domain A. Note that the variables in the higher order integration terms, such as convection and bottom friction, have been lumped into a simple form for approximation as self-explained in the preceding integrals.

For simplicity, the external inflow, the internal reaction, and the external loading terms in equation (3.3) are lumped into the following expression

$$QC_i - HR_{Ii} - HR_{Ei} \equiv f_{i1} HC_i + f_{i2} \quad (3.20)$$

where f_{i1} and f_{i2} are in general functions of Q , H , and C_i ($i=1,2,3, \dots, 9,0$). They are assumed to be values at previous time step, hence

they are constants in real calculation. Now each integral of equation (3.3) in an element is obtained as follows:

$$\iint_e H \frac{\partial C}{\partial t} \delta C = \{\delta C\}^T (M_{3H}) \left\{ \frac{\partial C}{\partial t} \right\}$$

$$\iint_e q_x \frac{\partial C}{\partial x} \delta C = \{\delta C\}^T (M_{bq_x}) \{C\}$$

$$\text{where } (M_{\alpha\beta}) = \frac{1}{24} \begin{pmatrix} \alpha_1(\bar{\beta}+\beta_1) & \alpha_2(\bar{\beta}+\beta_1) & \alpha_3(\bar{\beta}+\beta_1) \\ \alpha_1(\bar{\beta}+\beta_2) & \alpha_2(\bar{\beta}+\beta_2) & \alpha_3(\bar{\beta}+\beta_2) \\ \alpha_1(\bar{\beta}+\beta_3) & \alpha_2(\bar{\beta}+\beta_3) & \alpha_3(\bar{\beta}+\beta_3) \end{pmatrix}$$

$$\text{and } \bar{\beta} = \beta_1 + \beta_2 + \beta_3$$

$$\iint_e q_y \frac{\partial C}{\partial y} \delta C = \{\delta C\}^T (M_{cq_y}) \{C\}$$

$$\iint_e f_{1H} C \delta C = \{\delta C\}^T (f_1) (M_{3H}) \{C\}$$

$$\iint_e f_2 \delta C = \{\delta C\}^T \frac{f_2 \Delta}{3} \begin{pmatrix} 1 \\ 1 \\ 1 \end{pmatrix}$$

$$\iint_e \epsilon_{xH} \frac{\partial C}{\partial x} \frac{\partial \delta C}{\partial x} = \{\delta C\}^T \left(\frac{\epsilon_{xH}}{12\Delta} \right) (M_{bb}) \{C\}$$

$$\iint_e \epsilon_{yH} \frac{\partial C}{\partial y} \frac{\partial \delta C}{\partial y} = \{\delta C\}^T \left(\frac{\epsilon_{yH}}{12\Delta} \right) (M_{cc}) \{C\}$$

$$\int_{\partial e} F_{Dn}^* \delta C = \{\delta C\}^T \left(\frac{L_e}{2} \right) \{F_{Dn}^*\}$$

Now by substituting all the integrals into equation (3.3) and followed by global assemblage, the resultant equation in matrix form can be expressed

$$(M_c) \frac{\partial \{C\}}{\partial t} + (G_c)\{C\} + \{R_c\} = 0 \quad (3.21)$$

where the matrices (M_c) , (G_c) , and the vector $\{R_c\}$ are again obtained through the assemblage of all the element in domain A. Note that (M_c) is function of H and (G_c) and $\{R_c\}$ are in general functions of H, q_x , q_y and C_n ($n=1,2,\dots,9,0$).

3.3 Time Integration

After using the finite element integration in spatial coordinates, the original continuous system of equations (3.1), (3.2a and b) and (3.3) reduces to a system of first order ordinary differential equations in time, equations (3.17), (3.19) and (3.21). To complete the model, an effective technique must be used to advance the solution in time from a given initial condition. The choice of the scheme depends on the required features of accuracy, stability and efficiency. The literature on these features is very extensive (Richtmyer and Morton 1967, Roache 1972). In this study the split-time method with the forward difference for hydrodynamic equations (3.18) and (3.20) and the half-station central difference for water quality equation (3.21) is employed in order to achieve a faster and more efficient and economical computational procedure to deal with a large complicated water quality system. The computational procedure is expressed as follows:

Equations (3.17) and (3.19) can be reformed into

$$(M_h) \frac{\partial \{H\}}{\partial t} = \{P_h\} \quad (3.22a)$$

$$(M_m) \frac{\partial \{q\}}{\partial t} = \{P_m\} \quad (3.22b)$$

where the elements of $\{P_h\}$ and $\{P_m\}$ are in general functions of H , q , t .

If the trapezoidal rule in time is used and H and q are staggered in time such that H is evaluated at times $t_{n-\frac{1}{2}}$ and q at t_n ($n=1,2,3,\dots$),

equations (3.22a and b) reduce to

$$(M_h) \left\{ \{H\}_{n+\frac{1}{2}} - \{H\}_{n-\frac{1}{2}} \right\} = \Delta t \{P_h(\{H\}_{n-\frac{1}{2}}, \{q\}_n, t_n)\} \quad (3.23a)$$

$$(M_m) \left\{ \{q\}_{n+1} - \{q\}_n \right\} = \Delta t \{P_m(\{H\}_{n+\frac{1}{2}}, \{q\}_n, t_{n+\frac{1}{2}})\} \quad (3.23b)$$

or

$$\{H\}_{n+\frac{1}{2}} = \{H\}_{n-\frac{1}{2}} + \Delta t (M_h)^{-1} \{P_h(\{H\}_{n-\frac{1}{2}}, \{q\}_n, t_n)\} \quad (3.24a)$$

$$\{q\}_{n+1} = \{q\}_n + \Delta t (M_m)^{-1} \{P_m(\{H\}_{n+\frac{1}{2}}, \{q\}_n, t_{n+\frac{1}{2}})\} \quad (3.24b)$$

and equation (3.21) reduces to

$$(M_c) \frac{\{C\}_{n+1} - \{C\}_n}{\Delta t} + (G_c) \frac{\{C\}_{n+1} + \{C\}_n}{2} + \{R_c\} = 0$$

or

$$\{C\}_{n+1} = \left[(M_c) + \frac{\Delta t}{2} (G_c) \right]^{-1} \left\{ - \left[(M_c) - \frac{\Delta t}{2} (G_c) \right] \{C\}_n - \Delta t \{R_c\} \right\} \quad (3.25)$$

where $M_c = M_c(\{H\}_{n+\frac{1}{2}})$

$$G_c = G_c(\{H\}_{n+\frac{1}{2}}, \{q\}_n, \{C\}_n)$$

$$R_c = R_c(\{H\}_{n+\frac{1}{2}}, \{q\}_n, \{C\}_n)$$

by assuming given initial conditions $\{H\}_{n-\frac{1}{2}}$, $\{q\}_n$ and $\{C\}_n$, the solution is obtained by first solving equation (3.23a) and then equation (3.23b) and then equation (3.25) and then followed by sequentially repeating the process. The stability condition of this scheme for the present problem is difficult to obtain analytically since so many physical terms are considered. Nevertheless, according to the present study and the study by Wang and Connor (1975), the critical time step for onset of instability is about $1.5 \Delta t_{cr}$.

$$1.5 \Delta t_{cr} = 1.5 \Delta s^* / U^* > \Delta t \quad (3.26)$$

where Δs^* is typical grid size and $U^* = \sqrt{2gH}$ for equations (3.24a and b) and $U^* = \sqrt{u^2+v^2}$ for equation (3.25). Equation (3.26) without the factor 1.5 is the well known Courant condition. It should be noted that since \sqrt{gH} is in general greater than $\sqrt{u^2+v^2}$, it is practical and more efficient in numerical computation to decouple the hydrodynamic and the water quality systems into two separate models as it has been done in this study.

3.4 Treatment of Boundary Condition

The concept of "flow leaked in equals to flow leaked out across the boundaries" developed by Wang and Connor (1975) is adapted to define the normal in this study. Define the angle θ_n of the normal at point P_2 as shown in figure 3.2.

$$\cot \theta_n = \frac{L_2 \sin \theta_o}{L_1 - L_2 \cos \theta_o} \quad \frac{\pi}{2} < \theta_o < 2\pi \quad (3.27)$$

where P_1 , P_2 and P_3 are three immediate adjoining points, L_1 and L_2 are two lengths of element boundaries, and θ_o is the angle between L_1 and L_2 .

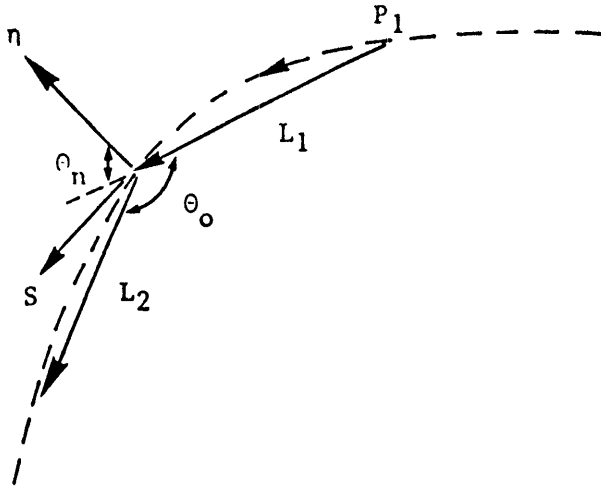


Figure 3.2. Definition sketch of boundary normal

Experience shows that the condition of zero velocity is appropriate for an acute angle, $\theta_0 \leq \frac{\pi}{2}$.

Boundary conditions are specified in terms of normal and tangential water transport q_n and q_s , instead of q_x and q_y . The transformation of field variables (water transport) from the global (x,y) coordinate system to local (n,s) coordinate system is performed according to the geometric relation

$$\begin{pmatrix} n \\ s \end{pmatrix} = (T) \begin{pmatrix} x \\ y \end{pmatrix}, \quad \begin{pmatrix} x \\ y \end{pmatrix} = (T)^T \begin{pmatrix} n \\ s \end{pmatrix} \quad (3.28a)$$

$$\begin{pmatrix} q_n \\ q_s \end{pmatrix} = (T) \begin{pmatrix} q_x \\ q_y \end{pmatrix}, \quad \begin{pmatrix} q_x \\ q_y \end{pmatrix} = (T)^T \begin{pmatrix} q_n \\ q_s \end{pmatrix} \quad (3.28b)$$

$$\text{where } (T) = \begin{pmatrix} \cos\theta & \sin\theta \\ -\sin\theta & \cos\theta \end{pmatrix} \quad (3.28c)$$

Note that (T) is an orthonormal matrix such that $(T)^{-1} = (T)^T$.

The boundary conditions (2.15), (2.16) and (2.38) are specified by using a standard row-column elimination technique on the coefficient matrixes of the respective equations (3.24a and b) and (3.25).

4. SOME COMPUTATIONAL ASPECTS

As it was noted in section 3.3, for economical and practical purposes, the entire biogeochemical water quality system is manipulated in actual calculation by treating the hydrodynamic and the water quality models separately; i.e., the hydrodynamic model is used first to calculate water elevation and circulation until the flow condition in the water body is simulated, then the result is used as hydrodynamic input to the water quality model to calculate the concentration distribution of the constituents. The computational procedures and program for the hydrodynamic and the water quality calculation have been developed according to Chapters 2 and 3. Since the approach for solving the hydrodynamic model described in Chapter 3 is somewhat similar to the works by Connor and Wang (1975), the associated computer program CAFE (Circulation Analysis by Finite Element) has been used with modifications in this study.

The layout of finite element system depends on variations of water elevation, coastal configuration, water depth and concentration distribution. The maximum element size is chosen, according to Chen and Mei (1974)

$$\frac{\ell^e}{\lambda} \leq 0.1 \quad (4.1)$$

i.e. the element size ℓ^e is chosen to be less than one tenth of wavelength, λ . A Numonics Digitizer which reads to the accuracy of one hundredth of a centimeter, has been used to measure the coordinates of nodal points. The critical time step for instability was found by computational trials to be $1.5 \Delta t_{cr}$ which is more relaxed than the Courant condition.

Computational experience also reached the same conclusions as found by Wang and Connor (1975); that the increase of the bottom friction coefficient c_f tends to increase the phase lag in the direction of water wave propagation. The water elevation was fairly insensitive to the change of c_f , but noticeable changes in the flow currents were calculated. Eddy viscosity (ϵ_{xx} , ϵ_{xy} and ϵ_{yy}) have little effect on phase and range of water elevation, but affect flow currents.

4.1 Verification by Studying Simple Problem

One way of verification of the numerical model is to solve some simple problem and then to compare the numerical result with the exact analytical solution. In this study for the time being there is no intention of verifying the hydrodynamic model since for most simple problems the program of the model is almost identical to the CAFE program which has been extensively used to study several simple problems (Wang and Connor 1975). However, the study of model application to the lower James River in the next chapter can be considered one of verification. The verification of the numerical model of the water quality is conducted by studying a rectangular channel, as shown in figure 4.1, with constant flow velocity, constant dispersion coefficients and constant decay rate, and with the following initial and boundary conditions for concentration $C(x,y,t)$.

Initial condition: $C(x,y,0) = 0$ for all (x,y)

Boundary conditions: (i) at upstream boundary $(x,y) = (0,y)$,
constant concentration $C(0,y,t) = 1$
for all y,t

- (ii) at downstream boundary (x_{42}, y) either constant concentration $C(x_{42}, y, t) = 0$ or dispersive flux condition $\epsilon H \frac{\partial C}{\partial n}$ at (x_{42}, y) , equal to the dispersive flux at previous time step.

Then the numerical results of the constituents of salinity and coliform bacteria are calculated to compare with the following exact analytical solution (equation 4.2) for the concentration distribution of an one-dimensional channel of infinite length and constant concentrations at upstream and downstream boundaries (Harleman, 1970).

$$\frac{C}{C_0} = \frac{1}{2} e^{\frac{xU}{2\epsilon}} \left(e^{\frac{x\Omega}{2\epsilon}} \operatorname{erfc} \left(\frac{x+\Omega t}{\sqrt{4\epsilon t}} \right) + e^{-\frac{x\Omega}{2\epsilon}} \operatorname{erfc} \left(\frac{x-\Omega t}{\sqrt{4\epsilon t}} \right) \right) \quad (4.2)$$

where erfc is the complementary error function and $\Omega = \sqrt{U^2 + 4k\epsilon}$, in which U is flow velocity, ϵ dispersive coefficient and k decay rate. The comparisons showing in figures 4.2, 4.3 and 4.4 agree quite well except at initial times which is effected by numerical discretization at initial time and near the downstream end where numerical result is effected by the finite length of the channel. Table 4.1 also shows the concentration results of the cases of different Δt . Note that the stability condition seems much relaxed by the conventional ones which are

$$S_u = \left(\frac{u}{\Delta x} + \frac{v}{\Delta y} \right) \Delta t \leq 1 \quad (4.3)$$

$$S_\epsilon = \left(\frac{\epsilon_{xx}}{2\Delta x^2} + \frac{\epsilon_{yy}}{2\Delta y^2} \right) \Delta t \leq \frac{1}{2}$$

The comparison for the other water quality constituents cannot be conducted since no analytical solution of the coupled system exists. However, by examining the numerical results and behavior, the calculated concentration distributions of the other constituents show the right trend and are very reasonable.

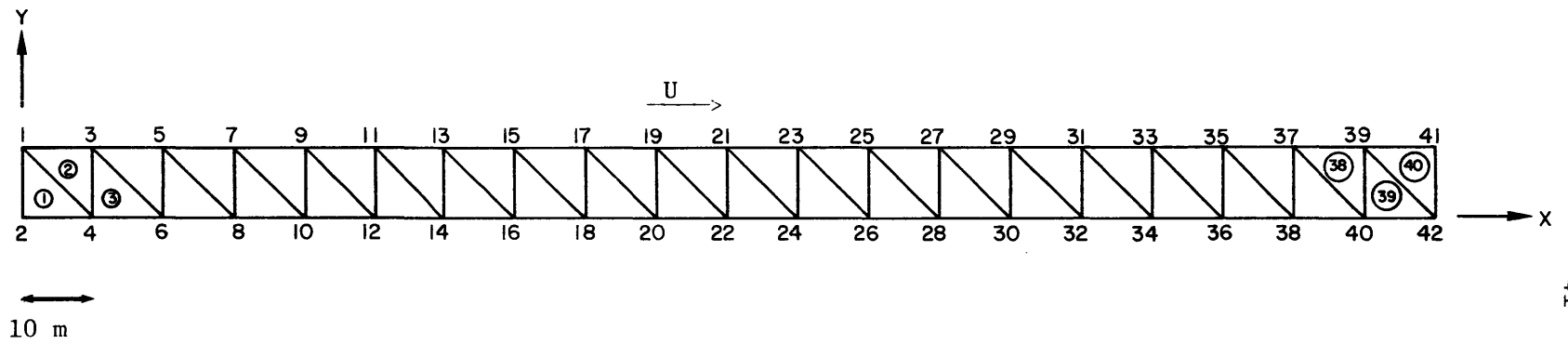


Figure 4.1. Finite element grid of rectangular channel.

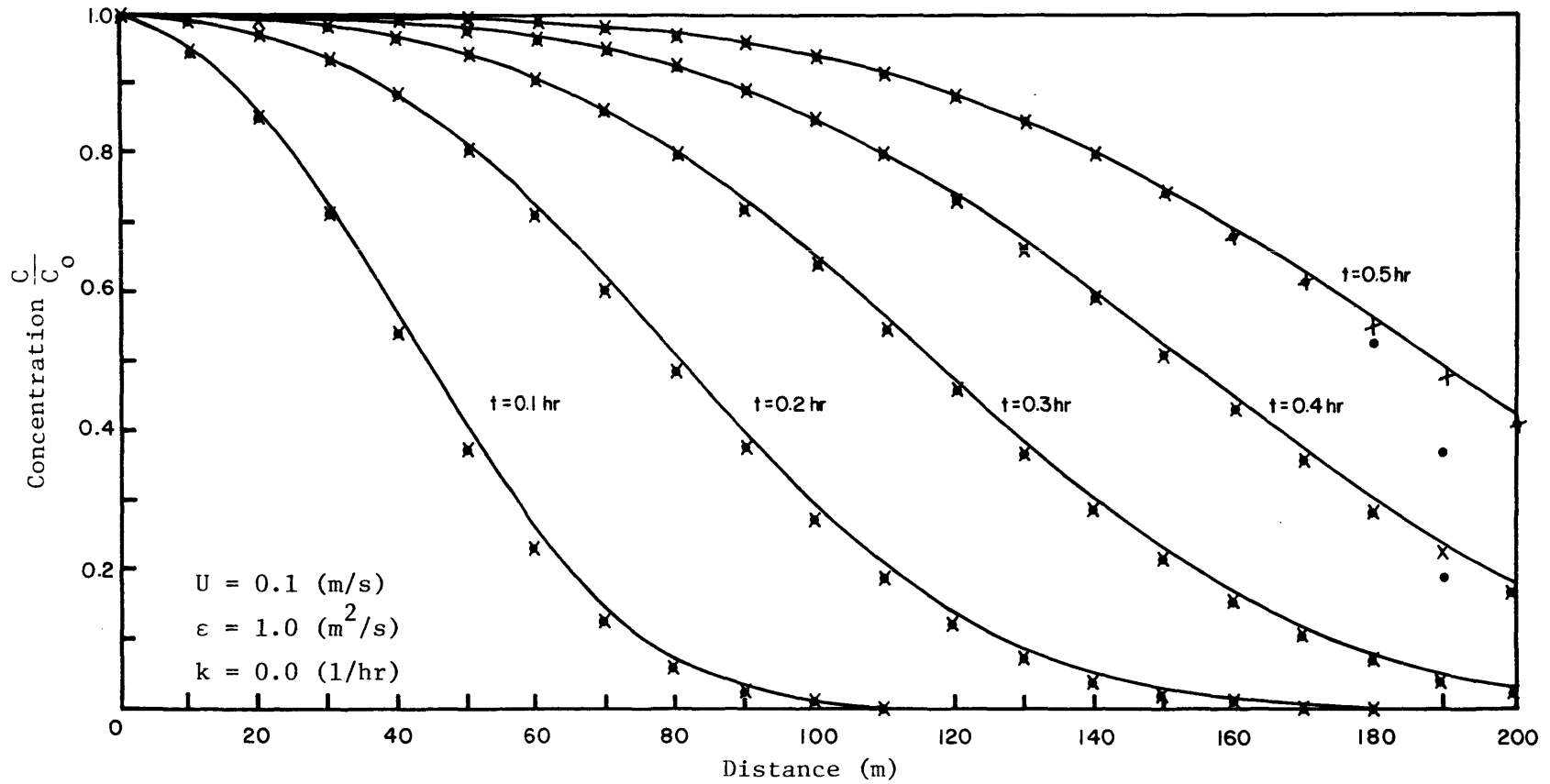


Figure 4.2. Comparison of concentration propagation of analytical solution and numerical solution ($\Delta t=0.01$ hr) without decay. (—, analytical, ...and xxx, FEM with zero concentration condition and dispersive flux condition respectively at downstream boundary).

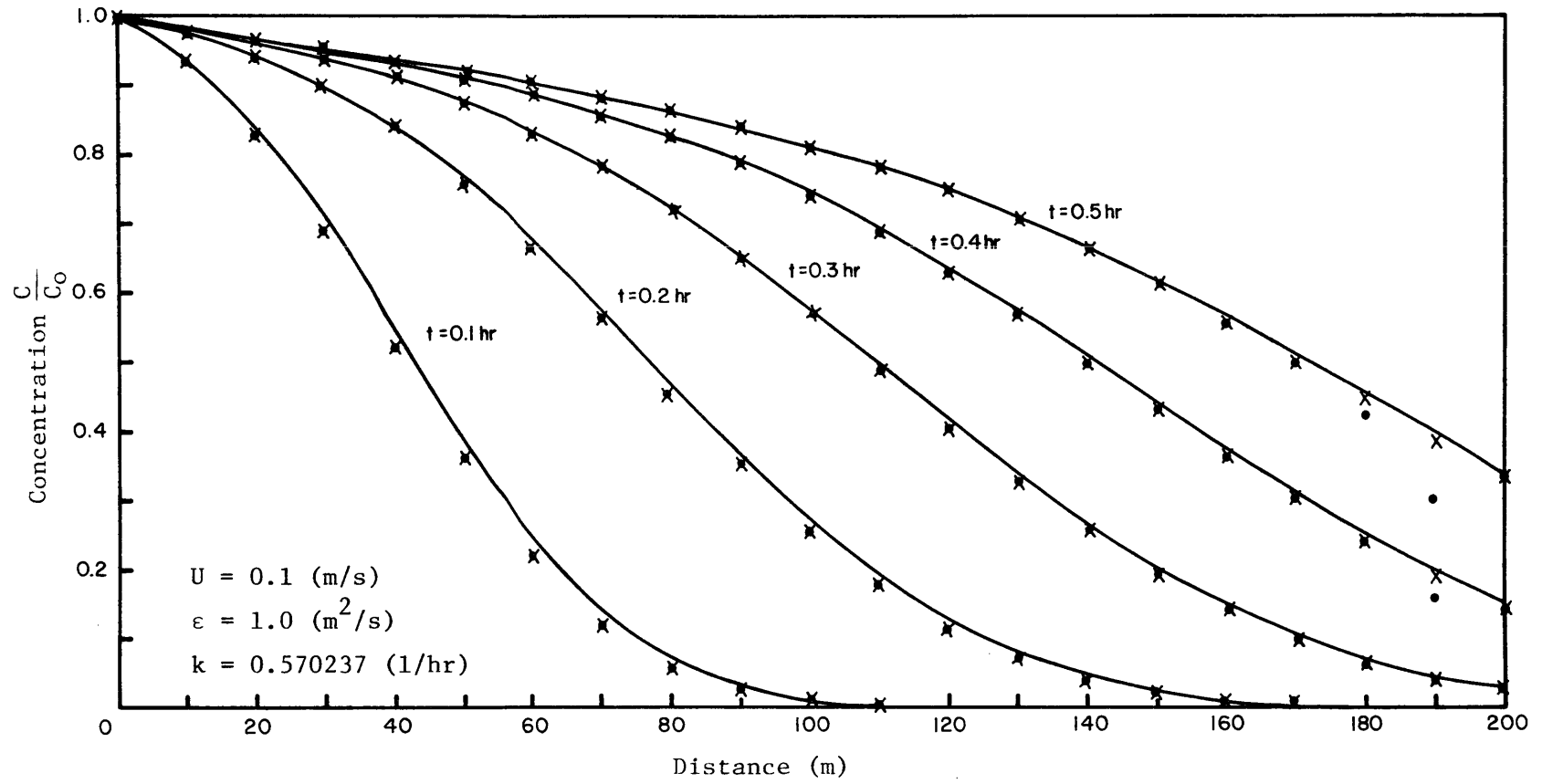


Figure 4.3. Comparison of concentration propagation of analytical solution and FEM numerical solution ($\Delta t=0.01$ hr) with decay. (—, analytical, ... and xxx, FEM with zero concentration condition and dispersive flux condition respectively at downstream boundary).

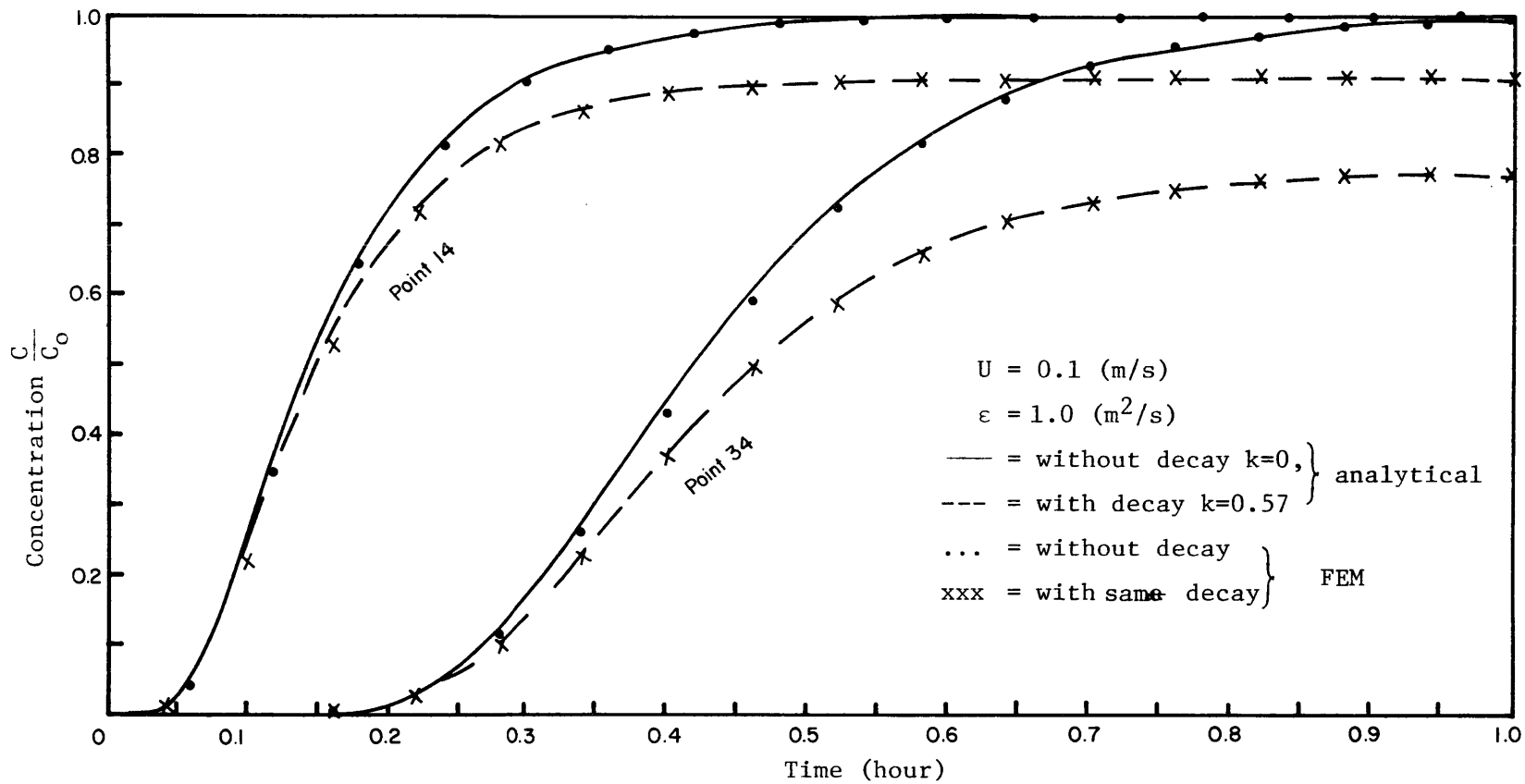


Figure 4.4. Time history of concentration of analytical solution and FEM numerical solution ($\Delta t=0.01$ hr). (Point location referred to figure 4.1).

Table 4.1. Convergence of $\frac{C}{C_0}$ With Respect to Δt at Point 24

Δt (hr)						
Time (hr)	Analytic Sol. (Eq. 4.2)	0.01	0.02	0.04	0.06	
0.12	0.017119	0.01207	0.01147	0.01365	0.01625	
0.24	0.354118	0.3366	0.3153	0.2676	0.2237	
0.36	0.725432	0.7140	0.7020	0.6756	0.6435	
0.48	0.902361	0.8976	0.8932	0.8848	0.8763	
0.60	0.967710	0.9661	0.9647	0.9625	0.9609	
0.72	0.993174	0.9892	0.9888	0.9882	0.9881	
0.84	0.996732	0.9966	0.9965	0.9964	0.9964	
0.96	0.998973	0.9989	0.9989	0.9989	0.9989	
1.08	0.999678	0.9997	0.9996	0.9996	0.9997	
Stability	S_u	0.36	0.72	1.44	2.16	
Eq. (4.3)	S_ϵ	0.72	1.44	2.88	4.32	

5. APPLICATION TO THE LOWER JAMES RIVER

In this Chapter the hydrodynamic and the water quality models are applied to the lower James River in Virginia. The area of the lower James River lies within the Peninsula and Southeastern Virginia Planning Districts as shown in Figure 5.1. In this study the lower James River is considered to begin near Sandy Point, just upstream from the confluence of the Chickahominy River. It meanders through the Southeastern Virginia Coastal Plains, while being augmented by its tributaries. Finally it ends at Old Point Comfort, where it exchanges water with Chesapeake Bay tidally. It has more than 26,000 square kilometers of drainage area (Seitz, 1971) and receives considerable wastes from point sources and non-point sources. It also absorbs and dilutes wastes from the upper James River and its tributaries. However, due to the large tidal prism of the James River, the present waste loads of the ten considered constituents seem not to have a strong environmental impact.

5.1 Finite Element Network of the River

Three U.S.C&G maps (1974), numbered 562, 529 and 530, were used to provide the information on coastal configuration and topography for the geometric input to the system. The finite element network of the lower James River, from Sandy Point and Sloop Point to the river mouth (Old Point Comfort and Willoughby Beach), is shown in Figure 5.1a and b. The figures illustrate the nodal and element positions. The typical length of an element is 1.2 to 4 km, depending on the desired accuracy. Figure 5.1c is the locally averaged mean water depth, being the mean water depth corrected by mean tidal height and NGVD (1929) (National Geodetic Vertical Datum 1929).

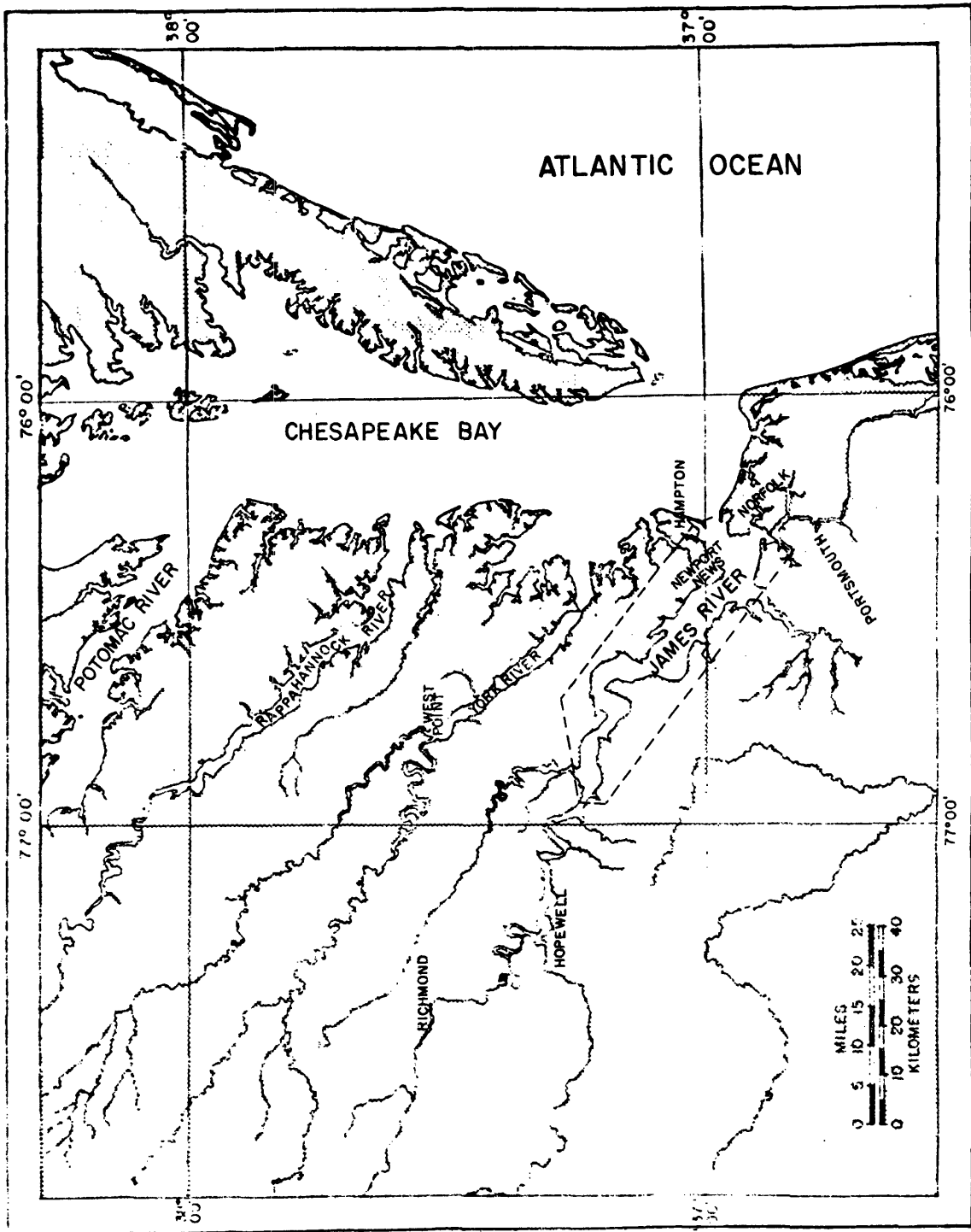


Figure 5.1. Tidewater Virginia showing the area of the lower James River.

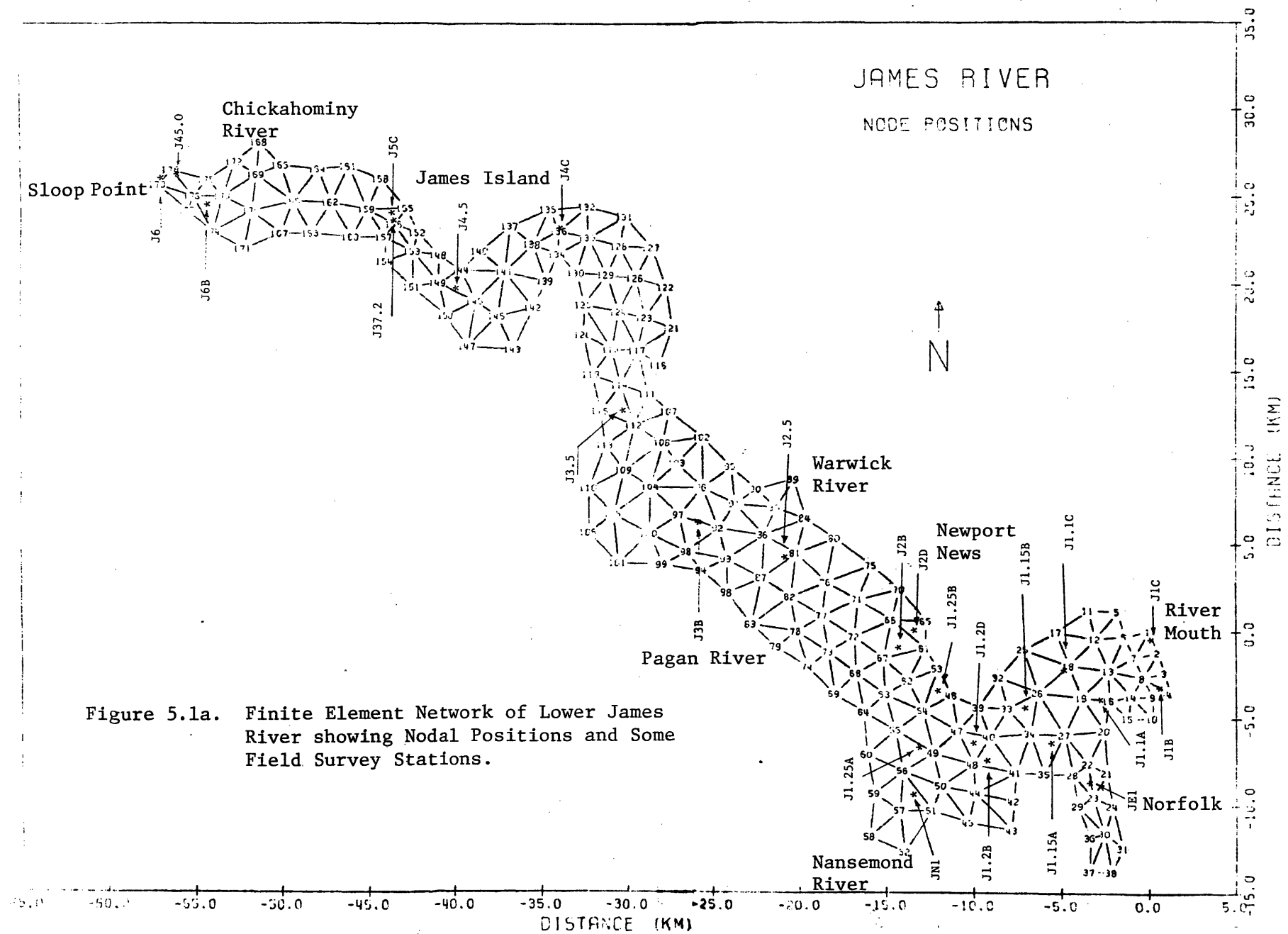


Figure 5.1a. Finite Element Network of Lower James River showing Nodal Positions and Some Field Survey Stations.

JAMES RIVER
FINITE ELEMENTS

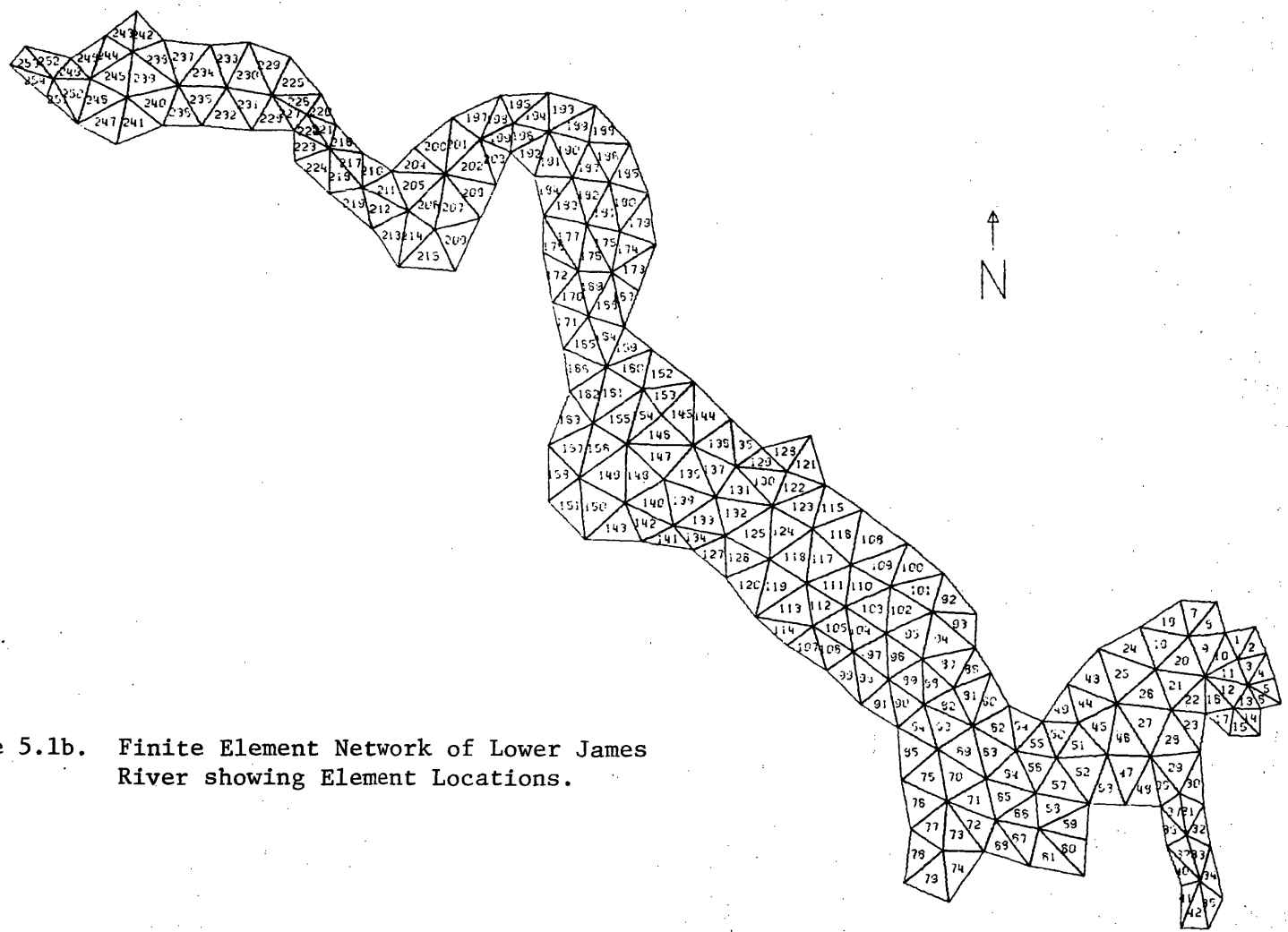


Figure 5.1b. Finite Element Network of Lower James River showing Element Locations.

35.0
30.0
25.0
20.0
15.0
10.0
5.0
0.0
-5.0
-10.0
-15.0
DISTANCE (KM)

-65.0 -60.0 -55.0 -50.0 -45.0 -40.0 -35.0 -30.0 -25.0 -20.0 -15.0 -10.0 -5.0 0.0 5.0
DISTANCE (KM)

5.2 Hydrodynamic Model

The tidal information is obtained from U. S. Tide Tables (1976) and is adjusted by NGVD (1929) data. The inputs of free surface super-elevation (mean sea level minus NGVD (1929)), tidal height and phase lag at fifteen locations are listed in Tables 5.1a and b. It is believed that the free surface super-elevation is partly contributed by freshwater discharge from upstream and from tributaries.

Tidal heights and tidal current from U. S. Tidal Table and U. S. Tidal Current (1976), and the intensive survey field current data from VIMS (Virginia Institute of Marine Science) were used to examine the bottom friction coefficient c_f and eddy viscosity coefficients ϵ_{ij} . The results show a good fit for $c_f = 0.0064$, $\epsilon_{xx} = \epsilon_{xy} = \epsilon_{yy} = 100 \text{ m}^2/\text{s}$. The time step is 2 minutes. The water elevation and flow current reached periodic equilibrium state in only about 2 hours after starting from initial conditions. Examples of transient response are illustrated in Figures 5.2a and b. This fast convergence is due to the even distribution of tidal forcing imposed over the water domain. The calculated results of water elevation and flow circulation within a tidal cycle are illustrated in Figures 5.3A,a thru F,f.

The computed results of flow circulation and water elevation serve as input to the biogeochemical water quality system.

5.3 Biogeochemical Water Quality Model

Waste loads to the lower James River are of two types: point sources which are the outfalls from municipal and industrial waste water treatment facilities and non-point sources which are the wastes contained in the storm runoff from the basins. In this work the point source data

Table 5.1a. Some Tide Data of Lower James River.

Location	NGVD (1929)- MLW (m)	Mean Tidal Height (m)	Phase Lag		
			High Water	Low Water (hr:min)	Average
Old Point Comfort	0.396	0.366	-00:11	-00:35	-00:23
Sewells Point	0.390	0.366	00:00	00:00	00:00
Norfolk Harbor	0.466	0.396	00:13	00:19	00:16
Newport News	0.399	0.396	00:20	00:18	00:19
Chuckatuck Creek Entrance	0.463	0.427	00:41	00:47	00:44
Menchville	0.421	0.396	00:54	01:09	01:02
Burwell Bay	0.357	0.366	01:14	01:42	01:28
Ferry Point Chickahominy R.	0.247	0.274	03:54	04:26	04:10
Claremont Wharf	0.238	0.274	04:02	04:38	04:20

Table 5.1b. Tidal Input for the Lower James River Hydrodynamic Model.

Nodal Point	Free Surface Superelevation (is Referenced to NGVD (1929)) (m)	Tidal Height (m)	Phase Lag (is Referenced to Sewells Point) (sec)
1	-0.015	0.38	-1380
2	-0.015	0.38	-1380
3	-0.015	0.38	-1380
4	-0.015	0.38	-1380
20	-0.009	0.38	0
37	-0.041	0.42	945
38	-0.041	0.42	945
46	-0.003	0.40	1140
59	-0.036	0.43	2640
60	-0.036	0.43	2640
89	-0.025	0.40	3696
106	0.009	0.36	5280
168	0.043	0.29	15000
178	0.052	0.29	15600
179	0.052	0.29	15600

(see Figure 5.1a for nodal point)

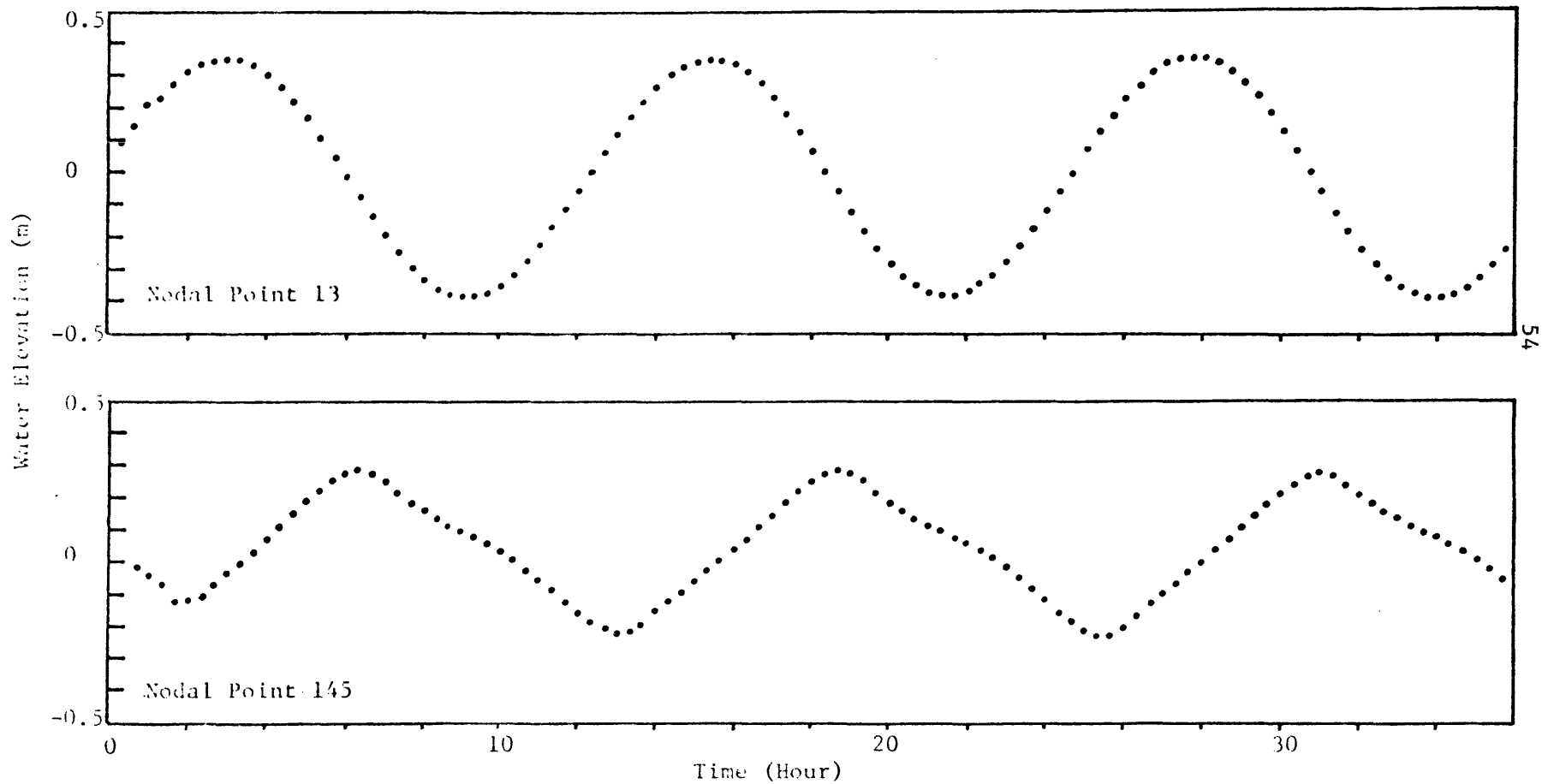


Figure 5.2a. Time history of water elevation at Node. (See Figure 5.1a for nodal position).

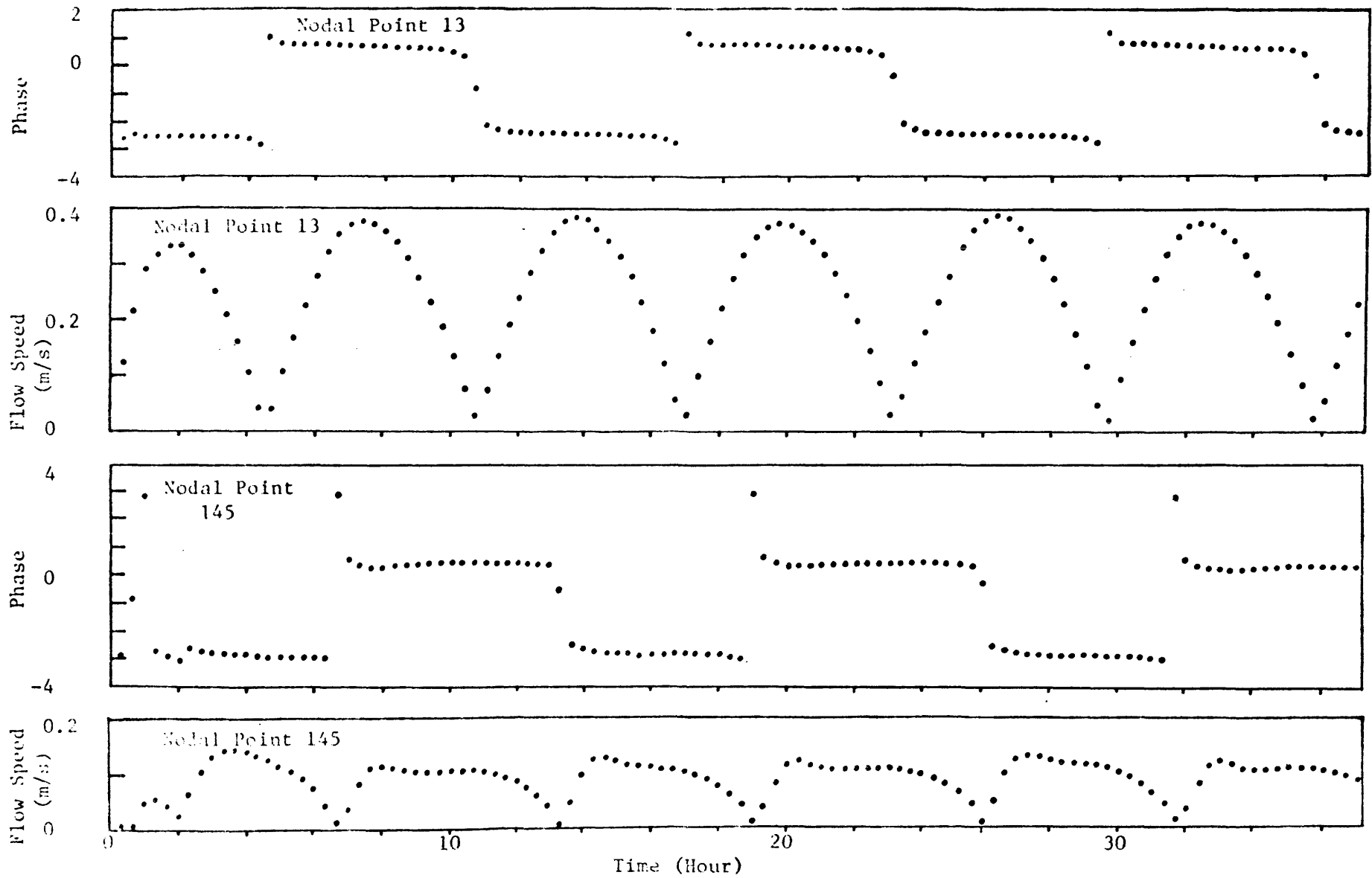
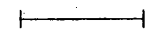


Figure 5.2b. Time history of flow velocity at node. (See Figure 5.1a for nodal position).

JAMES RIVER

CURRENT VECTOR SCALE: 1 INCH = 1 METER/SEC



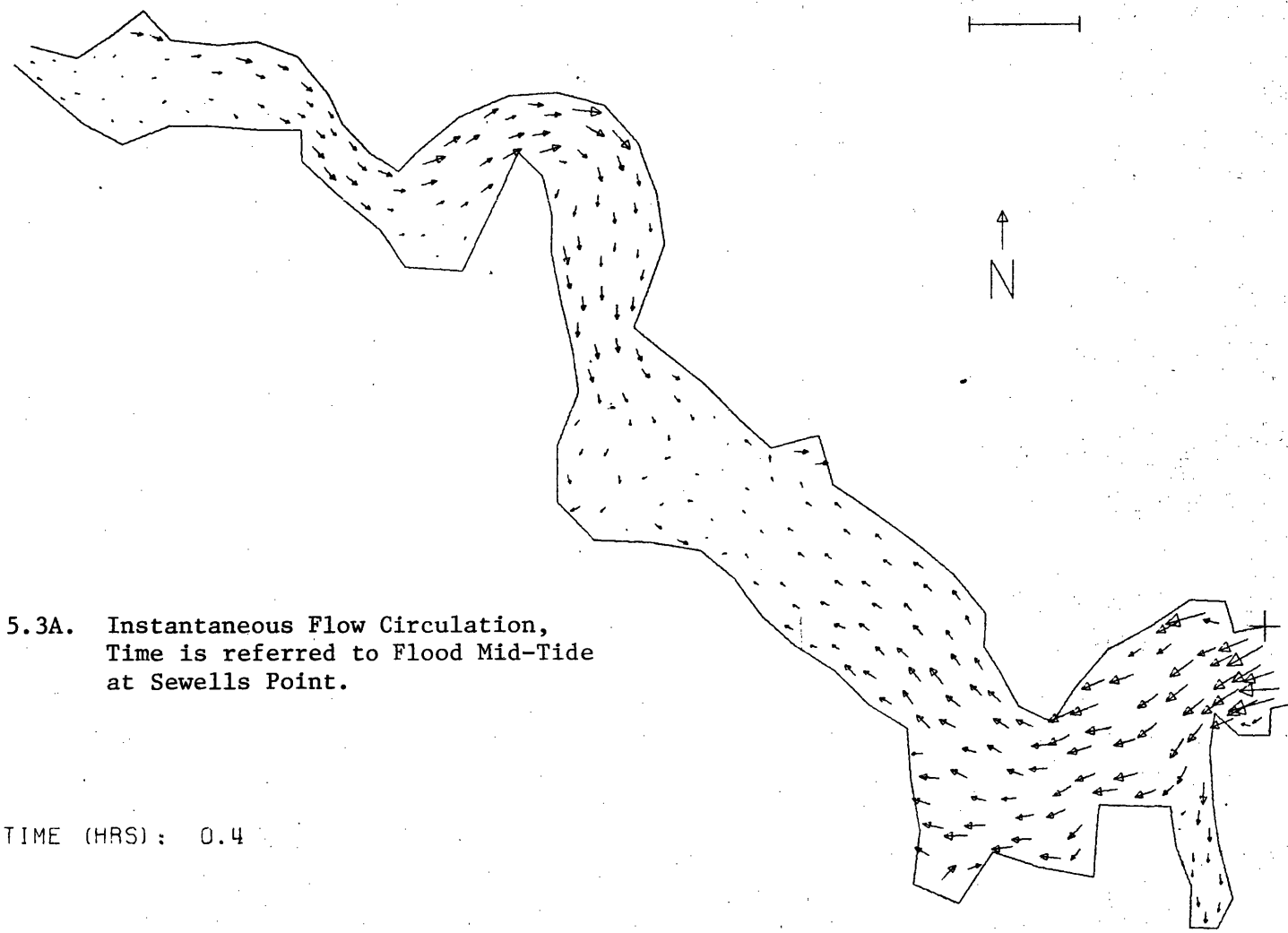
DISTANCE (KM)

SCALE (METERS/INCH) : 5000

Figure 5.3A. Instantaneous Flow Circulation,
Time is referred to Flood Mid-Tide
at Sewells Point.

TIME (HRS): 0.4

DISTANCE (KM)



JAMES RIVER
SURFACE ELEVATION IN METERS

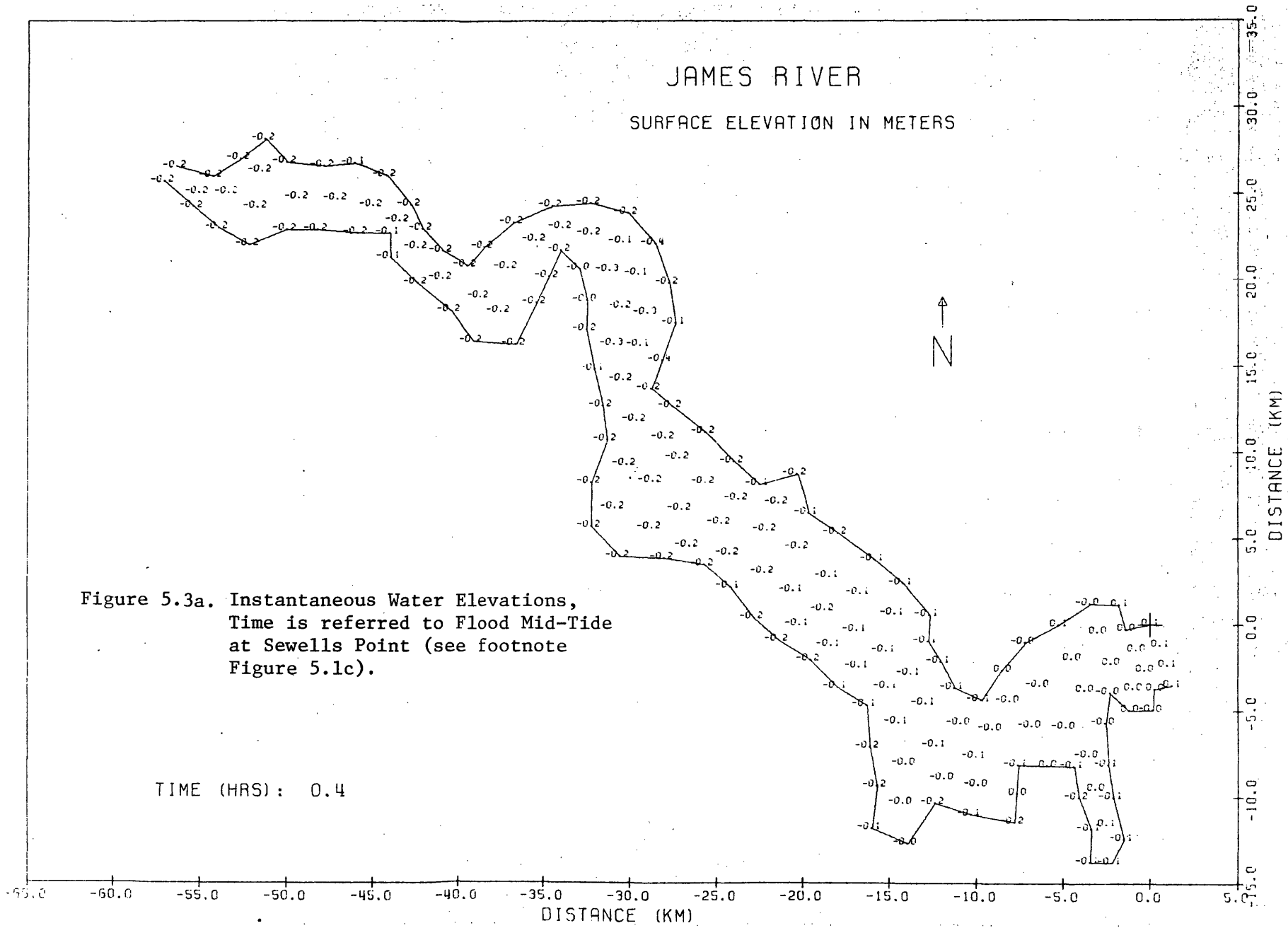


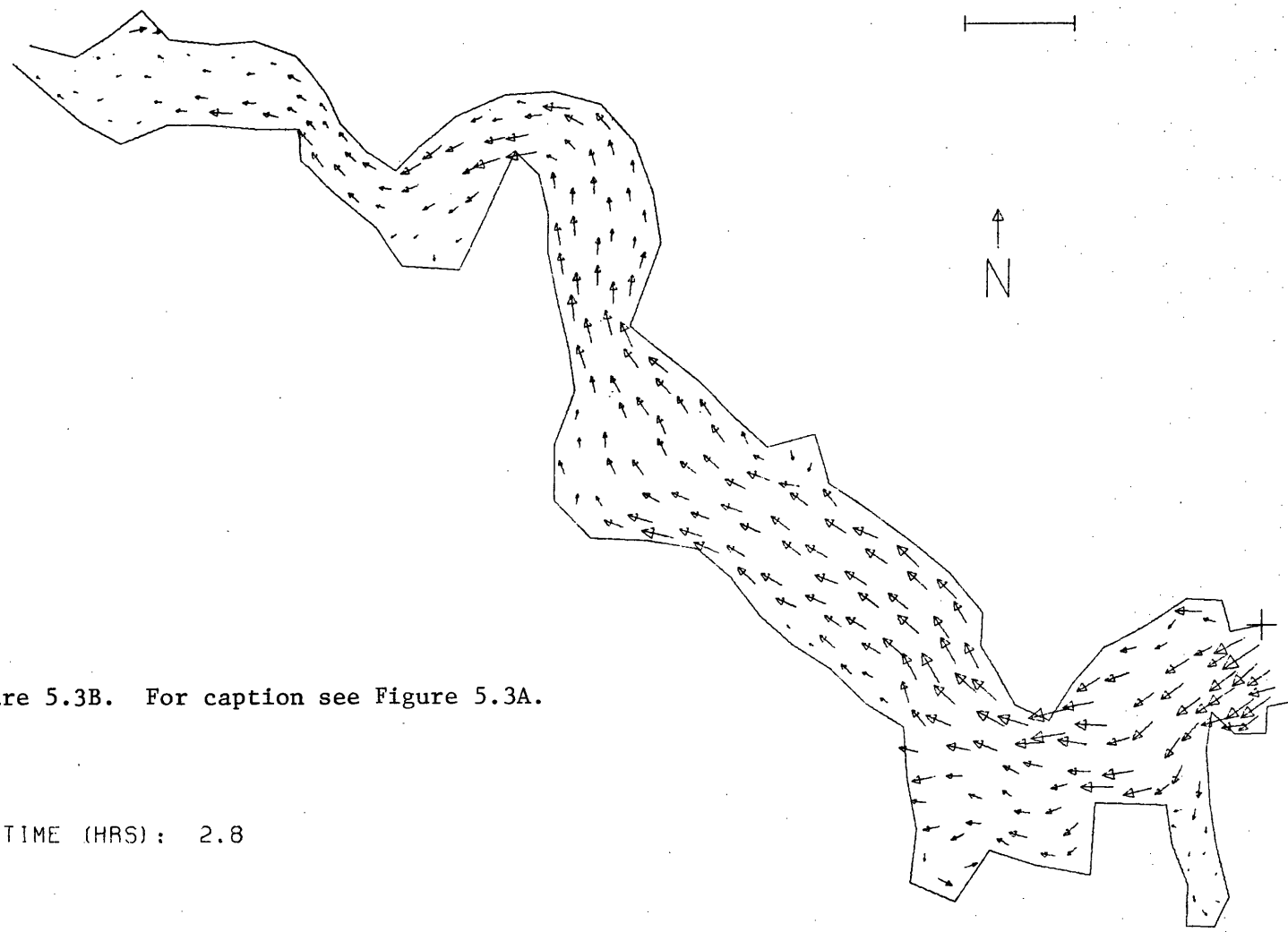
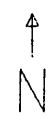
Figure 5.3a. Instantaneous Water Elevations,
Time is referred to Flood Mid-Tide
at Sewells Point (see footnote
Figure 5.1c).

TIME (HRS): 0.4

SCALE (METERS/INCH): 5000

JAMES RIVER

CURRENT VECTOR SCALE: 1 INCH = 1 METER/SEC



DISTANCE (KM)
35.0
30.0
25.0
20.0
15.0
10.0
5.0
0.0
-5.0
-10.0
-15.0

Figure 5.3B. For caption see Figure 5.3A.

TIME (HRS): 2.8

-55.0 -60.0 -65.0 -70.0 -75.0 -80.0 -85.0 -90.0
DISTANCE (KM)

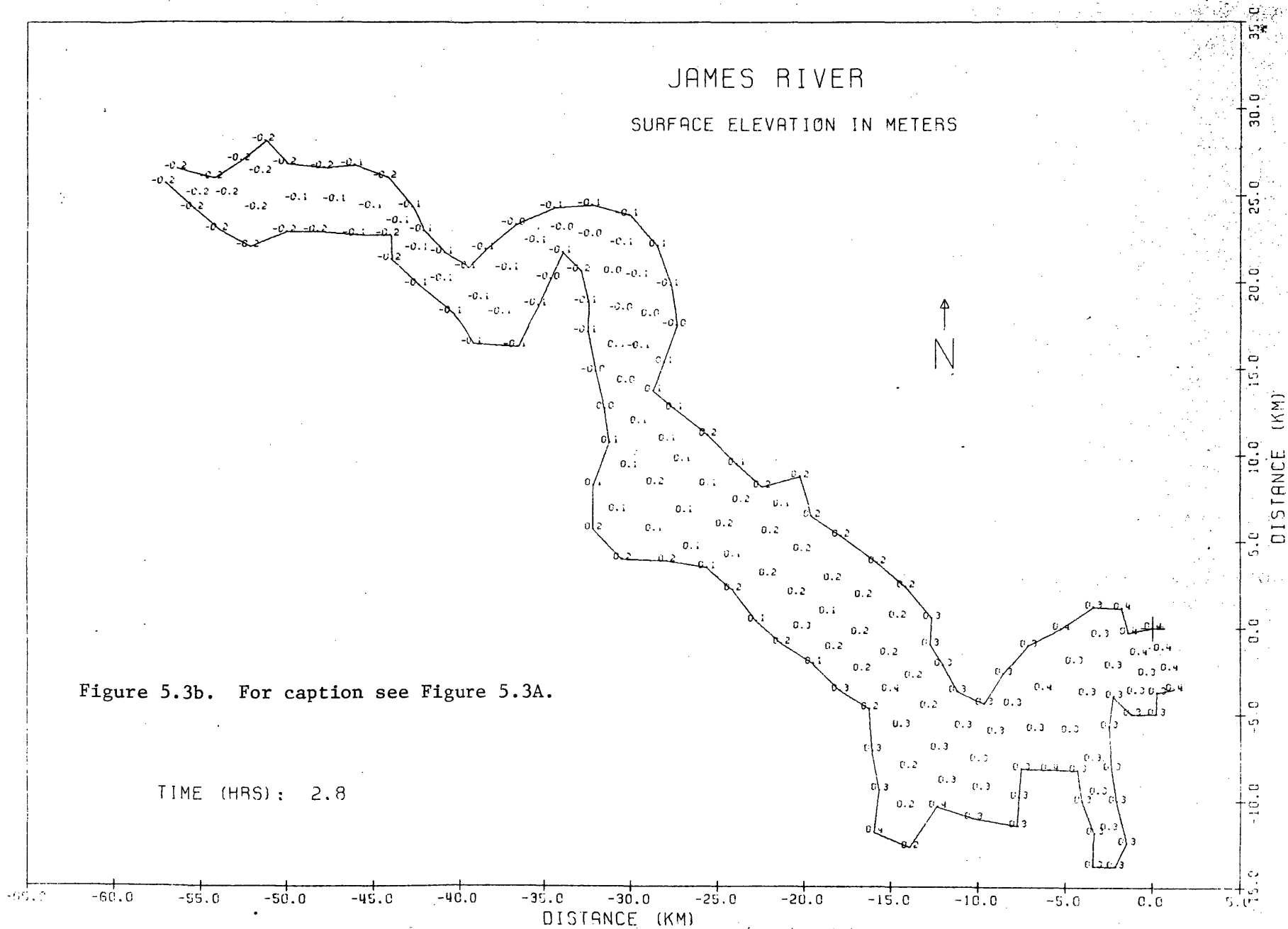
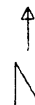


Figure 5.3b. For caption see Figure 5.3A.

JAMES RIVER

CURRENT VECTOR SCALE: 1 INCH = 1 METER/SEC

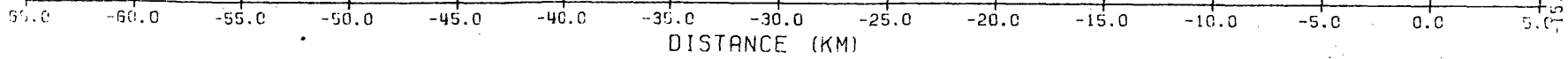


DISTANCE (KM)

09

Figure 5.3C. For caption see Figure 5.3A.

TIME (HRS): 5.2



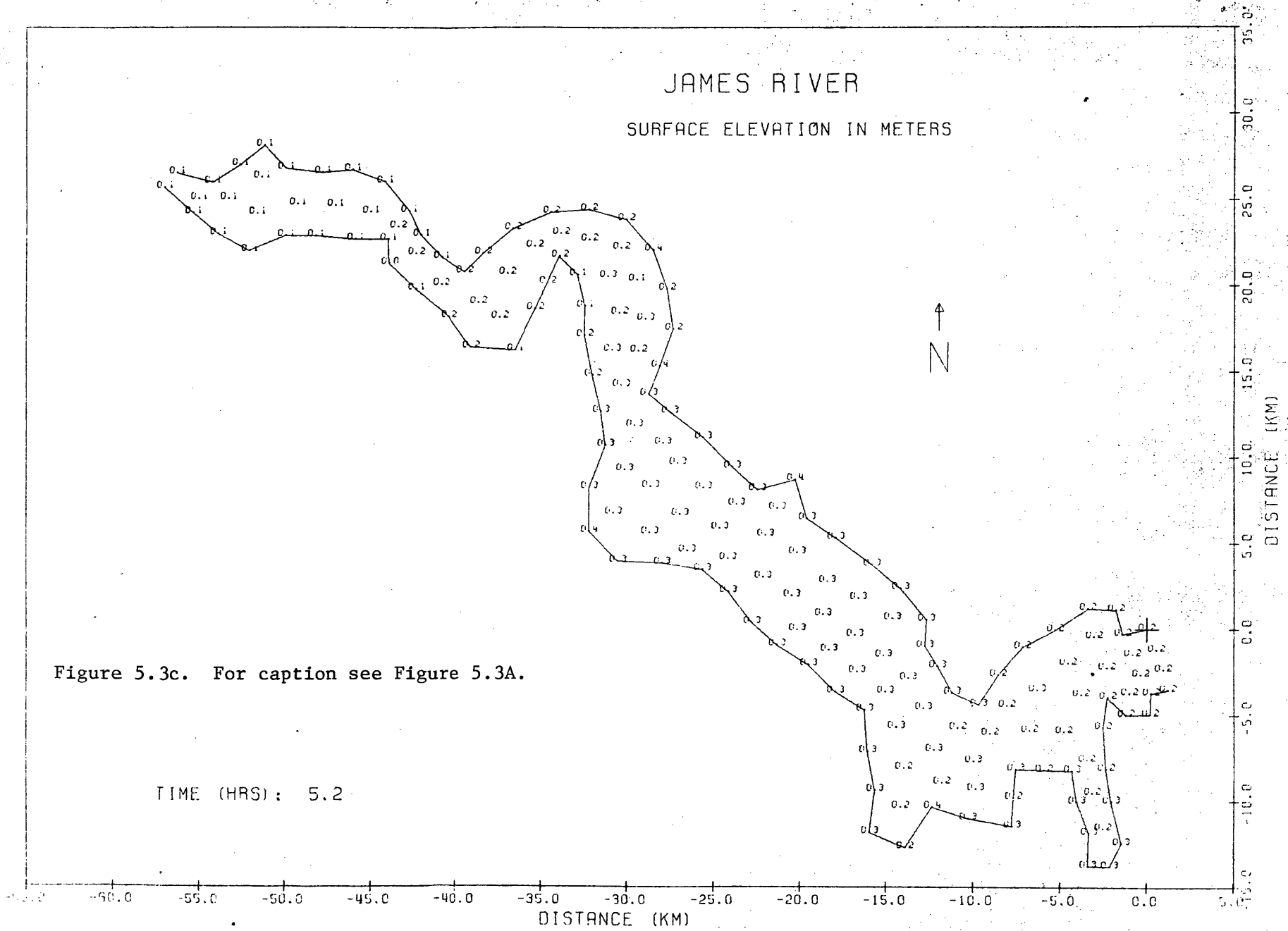


Figure 5.3c. For caption see Figure 5.3A.

JAMES RIVER

CURRENT VECTOR SCALE: 1 INCH = 1 METER/SEC



DISTANCE (KM)

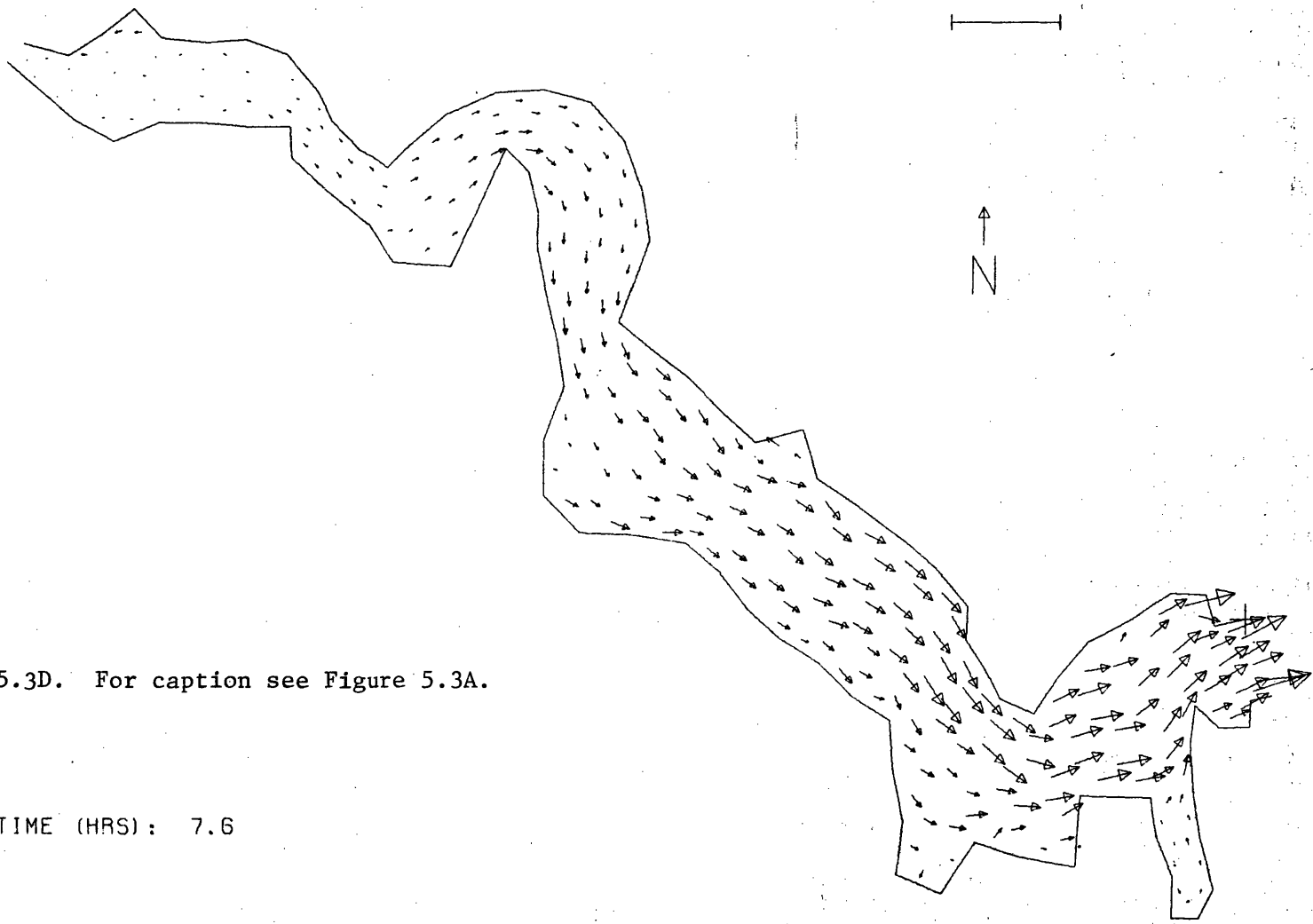
Figure 5.3D. For caption see Figure 5.3A.

TIME (HRS): 7.6

DISTANCE (KM)

-65.0 -60.0 -55.0 -50.0 -45.0 -40.0 -35.0 -30.0 -25.0 -20.0 -15.0 -10.0 -5.0 0.0 5.0

0.0 0.5 1.0 1.5 2.0 2.5 3.0 3.5 4.0 4.5 5.0 5.5 6.0 6.5 7.0 7.5 8.0 8.5 9.0 9.5 10.0



JAMES RIVER

SURFACE ELEVATION IN METERS

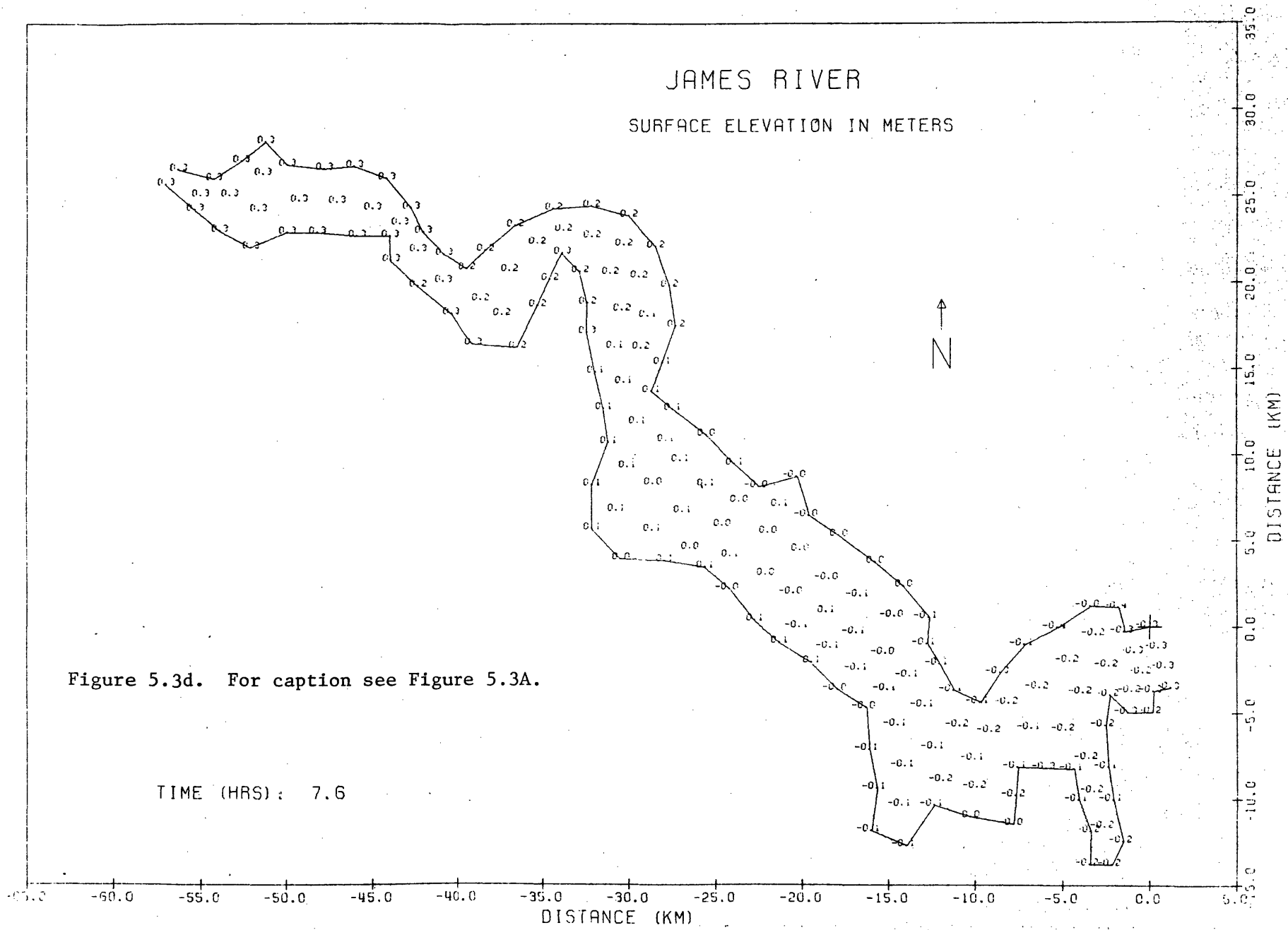
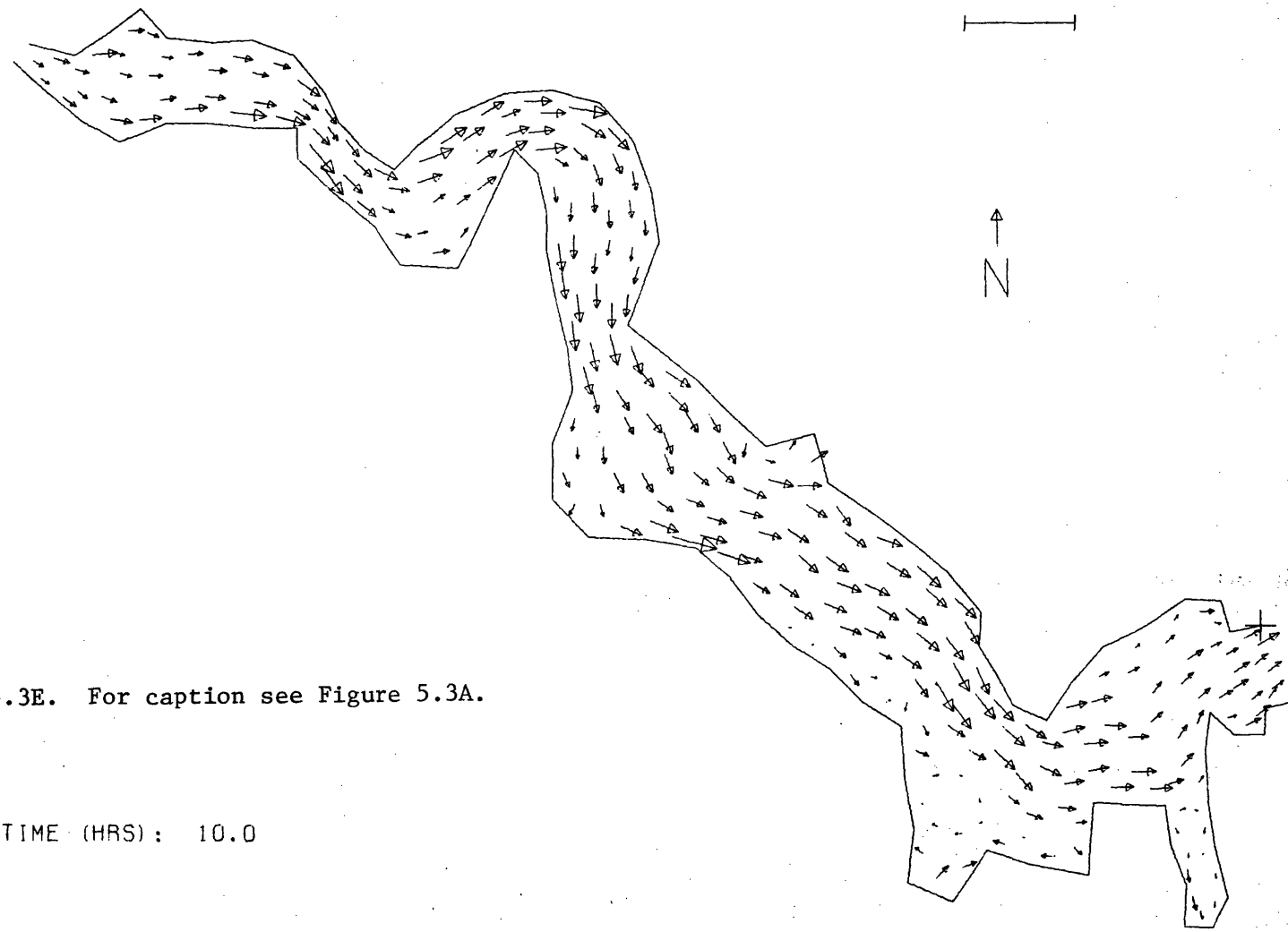
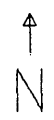


Figure 5.3d. For caption see Figure 5.3A.

TIME (HRS): 7.6

JAMES RIVER

CURRENT VECTOR SCALE: 1 INCH = 1 METER/SEC



DISTANCE (KM)
35.0
30.0
25.0
20.0
15.0
10.0
5.0
0.0
-5.0
-10.0
-15.0

-65.0 -60.0 -55.0 -50.0 -45.0 -40.0 -35.0 -30.0 -25.0 -20.0 -15.0 -10.0 -5.0 0.0
DISTANCE (KM)

Figure 5.3E. For caption see Figure 5.3A.

TIME (HRS): 10.0

JAMES RIVER

SURFACE ELEVATION IN METERS

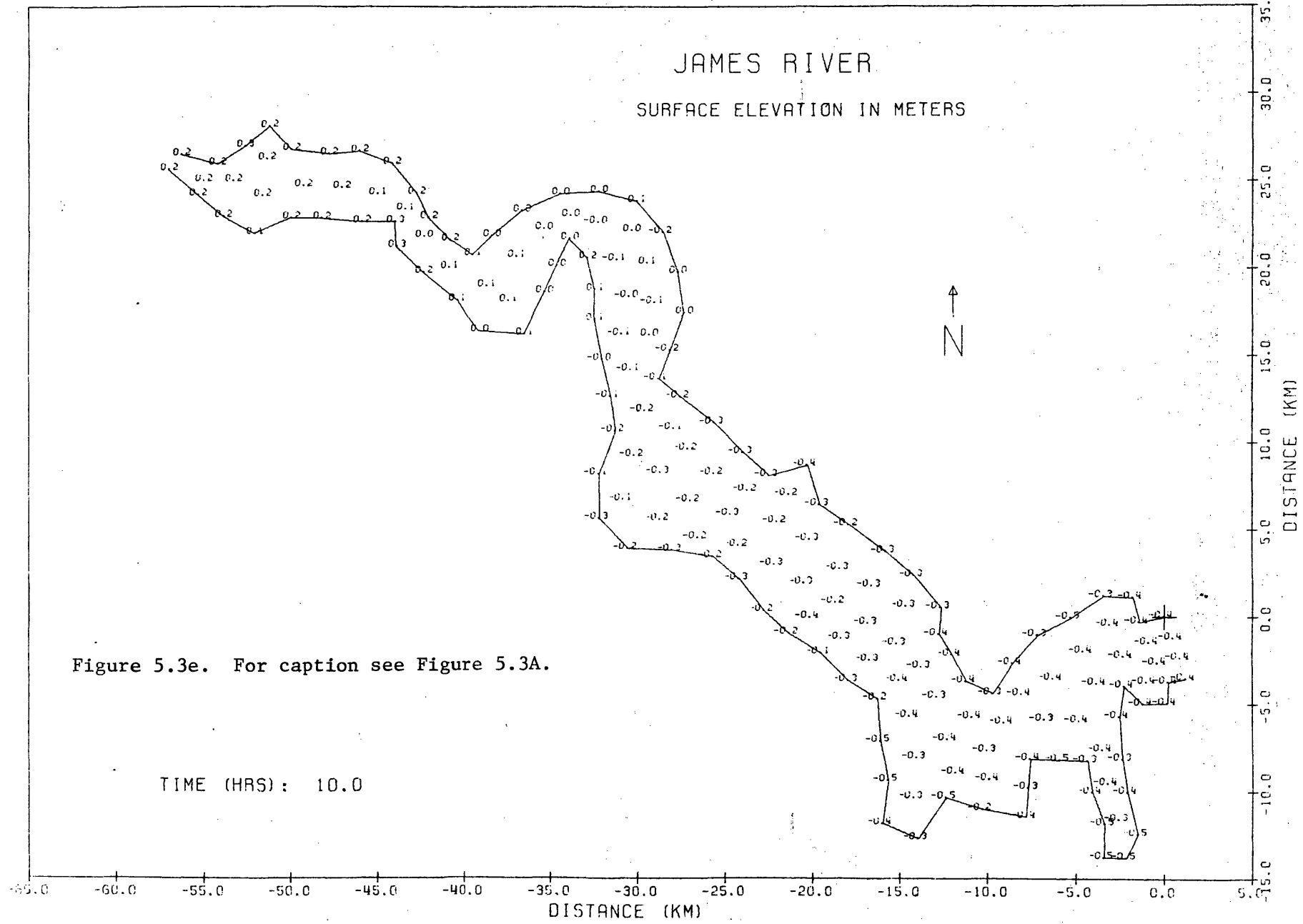
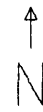


Figure 5.3e. For caption see Figure 5.3A.

JAMES RIVER

CURRENT VECTOR SCALE: 1 INCH = 1 METER/SEC



DISTANCE (KM)

35.0
30.0
25.0
20.0
15.0
10.0
5.0
0.0
-5.0
-10.0
-15.0

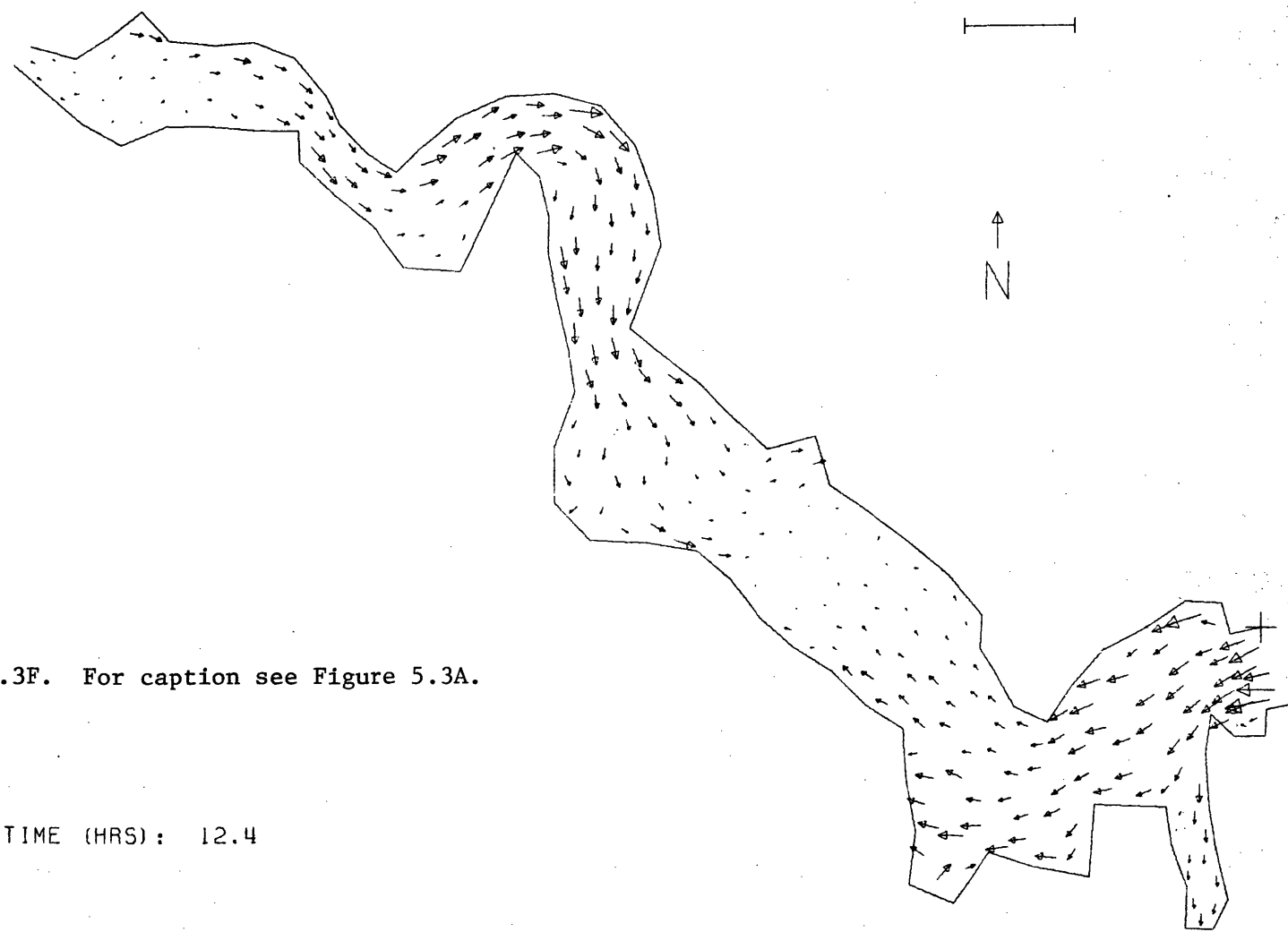


Figure 5.3F. For caption see Figure 5.3A.

TIME (HRS): 12.4

-65.0 -60.0 -55.0 -50.0 -45.0 -40.0 -35.0 -30.0 -25.0 -20.0 -15.0 -10.0 -5.0 0.0
DISTANCE (KM)

JAMES RIVER

SURFACE ELEVATION IN METERS

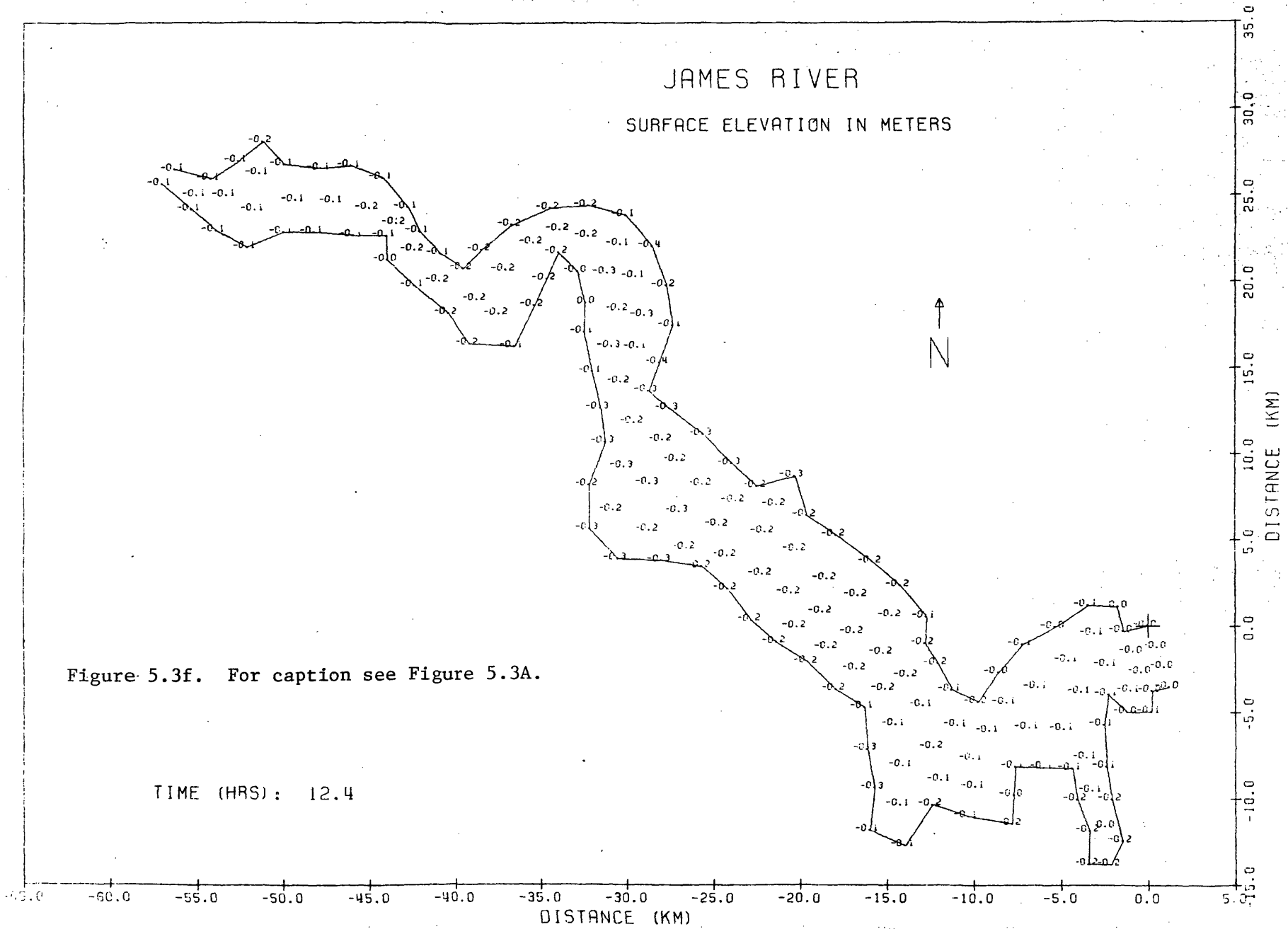


Figure 5.3f. For caption see Figure 5.3A.

TIME (HRS): 12.4

is supplied by Betz Engineering, Inc. and shown in Figure 5.4 and Tables 5.2a and b.

The non-point sources, calculated from the field data sampled by VIMS, were supplied by Malcolm Pirnie Engineers. The non-point source locations and data are shown in Figure 5.5 and Tables 5.3a and b. The values in Table 5.3b averaged over 61 days is used for calibration.

For the boundary conditions at ten locations, the concentration of each constituent is assumed to be constant and the average value of the intensive survey field data. They are tabulated in Table 5.4, see Figure 5.1a for nodal locations.

Calibration of the biogeochemical water quality system is rather difficult and time consuming since numerous parameter constants are involved. A trial and error approach by comparing the computer results with the field data is employed. The calibrated results of biogeochemical water quality and the field data at several locations show satisfactory agreement as illustrated in Figures 5.6a thru j. The calibrated physical and biogeochemical parameters are tabulated in Table 5.5. The computed result of each constituent averaged over a tidal cycle is shown in Figures 5.7a thru k.

5.4 Sensitivity

The model includes many biogeochemical water quality parameter constants. Much information can be gained by studying the sensitivity of predicted concentration distributions to one of the parameters, while keeping all others unchanged.

Several sensitivity runs were made, with typical results illustrated in Tables 5.6a thru j. Note that each set of water quality in the

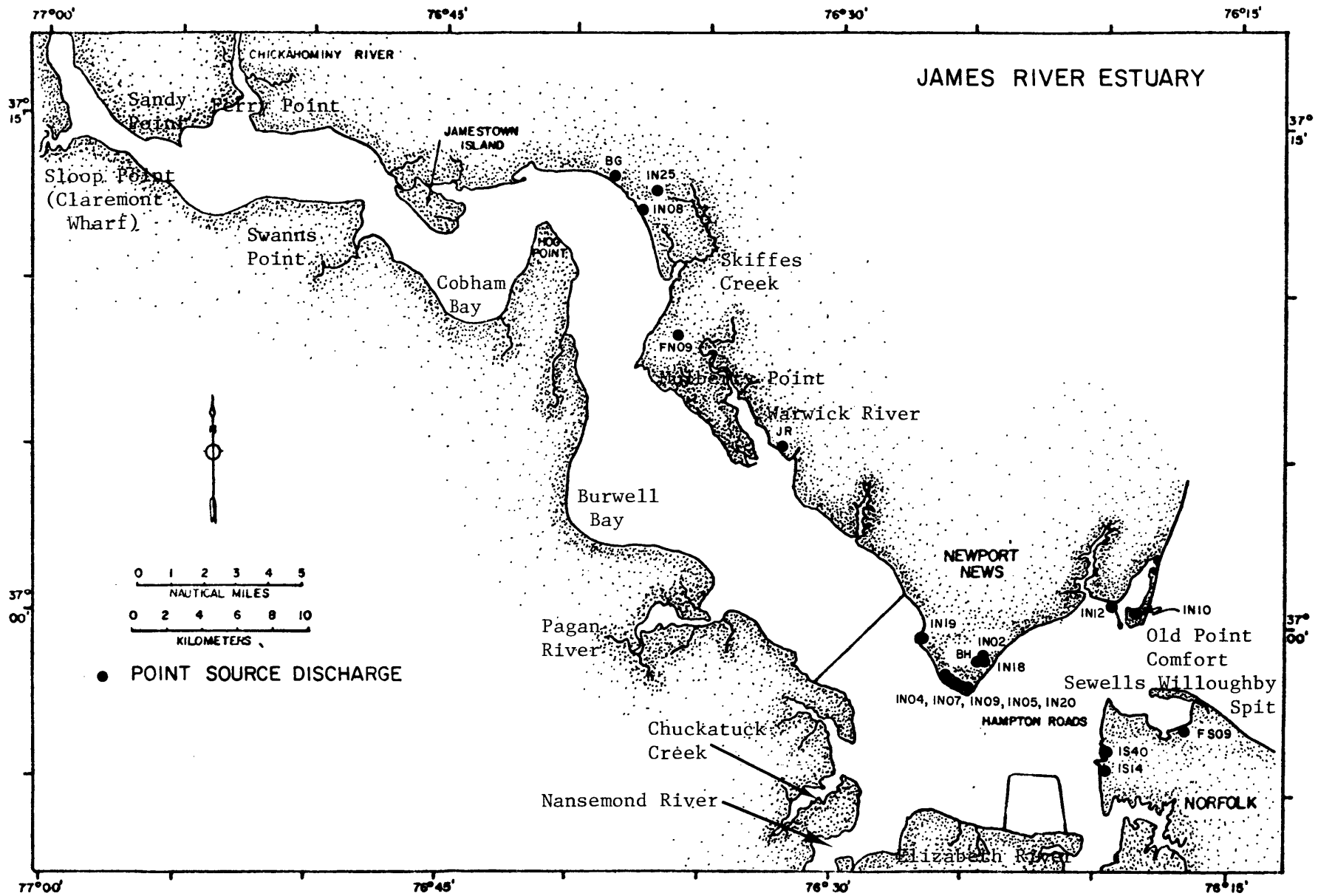


Figure 5.4. Locations of Point Waste Sources

Table 5.2a. Municipal And Industrial Waste Loads of Lower James River, 1976.

Element No	Effluent Outfall	Discharge Q (m3/s)	Coliform (bil-n/day)	Org-N	Ammon-N	Ni-Na-N	Org-P	Inorg-P	CBOD	DO deficit	Salinity
8	IN10	4.38E-5	-	4.33E-1	2.53E-2	9.84E-4	4.10E-3	1.76E-3	-	-	-
86	IN19	4.60E-3	-	1.27E 0	8.10E-2	1.80E-2	2.40E-1	6.40E-1	5.49E 0	1.96E 0	-
49	BH	9.75E-1	-	4.41E 2	1.80E 3	8.43E 0	4.25E 2	1.82E 2	2.19E 4	-	-
	IN02	2.15E-3	1.60E-1	5.56E-1	5.56E-1	3.70E-2	5.20E-2	2.00E-2	2.60E-1	-	-
	IN18	5.25E-6	2.00E-1	7.79E-1	1.99E-3	9.95E-4	3.83E-3	1.64E-4	3.40E-3	-	-
54	IN04	7.88E-6	-	-	6.40E-4	-	-	-	1.30E-2	-	-
	IN07	6.60E-5	-	-	-	-	-	-	1.70E-1	-	-
	IN09	4.10E-4	1.21E-2	-	-	-	-	-	-	-	-
	IN05	8.76E-6	-	7.30E-1	3.44E-2	3.20E-4	6.64E-3	2.85E-3	2.85E 1	-	-
	IN20	7.88E-6	-	1.45E-2	5.96E-3	0.00E 0	1.77E-4	7.50E-5	1.35E 1	-	-
128	JR	5.34E-1	-	8.91E 1	1.00E 3	2.10E 1	3.46E 2	1.48E 2	1.36E 3	-	-
152	FN09	6.13E-2	8.00E-1	5.30E 1	1.16E 2	4.24E 1	1.63E 1	3.18E 1	1.24E 2	1.21E 2	-
179	IN23	8.76E-5	-	9.10E-2	4.40E-3	2.00E-3	4.50E-3	1.90E-3	8.86E-1	-	-
185	IN08	2.62E-2	-	3.18E 1	9.53E 0	3.36E 1	4.08E 0	3.86E 0	8.74E 1	-	6.79E 2
188	BG	2.35E-1	-	2.64E 1	2.18E 2	7.16E 0	9.85E 1	4.23E 1	5.89E 2	-	-
30	IS40	8.00E-3	6.90E-1	0.00E-0	4.19E 0	6.90E-1	3.40E-1	1.10E 0	1.59E 1	3.41E 0	6.22E 1
14	FS09	1.97E-2	-	1.07E 1	1.70E-1	1.86E 1	6.80E-1	1.70E 0	6.12E 1	-	-

Table 5.2a. Continued

Industrial Sources (* "A" Industries)

IN10 - Fass Bros. Fish
IN19 - Newport News S&DD*
IN02 - Arkell Safety Bag
IN18 - Martin & Richardson
IN04 - Benson Phillips
IN07 - Chesapeake & Ohio RR
IN09 - Exxon Co.
IN05 - Blake & Bass Seafood
IN20 - GLD Dominion Crab
IN23 - Menzel Bros.
IN08 - Dow Badische*
IS40 - Sheller-Globe*

Municipal Treatment Plants

BH = Boat Harbor (HRSD)
JR = James River (HRSD)
WBG = Williamsburg (HRSD)

Federal Facilities

FN09 - Fort Eustis
FS09 - VSN Air Rework Fac.

Table 5.2b. Point Sources for the Lower James River Water Quality Model.

Element Number	Salinity (Kg/day)	Coliform (bil-n/day)	Chloroph	Org-N	Ammon-N	Ni-Na-N	Org-P (Kg/day)	Inorg-P	CBOD	DO Deficit
8	0.40	0.40	0.00	0.40	0.00	0.00	0.00	0.00	2.30	0.00
86	39.70	0.40	0.00	1.30	0.10	0.00	0.20	0.60	5.50	2.00
49	8441.30	0.30	0.00	442.10	1804.10	8.50	425.40	182.32	1997.10	395.90
54	4.30	0.00	0.00	0.70	0.00	0.00	0.00	0.00	42.20	0.20
128	4613.80	0.40	0.00	89.10	1003.40	21.00	346.40	148.50	1361.80	216.40
152	53.00	0.80	0.00	53.00	116.50	42.40	16.30	31.80	123.90	20.90
179	0.80	0.40	0.00	0.10	0.00	0.00	0.00	0.00	0.90	0.00
185	679.10	0.40	0.00	31.80	9.50	33.60	4.10	3.90	87.40	11.20
188	203.00	0.40	0.00	26.40	218.00	7.20	98.50	42.20	589.00	95.20
30	62.20	0.70	0.00	0.00	4.20	0.70	0.30	1.10	15.90	3.40
14	170.20	0.40	0.00	10.70	0.20	18.60	0.70	1.70	61.20	8.00

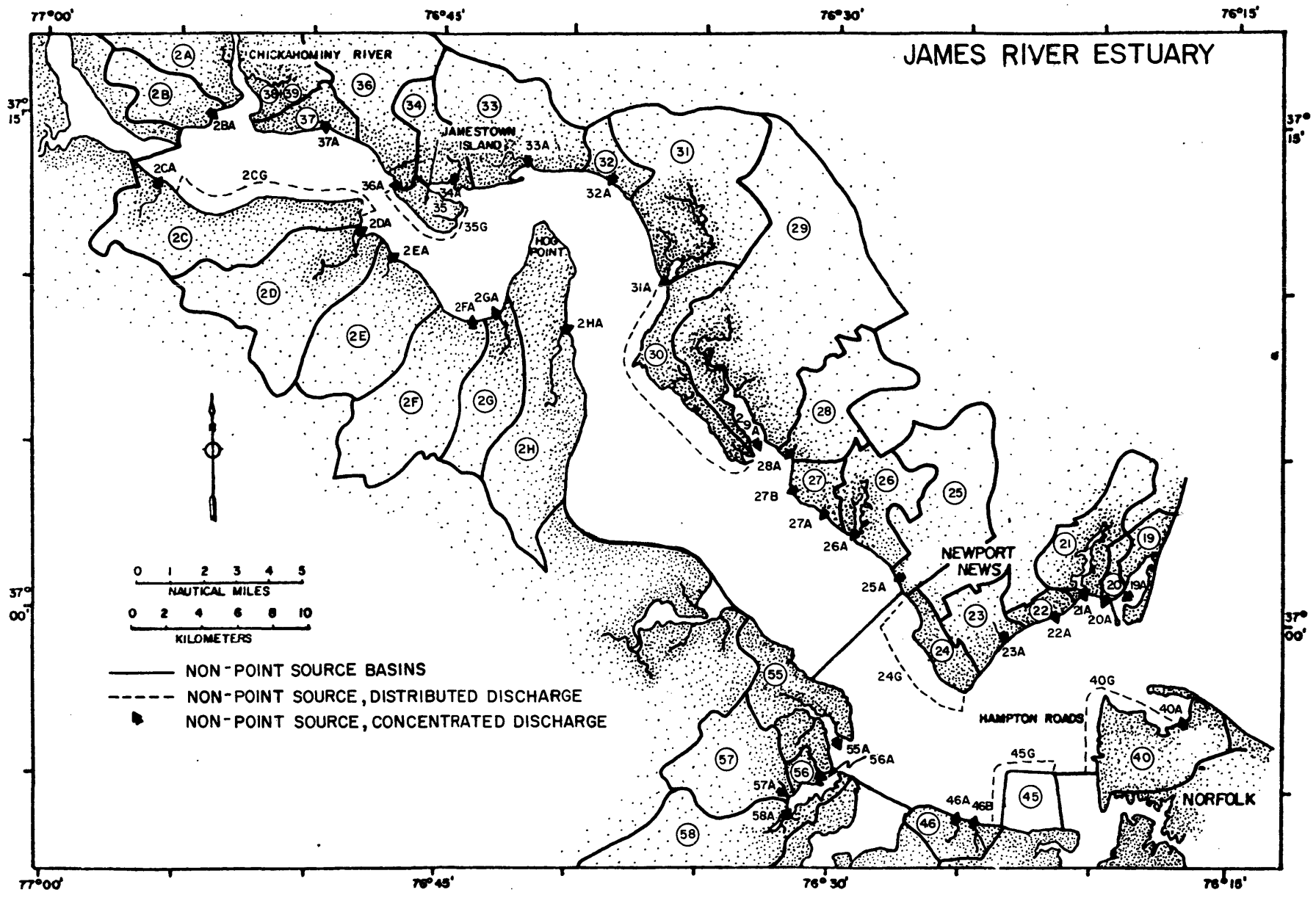


Figure 5.5. Basins of Non-point Waste Sources

Table 5.3a Total Non-point Sources of Wastes Over A Period of 61 Days from June 17 - Aug.16,1976

(If the basin number is three digits, the last two represent : 11=A,12=B,13=C, ... etc.)

Element Number	Basin No.	Contri.	Coliform (bil-n)	Org-N	Ammon-N	Ni-Na-N (kg)	Org-P	Inorg-P	BOD
8	19	1.00	22118.00	330.47	82.62	177.04	41.60	17.83	1602.57
	20	1.00							
7	21	0.77	48427.60	779.53	194.88	417.61	99.76	42.75	3918.15
18	21	0.23	11829.34	191.57	47.89	102.63	24.39	10.45	946.25
24	22	1.00	26647.00	383.82	95.95	205.62	47.63	20.41	1917.82
43	23	1.00	114007.00	989.39	247.35	530.03	125.74	53.89	5219.12
49	24	0.02	700.98	11.79	2.95	6.32	1.50	0.64	57.09
54	24	0.26	9112.71	153.29	38.32	82.12	19.48	8.35	742.17
80	24	0.27	9463.21	159.18	39.80	85.28	20.23	8.67	770.71
86	24	0.21	7360.27	123.81	30.95	66.33	15.74	6.74	599.44
93	24	0.24	8411.75	141.50	35.37	75.80	17.98	7.71	685.08
92	25	1.00	61365.00	886.01	221.50	474.65	111.77	47.90	4451.63
108	26	1.00	45321.00	676.19	169.05	362.24	84.78	36.33	3330.33
115	27	0.47	10465.46	176.57	44.14	94.59	22.24	9.53	905.21
	27	0.53							
121	28	1.00	48113.49	754.39	188.60	404.14	91.44	39.19	3675.24
	29	0.79							
128	30	0.02	118468.50	1888.06	472.01	1005.35	238.18	102.08	9511.90
135	30	0.14	1792.56	107.68	26.92	14.96	20.23	8.67	371.69
144	30	0.18	2304.72	138.44	34.61	19.23	26.00	11.14	477.89
152	30	0.18	2304.72	138.44	34.61	19.23	26.00	11.14	477.89
159	30	0.12	1536.48	92.29	23.07	12.82	17.34	7.43	318.59
167	30	0.13	1664.52	99.99	25.00	13.89	18.78	8.05	345.14
173	30	0.17	2176.68	130.75	32.69	18.16	24.56	10.53	451.34
	30	0.05							
179	31	1.00	42318.20	2213.23	553.31	307.39	352.37	151.01	7354.95
188	32	1.00	23895.00	526.14	131.53	73.07	156.22	66.95	1909.20

Table 5.3a. Continued-1

(If the basin number is three digits, the last two represent : 11=A,12=B,13=C, ... etc.)

Element Number	Basin No.	Contri.	Coliform (bil-n)	Org-N	Ammon-N	Ni-Na-N (kg)	Org-P	Inorg-P	BOD
195	33	0.50	73783.00	1641.61	410.40	228.00	431.03	184.73	6220.66
	33	0.50							
197	34	0.23	88836.25	1980.16	495.04	275.02	512.09	219.47	7480.39
	34	0.77							
200	35	0.07	50981.43	1152.51	288.13	160.07	277.34	118.86	4285.71
204	35	0.29	2420.34	79.18	19.79	11.00	24.68	10.58	282.95
210	35	0.28	2336.88	76.45	19.11	10.62	23.83	10.21	273.19
216	35	0.26	2169.96	70.99	17.75	9.86	22.12	9.48	253.68
	35	0.10							
220	36	1.00	233302.50	5100.25	1275.06	708.37	1380.83	591.78	19081.16
229	37	1.00	18089.00	686.82	171.71	95.39	151.14	64.77	2610.92
	38	1.00							
	39	1.00							
242	211	1.00	328681.00	13207.30	3301.84	1834.35	2864.02	1227.44	45846.16
243	212	1.00	14959.00	1859.29	464.82	258.23	260.37	111.59	4752.36
254	213	0.44	5864.75	845.53	211.38	117.44	120.29	51.55	2552.88
251	213	0.05	666.45	96.08	24.02	13.34	13.67	5.86	290.10
247	213	0.09	1199.61	172.95	43.24	24.02	24.60	10.54	522.18
241	213	0.10	1332.90	192.17	48.04	26.69	27.34	11.72	580.20
236	213	0.09	1199.61	172.95	43.24	24.02	24.60	10.54	522.18
232	213	0.10	1332.90	192.17	48.04	26.69	27.34	11.72	580.20
228	213	0.09	1199.61	172.95	43.24	24.02	24.60	10.54	522.18
	213	0.03							
223	214	0.39	7850.80	1149.98	287.50	159.72	168.19	72.08	3452.44
	214	0.61							
224	215	0.50	17554.03	2460.33	615.08	341.71	354.86	152.09	7079.75
219	215	0.50	5900.00	751.81	187.95	104.42	104.62	44.84	1952.07

Table 5.3a. Continued-2

(If the basin number is three digits, the last two represent : 11=A,12=B,13=C, ... etc.)

Element Number	Basin No.	Contri.	Coliform (bil-n)	Org-N	Ammon-N	Ni-Na-N (kg)	Org-P	Inorg-P	BOD
	216	1.00							
215	217	0.50	25079.50	3094.94	773.73	429.85	418.01	179.15	7457.38
209	217	0.50	10123.50	1252.64	313.16	173.98	168.44	72.19	2965.86
172	218	1.00	32161.00	4314.28	1078.57	599.20	598.52	256.51	11555.89
	55	0.10							
	56	0.10							
	57	0.10							
85	58	0.10	23312.52	714.29	178.57	99.21	174.95	74.98	2065.87
	55	0.90							
	56	0.90							
	57	0.90							
76	58	0.90	209812.00	6428.57	1607.14	892.86	1574.57	674.82	18592.79
61	46	1.00	28812.00	1044.11	261.03	145.02	125.42	53.75	3874.65
60	45	0.26	157.82	16.91	4.23	9.06	1.98	0.85	95.53
59	45	0.25	151.75	16.26	4.06	8.71	1.91	0.82	91.85
53	45	0.25	151.75	16.26	4.06	8.71	1.91	0.82	91.85
48	45	0.24	145.68	15.61	3.90	8.36	1.83	0.78	88.18
30	40	0.12	13827.81	254.43	63.61	136.30	32.04	13.73	1228.47
23	40	0.09	10370.85	190.82	47.71	102.23	24.03	10.30	921.35
17	40	0.07	8066.23	148.42	37.10	79.51	18.69	8.01	716.61
15	40	0.07	8066.23	148.42	37.10	79.51	18.69	8.01	716.61
14	40	0.66	76053.00	1399.38	349.84	749.67	176.24	75.53	6756.61

Table 5.3b. Daily Non-point Sources for the Lower James River Water Quality Model.

Element Number	Salinity (kg/day)	Coliform (bil-n/day)	Chloroph	Org-N	Ammon-N	Ni-Na-N	Org-P (kg/day)	Inorg-P	CBOD	DO Deficit
8	432.00	362.59	0.02	5.42	1.35	2.90	0.68	0.29	26.27	4.32
7	1036.80	793.90	0.05	12.78	3.19	6.85	1.64	0.70	64.23	10.36
18	259.20	193.92	0.01	3.14	0.79	1.68	0.40	0.17	15.51	2.59
24	518.40	436.84	0.02	6.29	1.57	3.37	0.78	0.33	31.44	5.18
43	1123.20	1868.97	0.05	16.22	4.05	8.69	2.06	0.88	85.56	11.23
49	0.00	11.49	0.00	0.19	0.05	0.10	0.02	0.01	0.94	0.00
54	172.80	149.39	0.01	2.51	0.63	1.35	0.32	0.14	12.17	1.72
80	172.80	155.13	0.01	2.61	0.65	1.40	0.33	0.14	12.63	1.72
86	86.40	120.66	0.00	2.03	0.51	1.09	0.26	0.11	9.83	0.86
93	172.80	137.90	0.01	2.32	0.58	1.24	0.29	0.13	11.23	1.72
92	1382.40	1005.98	0.06	14.52	3.63	7.78	1.83	0.79	72.98	13.82
108	950.40	742.97	0.04	11.09	2.77	5.94	1.39	0.60	54.60	9.50
115	259.20	171.56	0.01	2.89	0.72	1.55	0.36	0.16	14.84	2.59
121	1209.60	788.75	0.06	12.37	3.09	6.63	1.50	0.64	60.25	12.09
128	4320.00	1942.11	0.21	30.95	7.74	16.48	3.90	1.67	155.93	43.20
135	86.40	29.39	0.00	1.77	0.44	0.25	0.33	0.14	6.09	0.86
144	86.40	37.78	0.00	2.27	0.57	0.32	0.43	0.18	7.83	0.86
152	86.40	37.78	0.00	2.27	0.57	0.32	0.43	0.18	7.83	0.86
159	86.40	25.19	0.00	1.51	0.38	0.21	0.28	0.12	5.22	0.86
167	86.40	27.29	0.00	1.64	0.41	0.23	0.31	0.13	5.66	0.86
173	86.40	35.68	0.00	2.14	0.54	0.30	0.40	0.17	7.40	0.86
179	1728.00	693.74	0.08	36.28	9.07	5.04	5.78	2.48	120.57	17.28
188	259.20	391.72	0.01	8.63	2.16	1.20	2.56	1.10	31.30	2.59
195	1036.80	1209.56	0.05	26.91	6.73	3.74	7.07	3.03	101.98	10.36
197	1209.60	1456.33	0.06	32.46	8.12	4.51	8.39	3.60	122.63	12.09
200	604.80	835.76	0.03	18.89	4.72	2.62	4.55	1.95	70.26	6.04
204	0.00	39.68	0.00	1.30	0.32	0.18	0.40	0.17	4.64	0.00
210	0.00	38.31	0.00	1.25	0.31	0.17	0.39	0.17	4.48	0.00
216	0.00	35.57	0.00	1.16	0.29	0.16	0.36	0.16	4.16	0.00
220	2592.00	3824.63	0.12	83.61	20.90	11.61	22.64	9.70	312.81	25.92
229	604.80	296.54	0.03	11.26	2.81	1.56	2.48	1.06	42.80	6.04
242	9590.40	5388.21	0.47	216.51	54.13	30.07	46.95	20.12	751.58	95.90

Table 5.3b. Continued

Element Number	Salinity (kg/day)	Coliform (bil-n/day)	Chloroph	Org-N	Ammon-N	Ni-Na-N (kg/day)	Org-P	Inorg-P	CBOD	DO Deficit
243	1123.20	245.23	0.05	30.48	7.62	4.23	4.27	1.83	77.91	11.23
254	691.20	96.14	0.03	13.86	3.47	1.93	1.97	0.85	41.85	6.91
251	86.40	10.93	0.00	1.58	0.39	0.22	0.22	0.10	4.76	0.86
247	172.80	19.67	0.01	2.84	0.71	0.39	0.40	0.17	8.56	1.72
241	172.80	21.85	0.01	3.15	0.79	0.44	0.45	0.19	9.51	1.72
236	172.80	19.67	0.01	2.84	0.71	0.39	0.40	0.17	8.56	1.72
232	172.80	21.85	0.01	3.15	0.79	0.44	0.45	0.19	9.51	1.72
228	172.80	19.67	0.01	2.84	0.71	0.39	0.40	0.17	8.56	1.72
223	950.40	128.70	0.04	18.85	4.71	2.62	2.76	1.18	56.60	9.50
224	1900.80	287.77	0.09	40.33	10.08	5.60	5.82	2.49	116.06	19.00
219	518.40	96.72	0.02	12.32	3.08	1.71	1.72	0.74	32.00	5.18
215	1814.40	411.14	0.09	50.74	12.68	7.05	6.85	2.94	122.25	18.14
209	691.20	165.96	0.03	20.54	5.13	2.85	2.76	1.18	48.62	6.91
172	3196.80	527.23	0.15	70.73	17.68	9.82	9.81	4.21	189.44	31.96
85	259.20	382.17	0.01	11.71	2.93	1.63	2.87	1.23	33.87	2.59
76	2419.20	3439.54	0.12	105.39	26.35	14.64	25.81	11.06	304.80	24.19
61	691.20	472.33	0.03	17.12	4.28	2.38	2.06	0.88	63.52	6.91
60	172.80	2.59	0.01	0.28	0.07	0.15	0.03	0.01	1.57	1.72
59	172.80	2.49	0.01	0.27	0.07	0.14	0.03	0.01	1.51	1.72
53	172.80	2.49	0.01	0.27	0.07	0.14	0.03	0.01	1.51	1.72
48	172.80	2.39	0.01	0.26	0.06	0.14	0.03	0.01	1.45	1.72
30	345.60	226.69	0.01	4.17	1.04	2.23	0.53	0.23	20.14	3.45
23	259.20	170.01	0.01	3.13	0.78	1.68	0.39	0.17	15.10	2.59
17	172.80	132.23	0.01	2.43	0.61	1.30	0.31	0.13	11.75	1.72
15	172.80	132.23	0.01	2.43	0.61	1.30	0.31	0.13	11.75	1.72
14	1814.40	1246.77	0.09	22.94	5.74	12.29	2.89	1.24	110.76	18.14

Table 5.4. Values of Boundary Condition for Biogeochemical Water Quality Model.

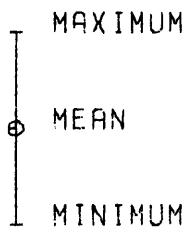
Node Number	Salinity (ppm)	Coliform (MPN/100ml)	Chloroph (ppm)	Org-N (ppm)	Ammon-N (ppm)	Ni-Na-N (ppm)	Org-P (ppm)	Inorg-P (ppm)	CBOD (ppm)	DO Deficit (ppm)
1	20.94	3.82	4.75	0.34	0.09	0.05	0.08	0.02	1.77	1.24
2	21.33	4.63	4.94	0.19	0.19	0.06	0.09	0.03	1.68	0.78
3	21.72	5.44	5.13	0.23	0.09	0.06	0.10	0.02	1.58	0.32
4	21.65	5.54	5.59	0.25	0.10	0.08	0.09	0.03	1.75	0.53
23	22.87	246.89	9.25	0.25	0.23	0.08	0.10	0.05	2.77	0.60
58	18.69	3.30	9.81	0.29	0.06	0.05	0.13	0.02	2.22	0.36
83	11.08	11.32	14.86	0.22	0.21	0.68	0.19	0.05	3.17	1.22
88	11.08	11.32	14.86	0.22	0.21	0.68	0.19	0.05	3.17	1.22
178	0.17	5.14	3.30	0.22	0.10	0.64	0.24	0.02	1.76	1.10
179	0.17	5.14	3.30	0.22	0.10	0.64	0.24	0.02	1.76	1.10

Note: Nodal points shown in Figure 5.1a

JAMES RIVER WATER QUALITY

MEANING OF SYMBOLS

INTENSIVE SURVEYS



SLACK WATER SURVEYS

- * SLACK BEFORE EBB
- x SLACK BEFORE FLOOD

MODEL PROJECTIONS



Showing the values at nodal numbers (—●—): 2,18,26,47, 48,49,67,81,92,112,136,149, 156,173 and 178.

Figure 5.6. Meaning of symbols for the Figures 5.6a through 5.6j.

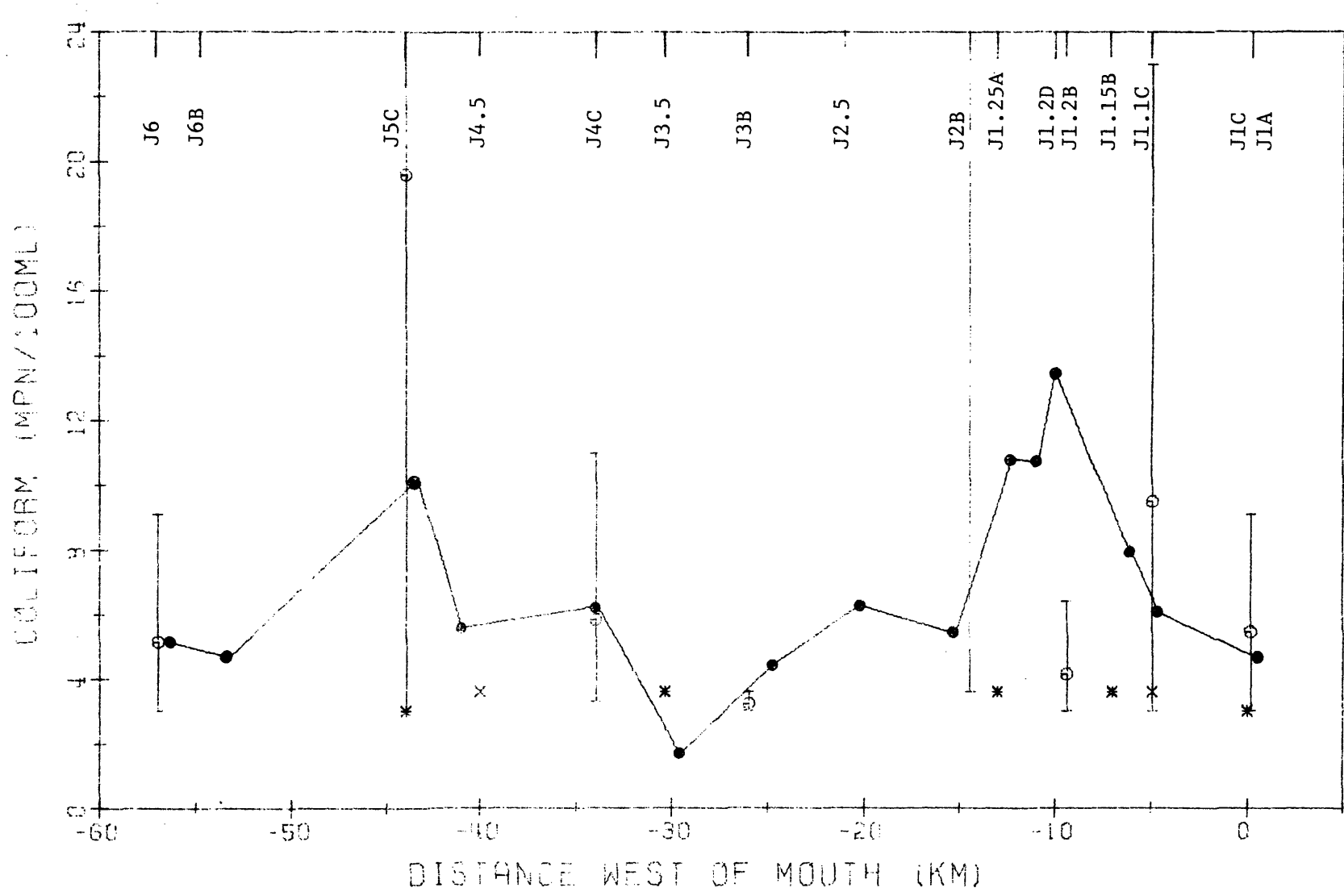


Figure 5.6b. Field data and calibrated results of fecal coliform at some locations along the lower James River. See Figure 5.6 for the meaning of the symbols and Figure 5.1a for the field stations and nodal points.

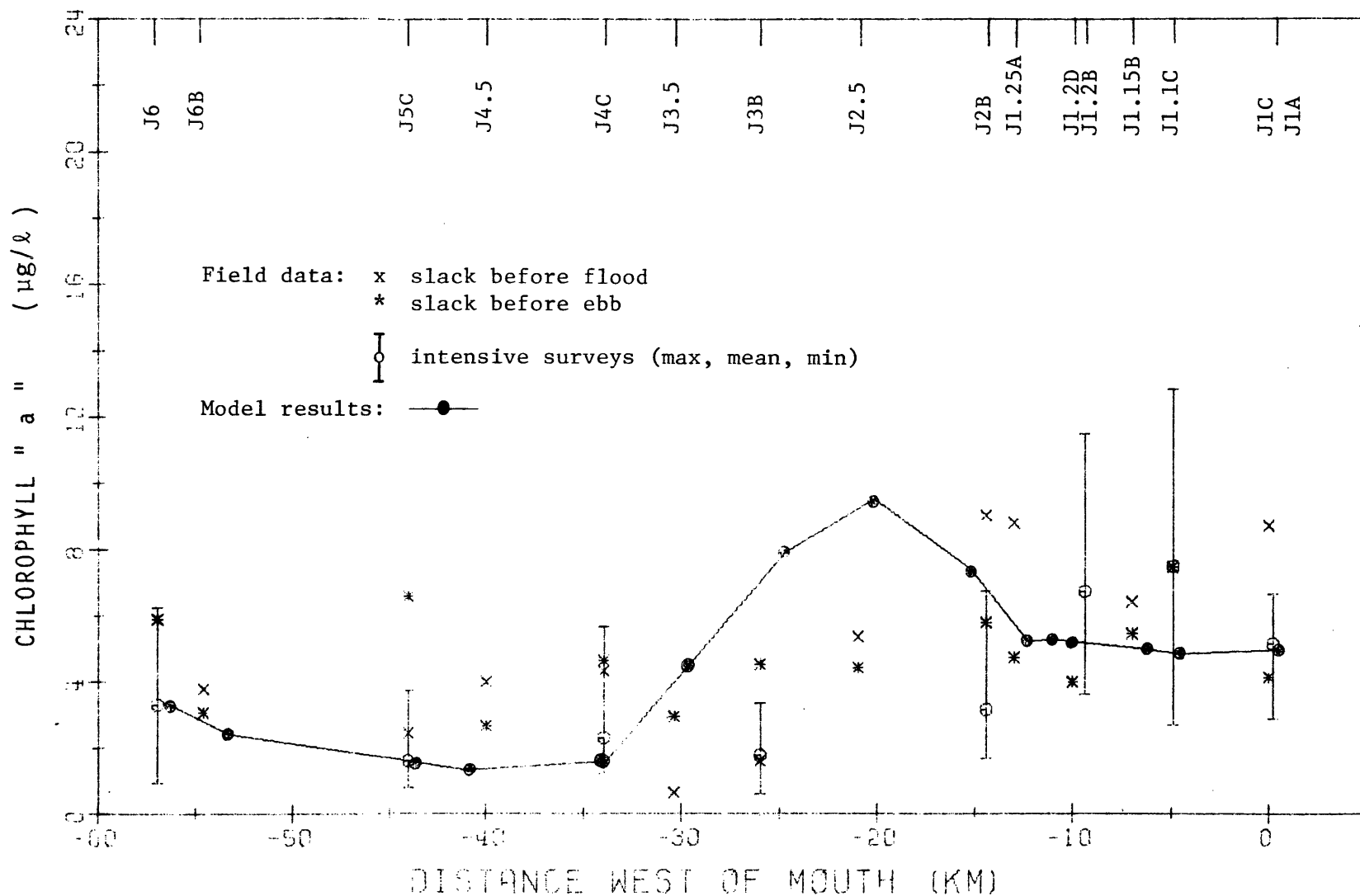


Figure 5.6c. Field data and calibrated results of chlorophyll 'a' at some locations along the lower James River. See Figure 5.6 for the meaning of the symbols and Figure 5.1a for the field stations and nodal points.

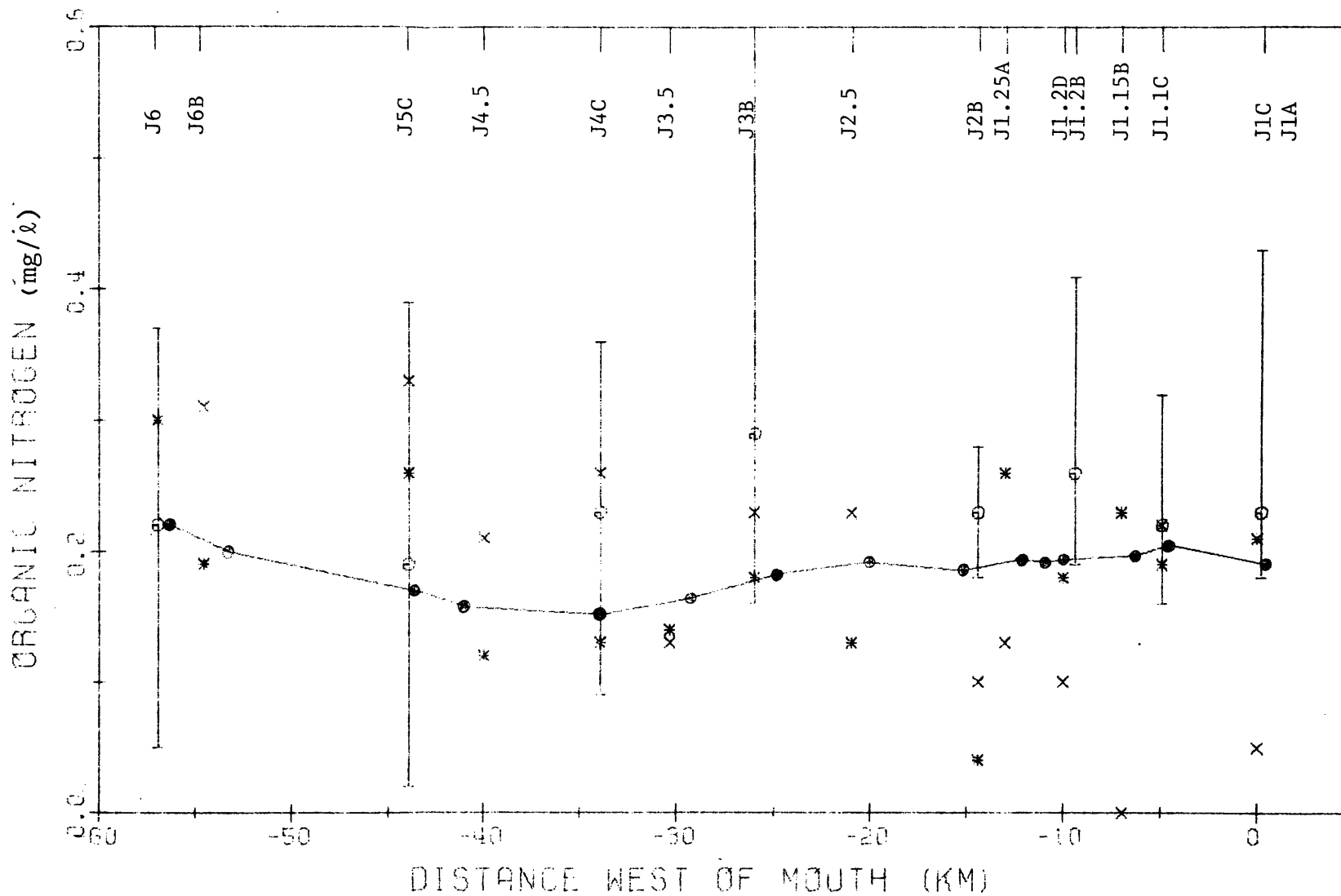


Figure 5.6d. Field data and calibrated results of organic-N at some locations along the lower James River. See Figure 5.6 for the meaning of the symbols and Figure 5.1a for the field stations and nodal points.

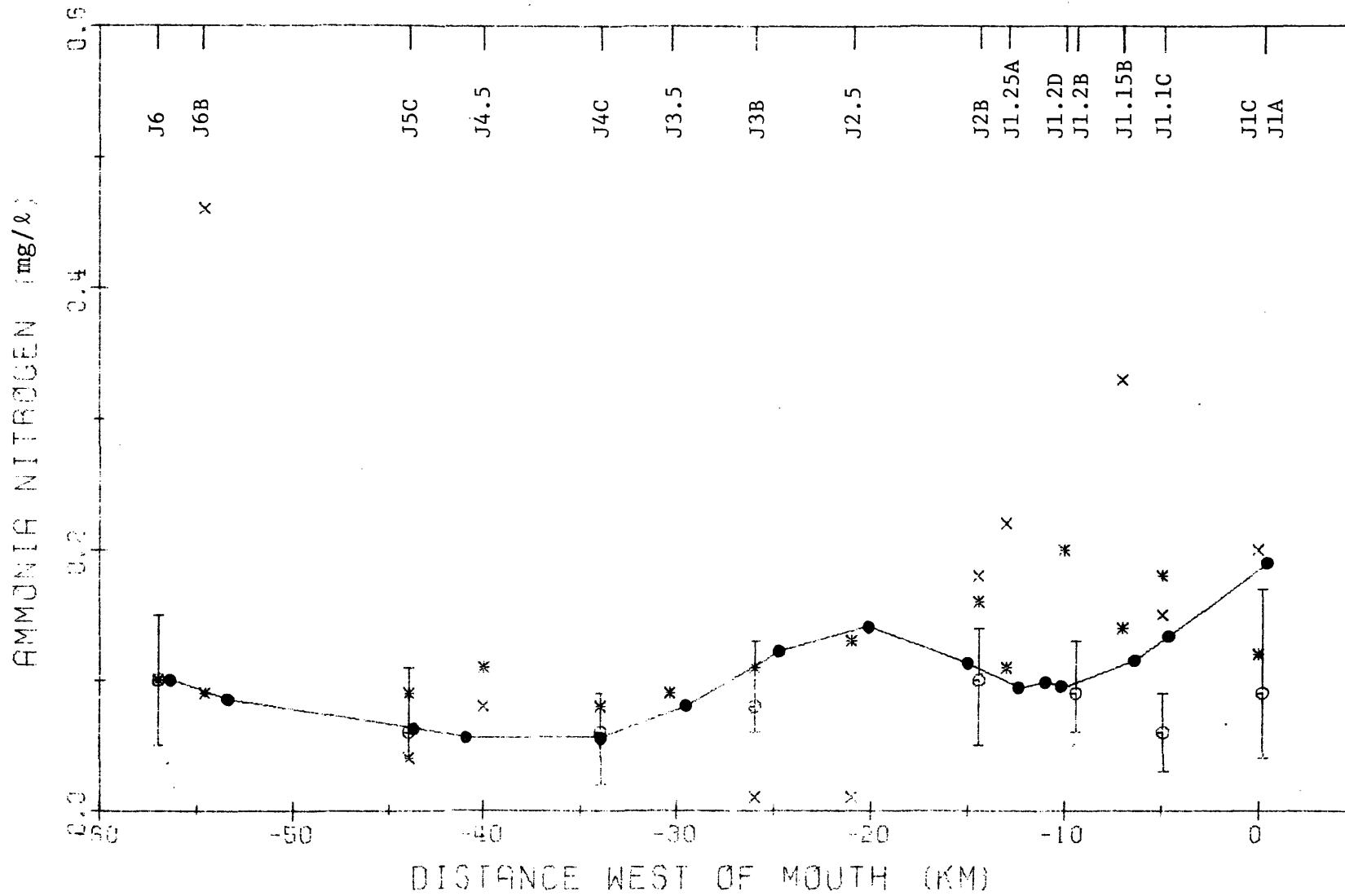


Figure 5.6e. Field data and calibrated results of ammonia-N at some locations along the lower James River. See Figure 5.6 for the meaning of the symbols and Figure 5.1a for the field stations and nodal points.

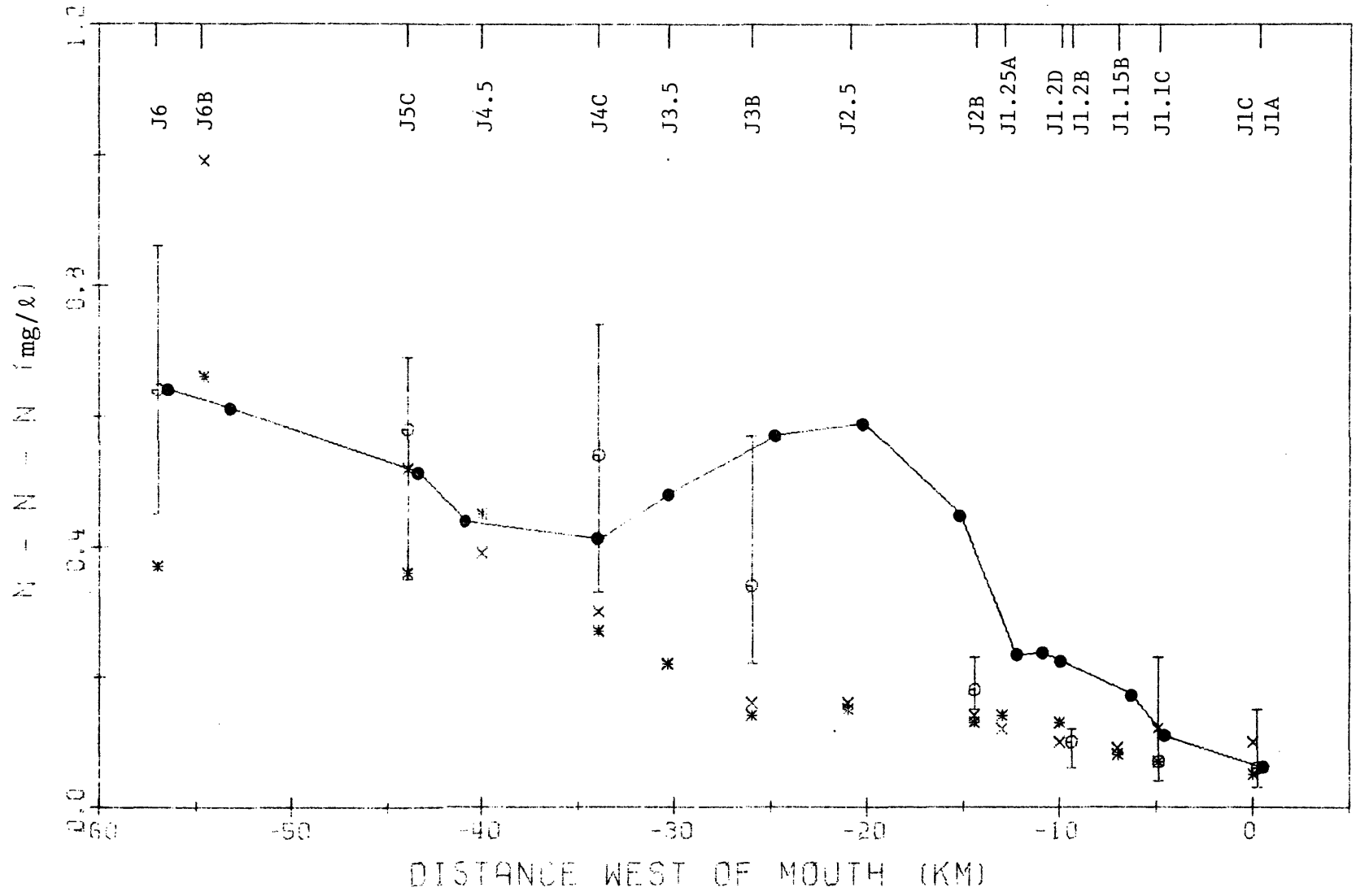


Figure 5.6f. Field data and calibrated results of nitrite-nitrate-N at some locations along the lower James River. See Figure 5.6 for the meaning of the symbols and Figure 5.1a for the field stations and nodal points.

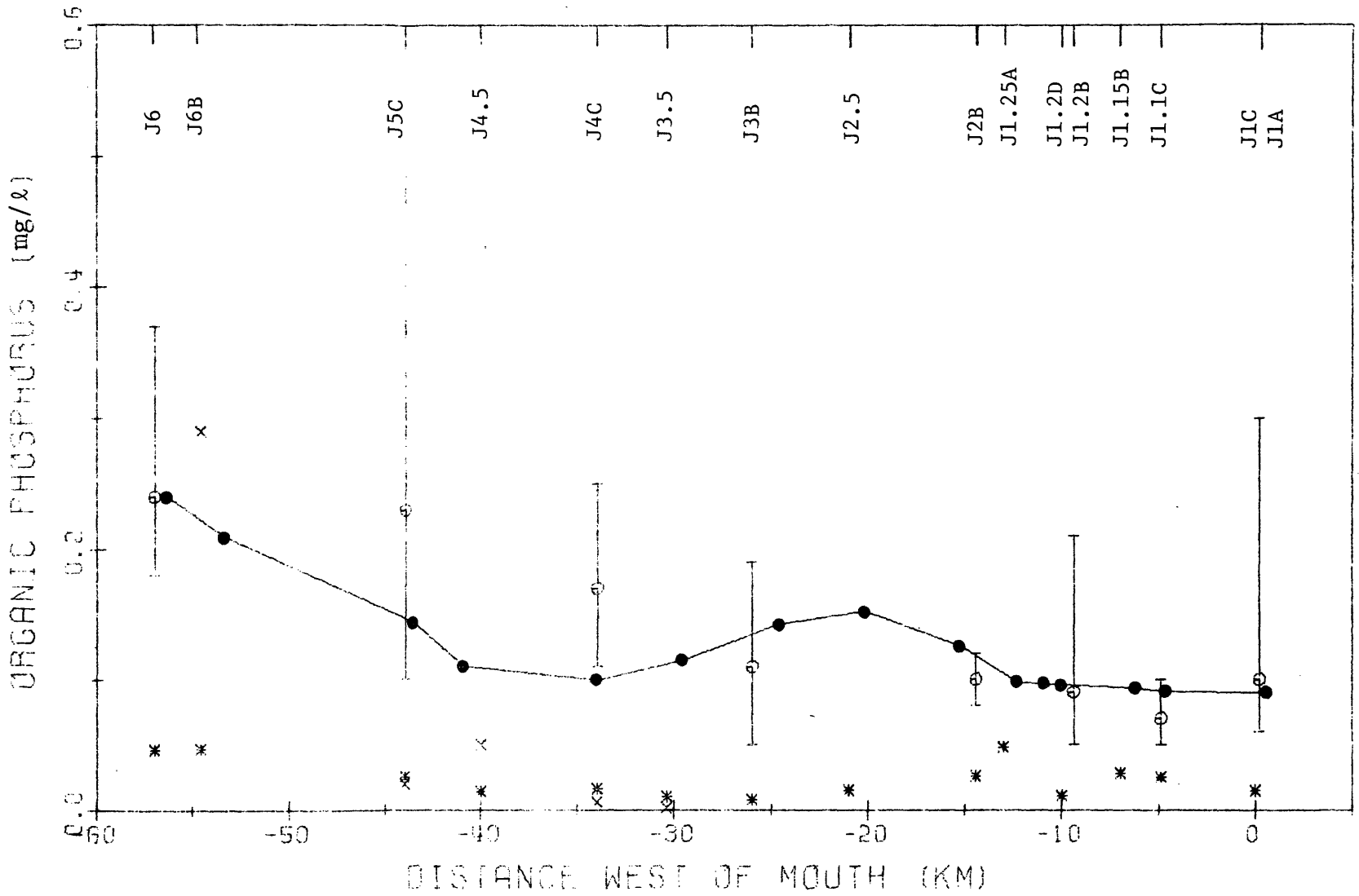


Figure 5.6g. Field data and calibrated results of organic phosphorus at some locations along the lower James River. See Figure 5.6 for the meaning of the symbols and Figure 5.1a for the field stations and nodal points.

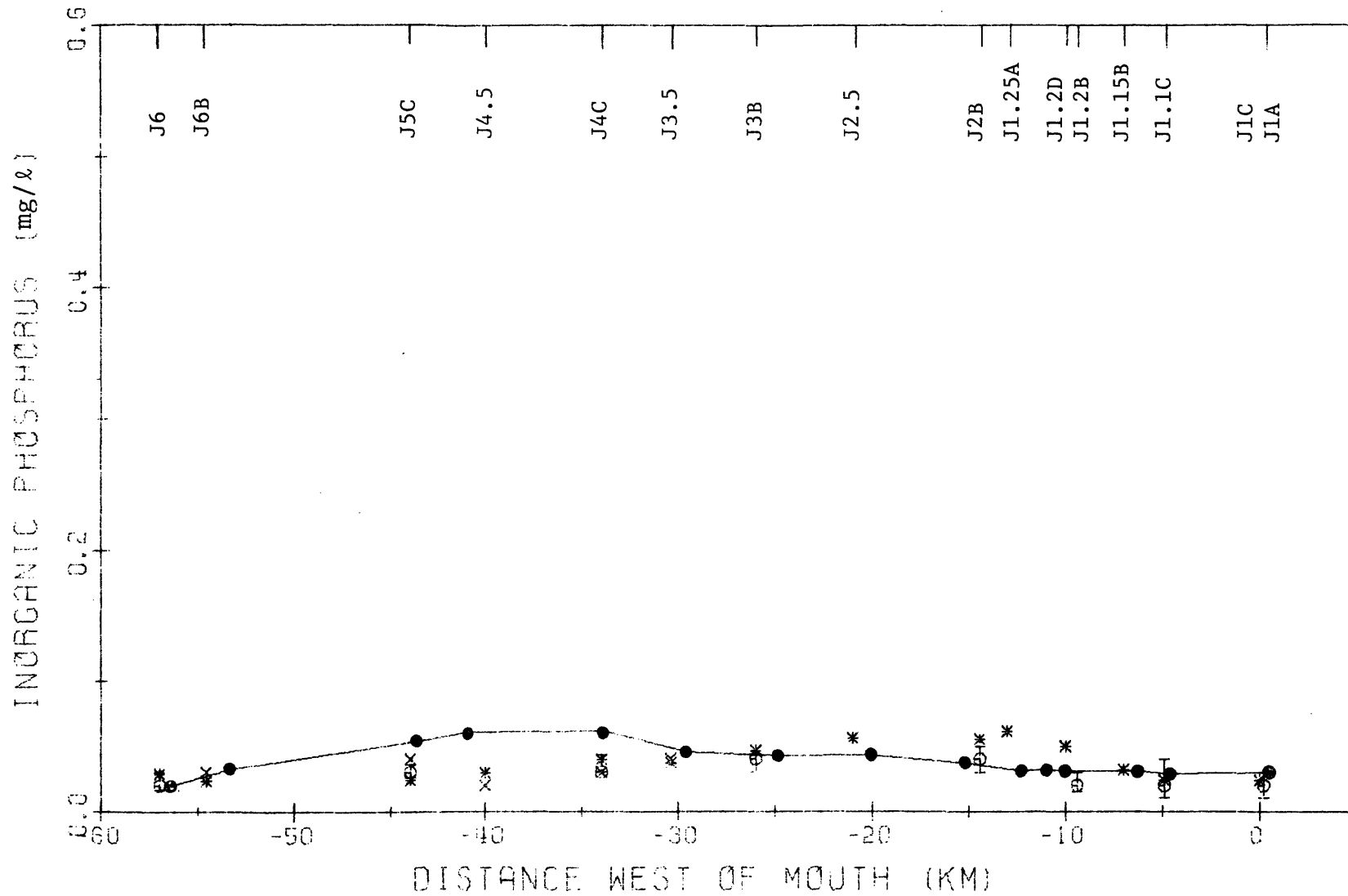


Figure 5.6h. Field data and calibrated results of inorganic phosphorus at some locations along the lower James River. See Figure 5.6 for the meaning of the symbols and Figure 5.1a for the field stations and nodal points.

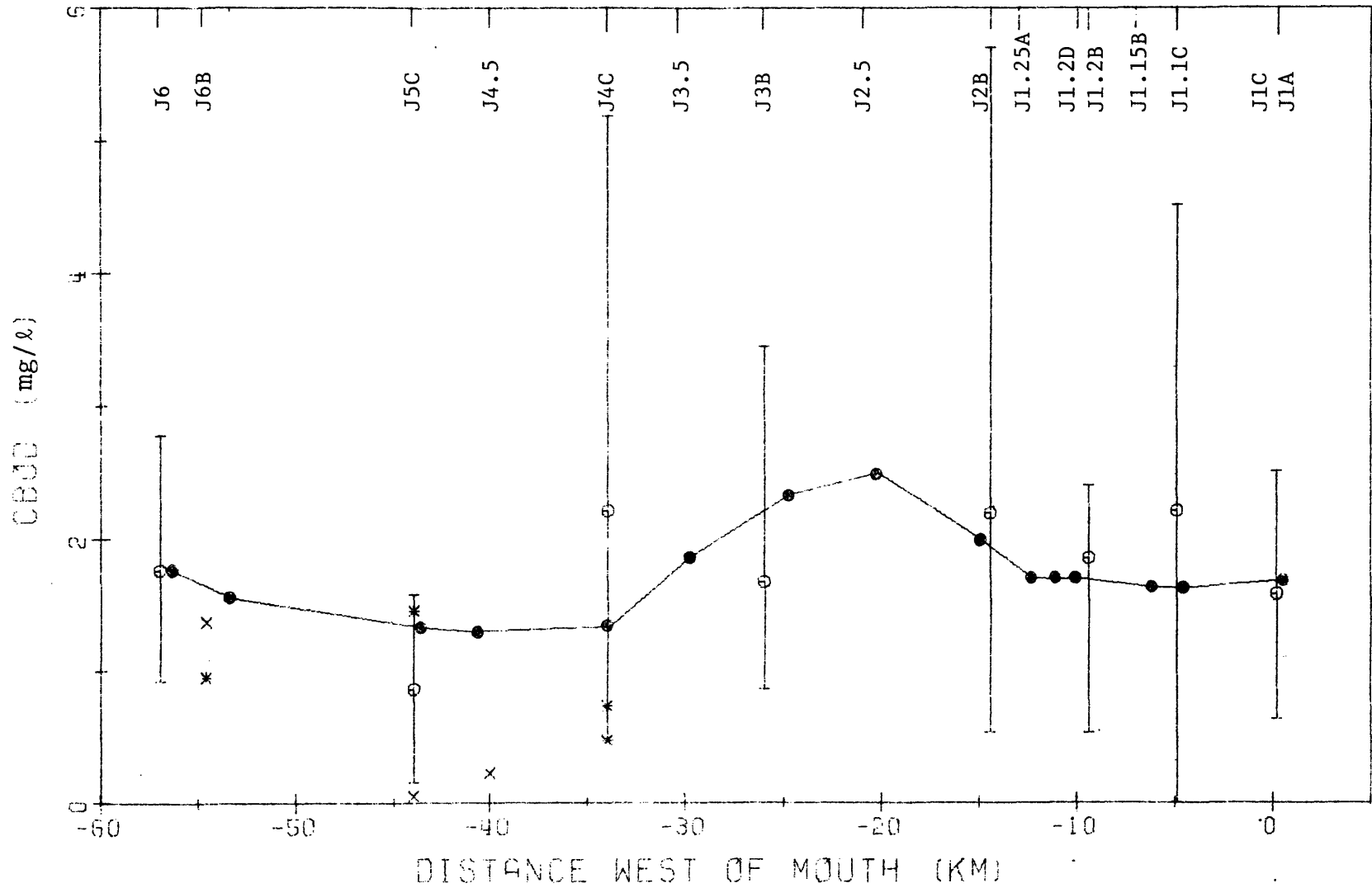


Figure 5.6i. Field data and calibrated results of CBOD at some locations along the lower James River. See Figure 5.6 for the meaning of the symbols and Figure 5.1a for the field stations and nodal points.

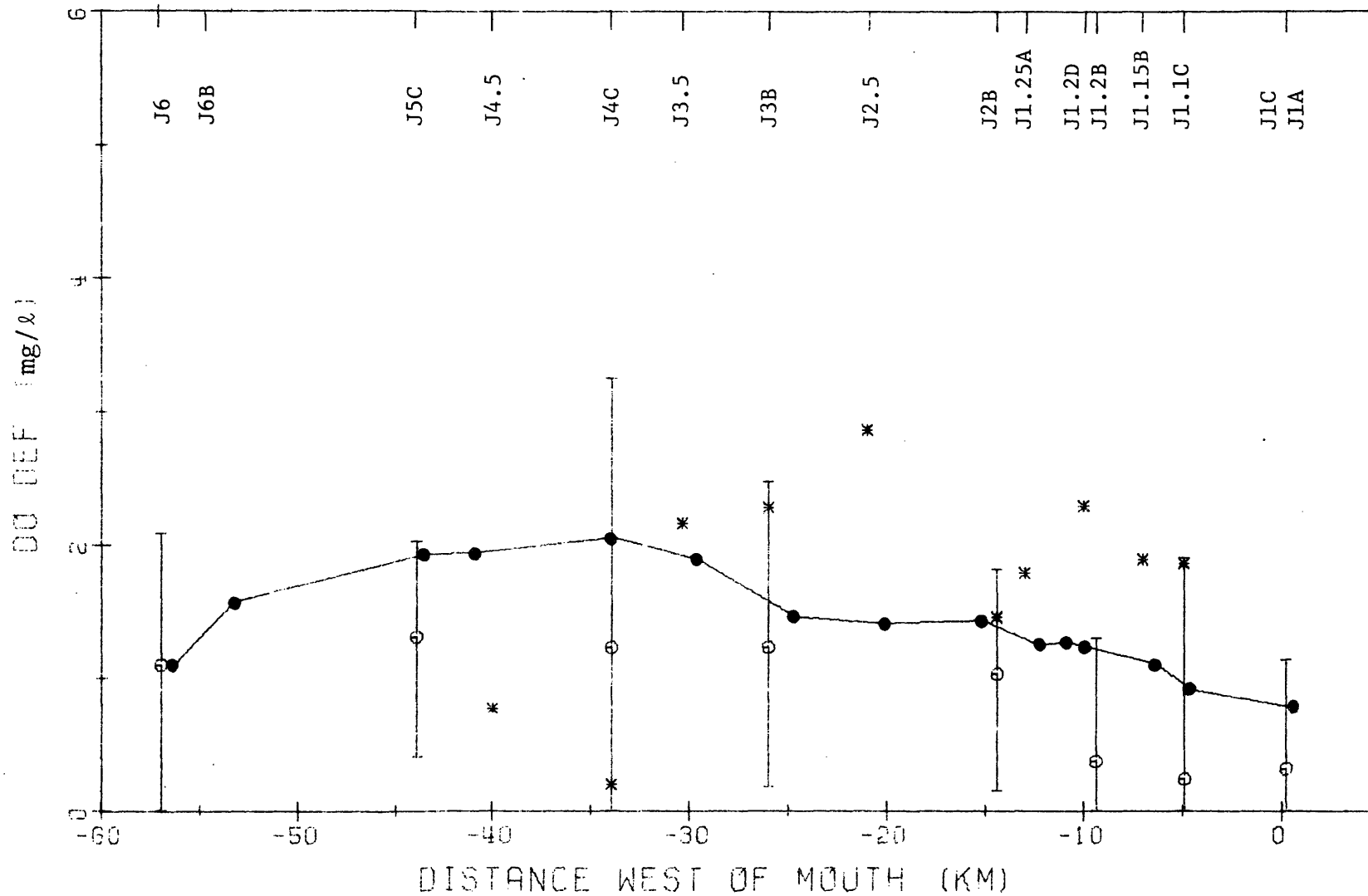


Figure 5.6j. Field data and calibrated results of dissolved oxygen deficit at some locations along the lower James River. See Figure 5.6 for the meaning of the symbols and Figure 5.1a for the field stations and nodal points.

Table 5.5. Calibrated Values for Hydrodynamic and Biogeochemical Water Quality Parameters.

Parameter Name	Value and Unit
Dispersion coefficient	$\epsilon_1 = 400 (-)$, $\epsilon_2 = 28 (m^2/s)$
Reaeration coefficient	$k_0 = 8 (-)$
Coliform dieoff rate at 20°C	$k_2 = 0.41 (1/day)$
Phytoplankton optimum growth rate	$k_g = 0.131 (1/day/°C)$
Extinction coefficient at zero chlorophyll concentration	$k_e = 1.5 (1/m)$
Phytoplankton endogeneous respiration rate	$k_r = 0.005 (1/day/°C)$
Zooplankton grazing rate	$k_z = 0.08 (1/day)$
Michaelis nitrogen constant	$k_{mn} = 0.018 (mg/l)$
Michaelis phosphorous constant	$k_{mp} = 0.006 (mg/l)$
Organic N-NH ₃ hydrolysis rate	$k_4 = 0.0021 (1/day/°C)$
Nitrogen-chlorophyll ratio	$r_n = 0.0085 (mg/\mu g)$
NH ₃ - NO ₃ nitrification rate	$k_5 = 0.009 (1/day/°C)$
Organic P - inorganic P conversion rate	$k_7 = 0.002 (1/day/°C)$
Phosphate - chlorophyll ratio	$r_p = 0.005 (mg/\mu g)$
CBOD oxidation rate	$k_9 = 0.07 (1/day)$
Carbon - chlorophyll ratio	$r_c = 0.04 (mg/\mu g)$
Photosynthetic quotient	$k_{op} = 1.4 (-)$
Respiratory quotient	$k_{or} = 1.0 (-)$
Benthic oxygen demand	$\ell_0 = 0.8 (gm/m^2/day)$
	Salinity $k_{1s} = 0.0$
	Coliform $k_{2s} = 0.0$
	Chlorophyll $k_{3s} = 0.0$
	Organic-N $k_{4s} = 0.01$
Settling and escaping rate	Ammonia-N $k_{5s} = 0.0 (1/day)$
	Nitrite- $k_{6s} = 0.04$
	Nitrate-N $k_{7s} = 0.02$
	Organic-P $k_{8s} = 0.05$
	Inorganic-P $k_{9s} = 0.0$
	CBOD $k_{0s} = 0.0$
	DO deficit $k_{0s} = 0.0$

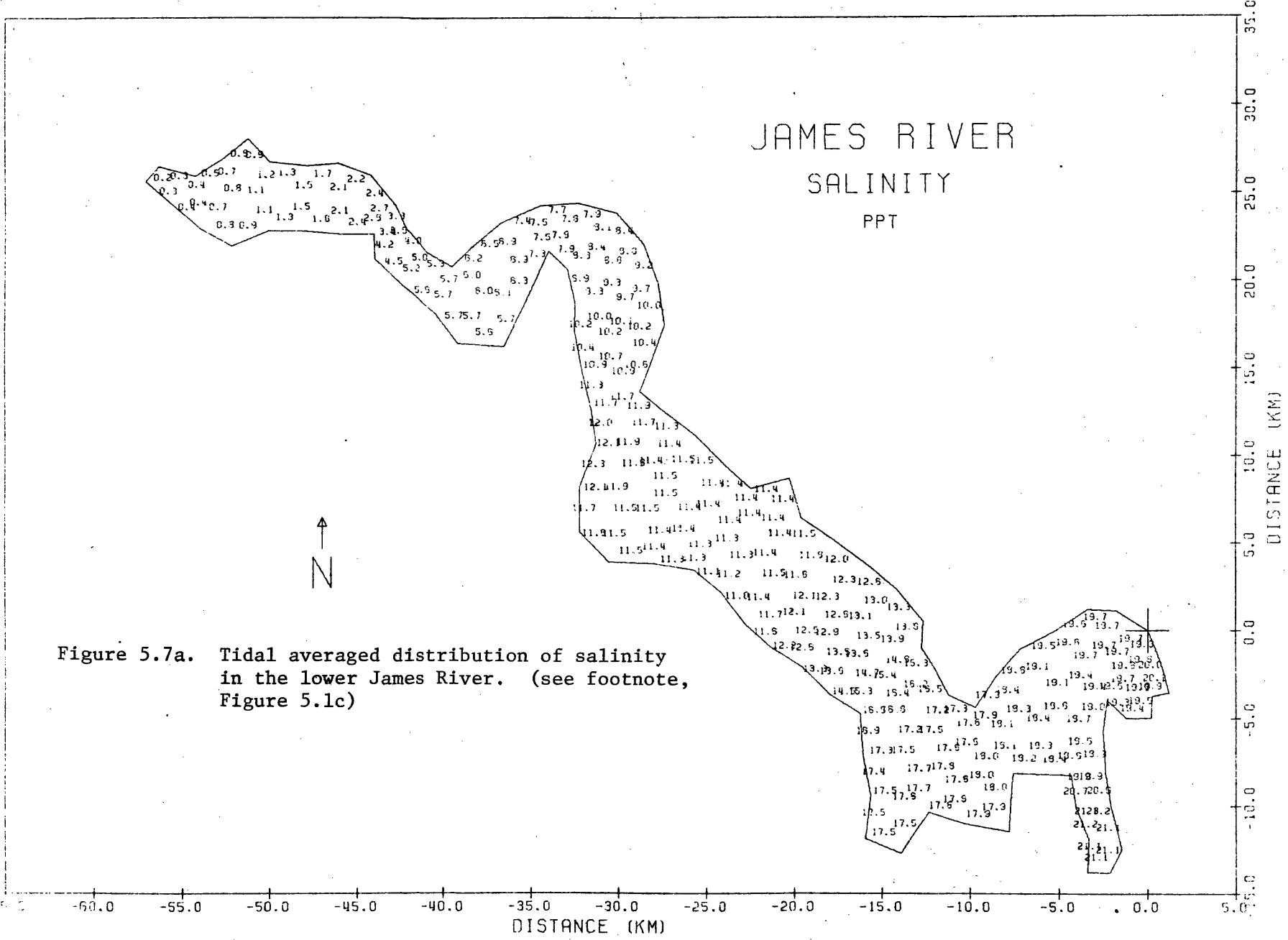


Figure 5.7a. Tidal averaged distribution of salinity in the lower James River. (see footnote, Figure 5.1c)

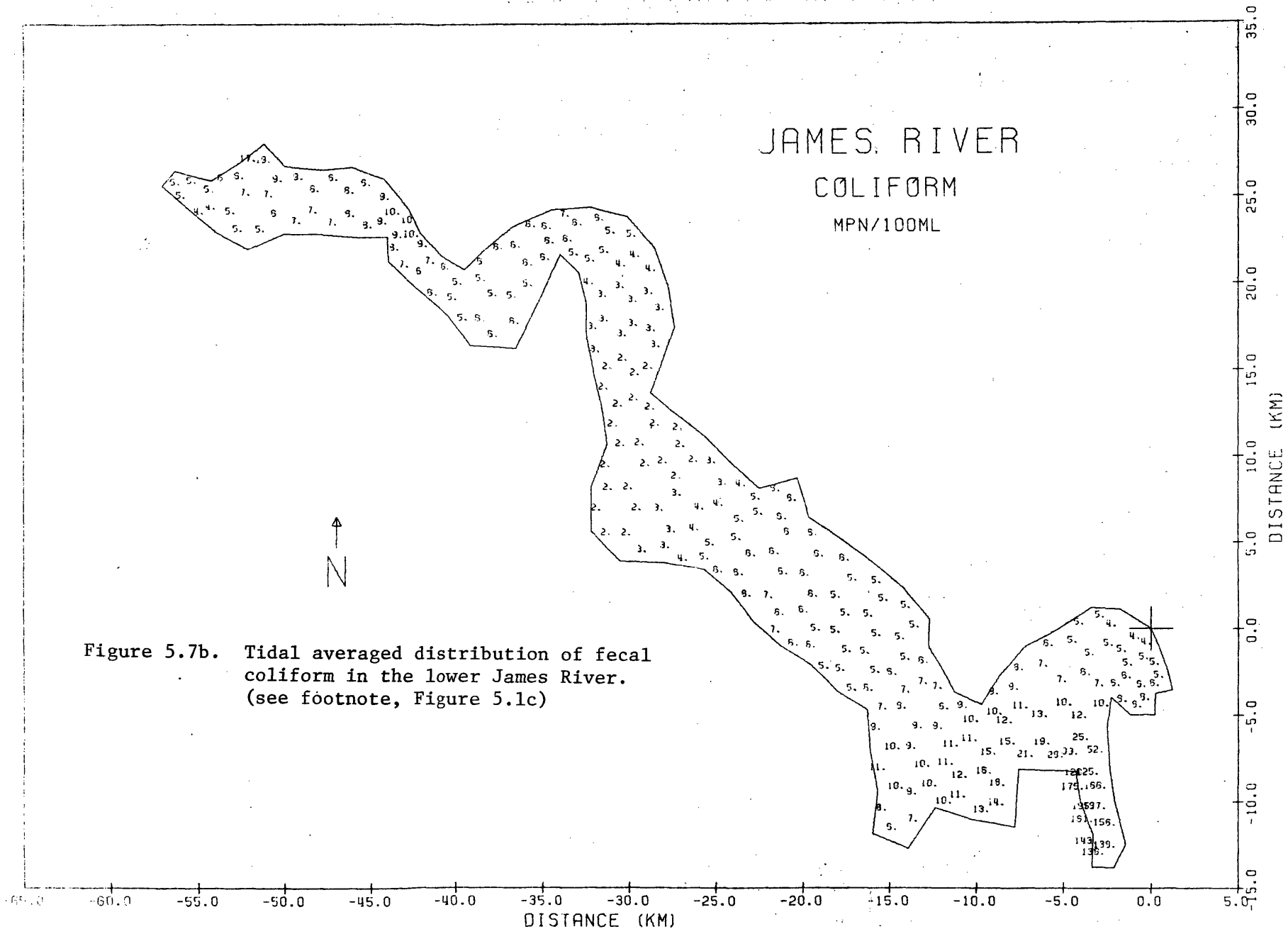


Figure 5.7b. Tidal averaged distribution of fecal coliform in the lower James River. (see footnote, Figure 5.1c)

JAMES RIVER CHLOROPHYLL µg/l

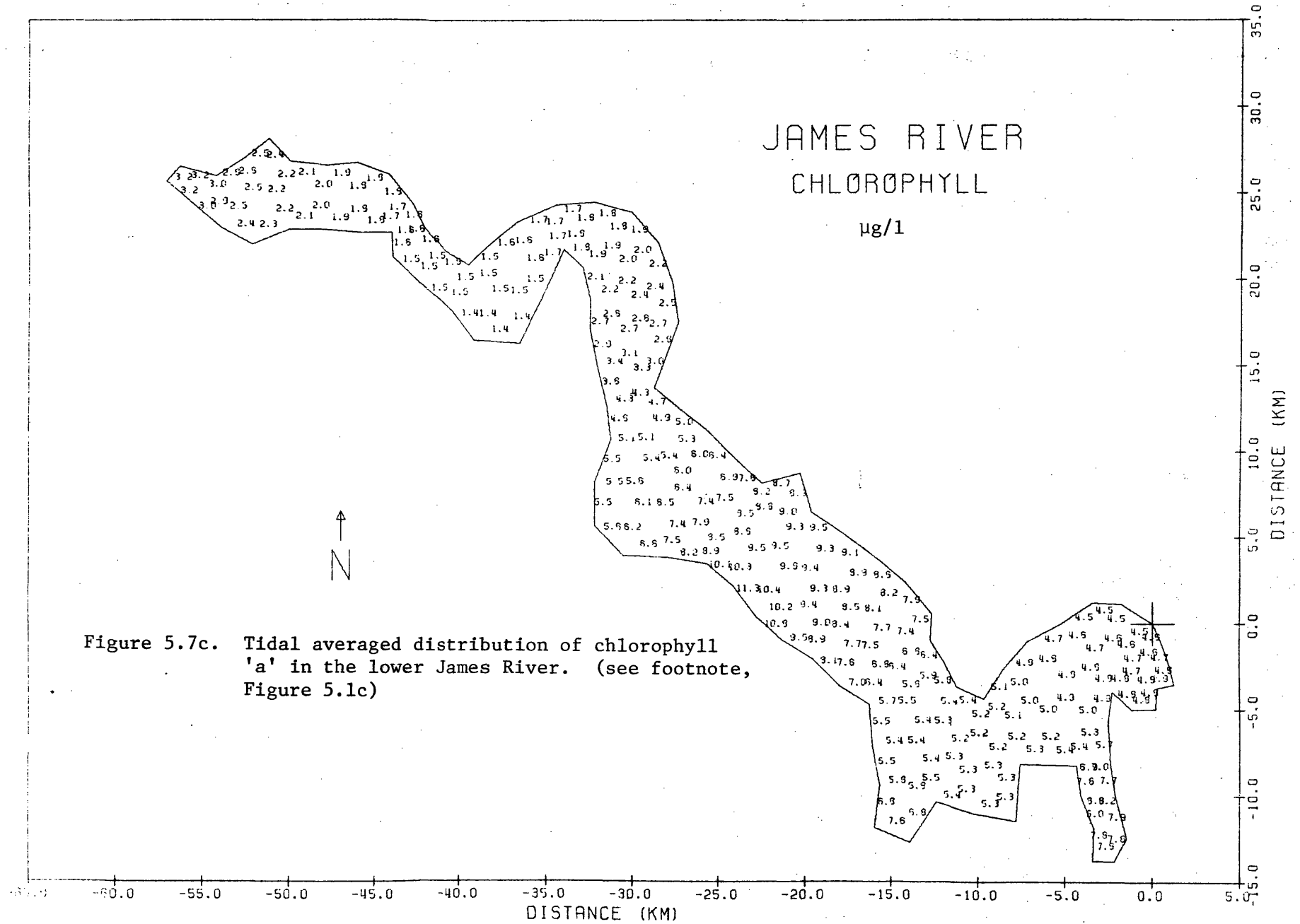
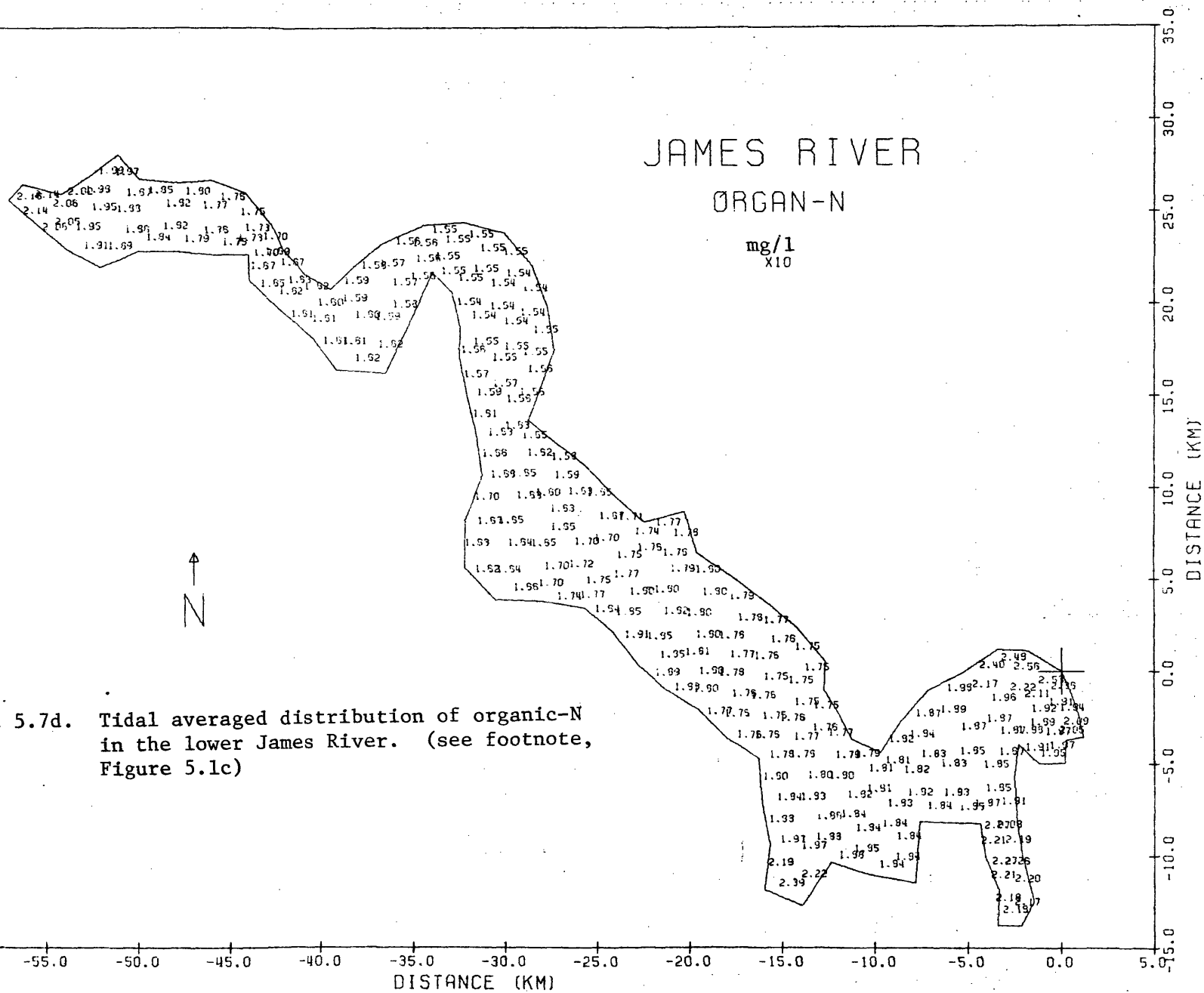


Figure 5.7c. Tidal averaged distribution of chlorophyll 'a' in the lower James River. (see footnote, Figure 5.1c)

Figure 5.7d. Tidal averaged distribution of organic-N in the lower James River. (see footnote, Figure 5.1c)



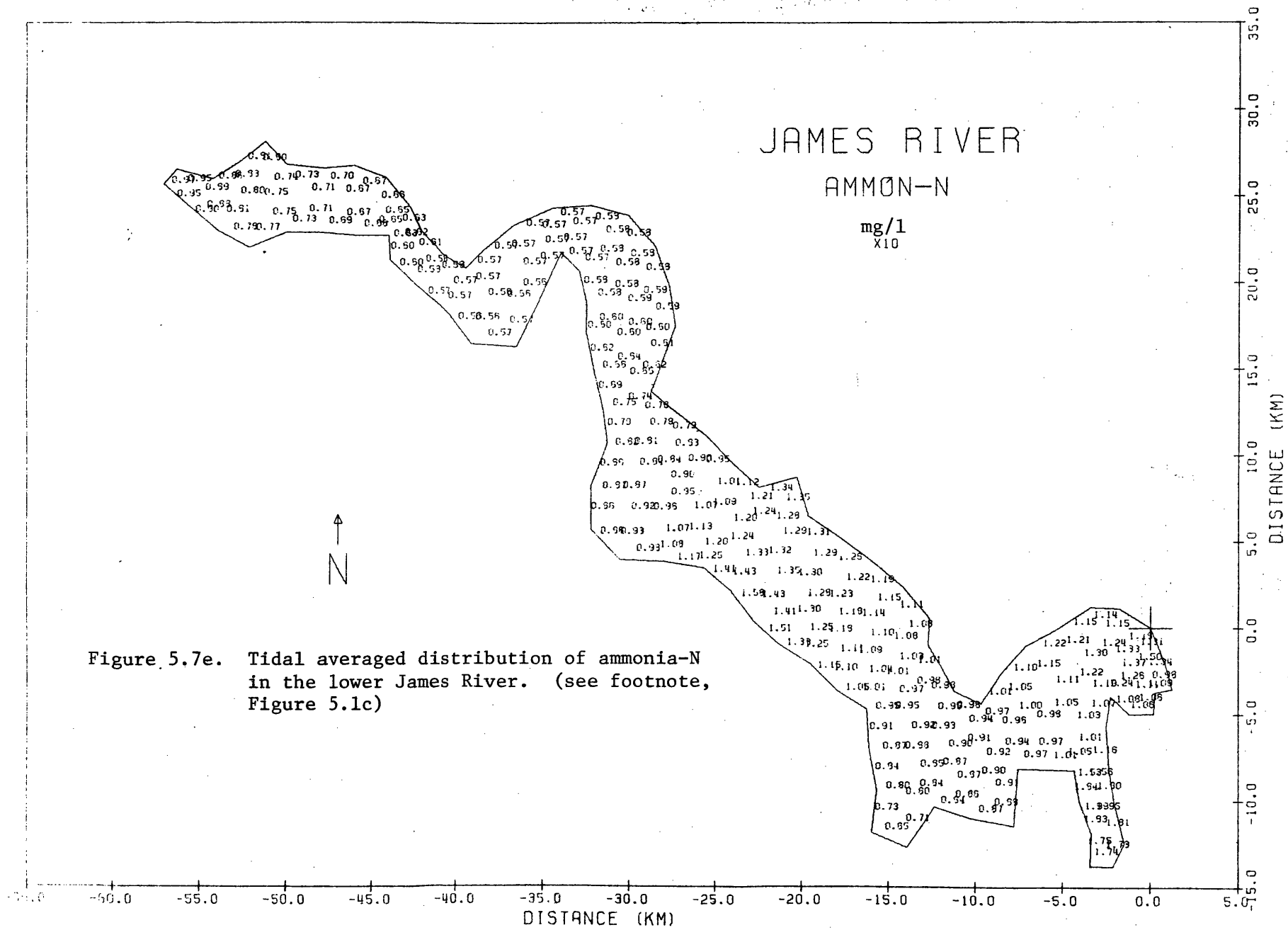


Figure 5.7e. Tidal averaged distribution of ammonia-N in the lower James River. (see footnote, Figure 5.1c)

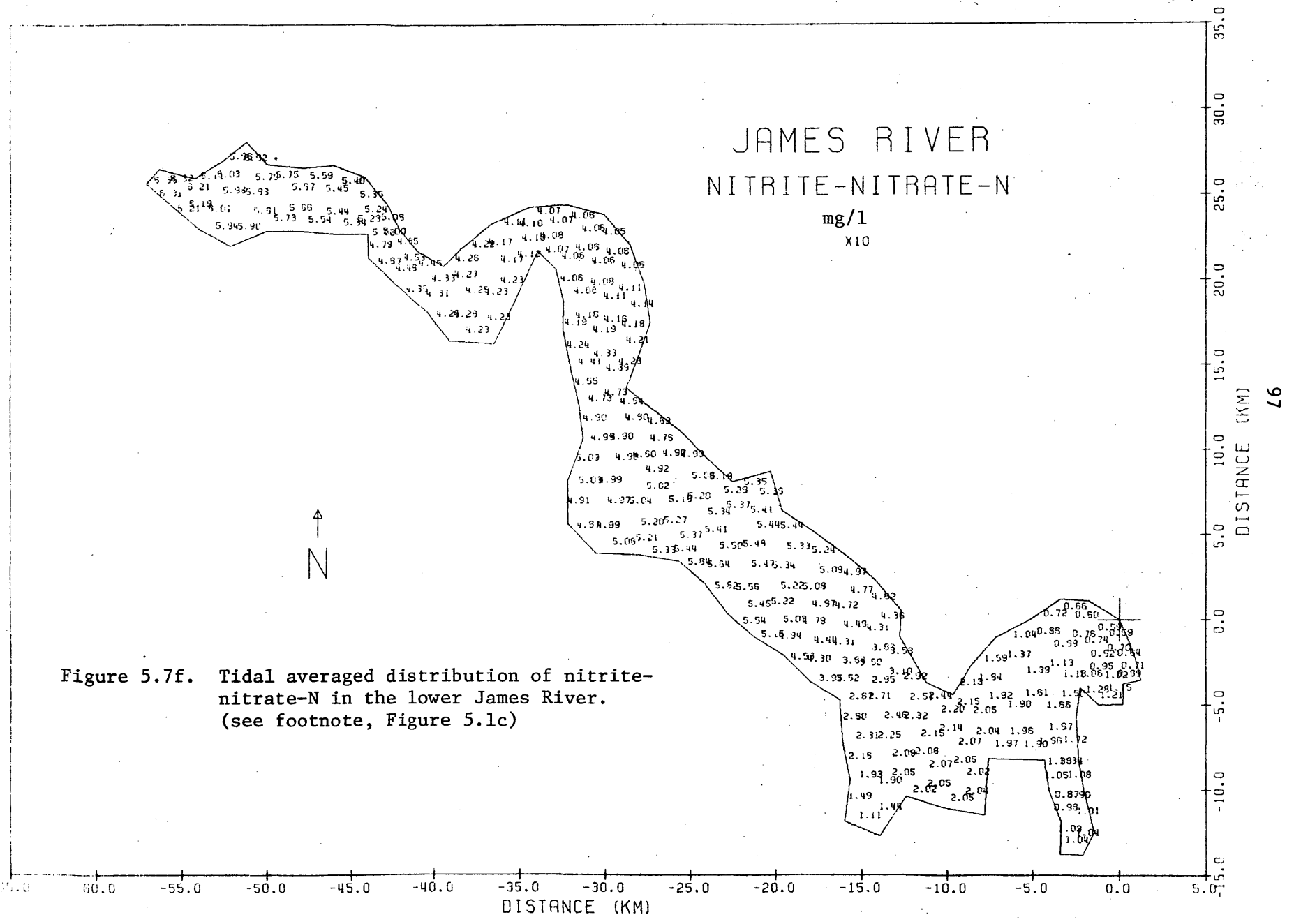


Figure 5.7f. Tidal averaged distribution of nitrite-nitrate-N in the lower James River.
 (see footnote, Figure 5.1c)

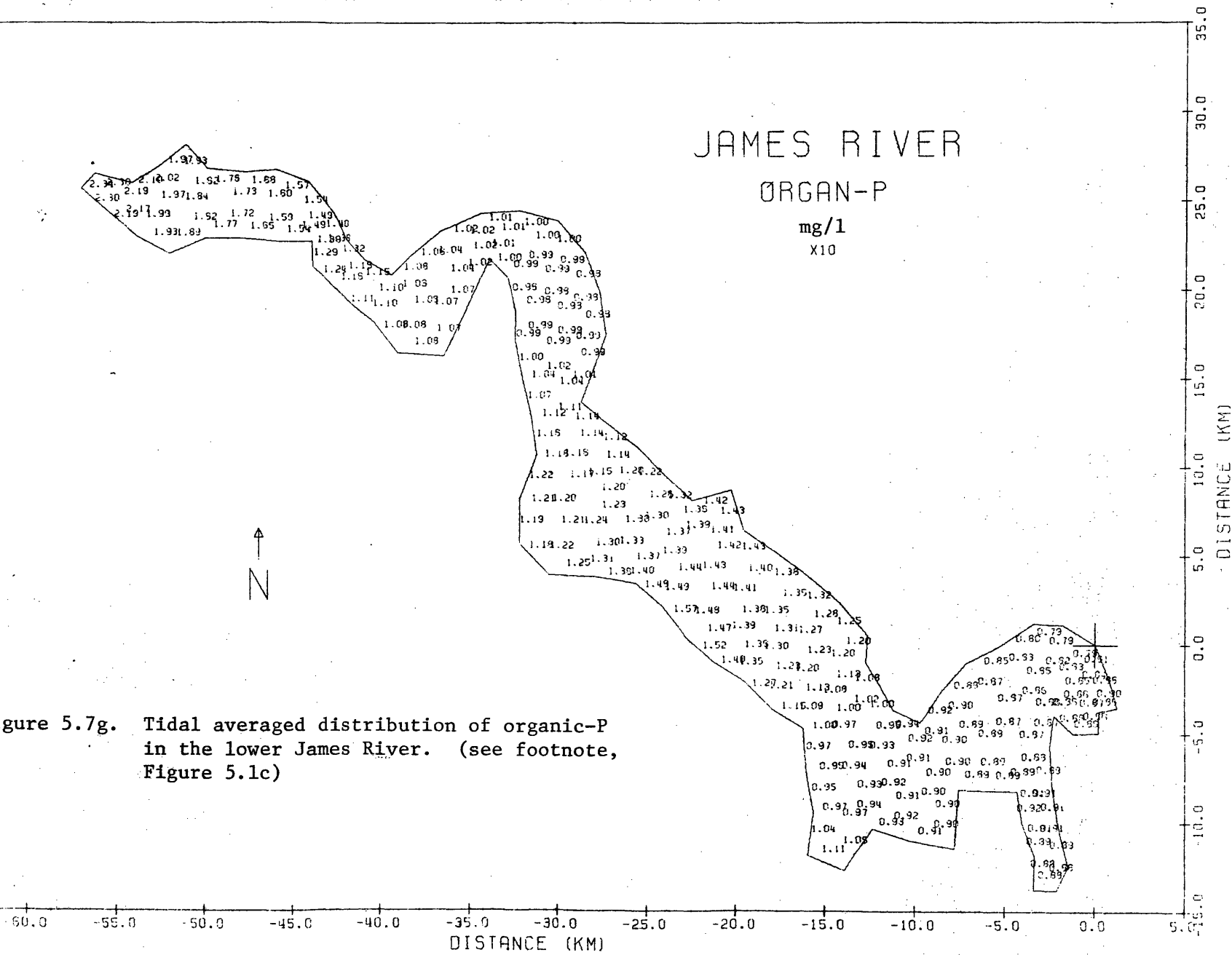


Figure 5.7g. Tidal averaged distribution of organic-P in the lower James River. (see footnote, Figure 5.1c)

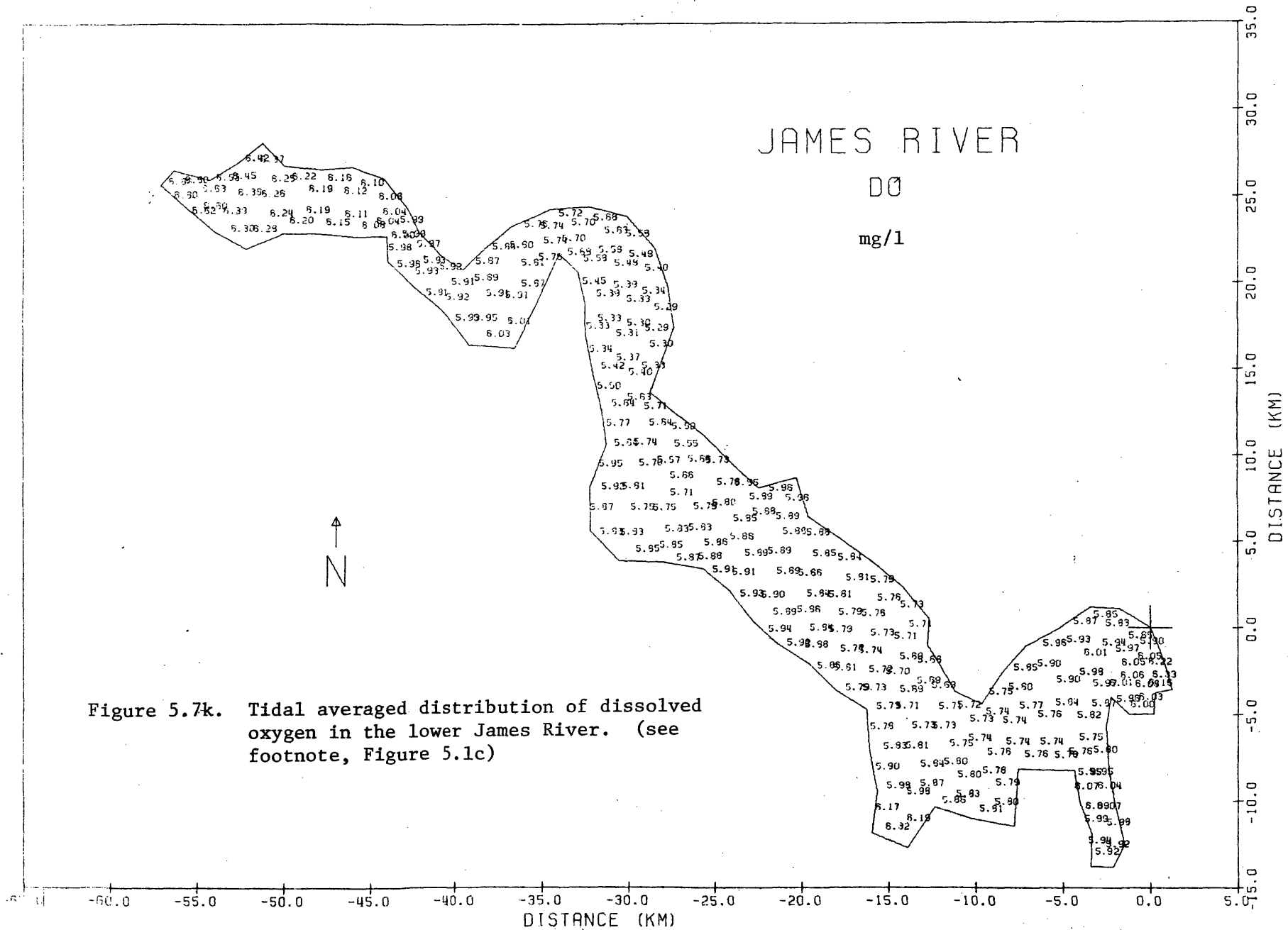


Figure 5.7k. Tidal averaged distribution of dissolved oxygen in the lower James River. (see footnote, Figure 5.1c)

Table 5.6a. Sensitivity of Salinity Distribution to the Change of Various Parameters.

Salinity (ppt)		
Node Number	*Calibrated Result	** $\epsilon_1 = 800$ $\epsilon_2 = 56$
2	21.33	21.33
18	20.89	20.89
26	20.02	20.05
47	18.93	18.97
48	19.07	19.18
49	18.90	18.96
67	15.03	15.32
81	12.22	12.35
92	12.11	11.95
112	11.91	11.32
136	7.55	7.58
149	5.50	5.74
156	3.00	3.56
173	0.52	0.86
178	0.17	0.17

Table 5.6b. Sensitivity of Coliform Bacteria Distribution to the Change of Various Parameters.

Coliform Bacteria (MPN/100ml)			
Node Number	*Calibrated Result	** $\epsilon_1 = 800$ $\epsilon_2 = 56$	$k_2 = 0.82$
2	4.63	4.63	4.63
18	6.06	8.55	4.18
26	8.30	14.42	4.43
47	10.71	20.85	5.26
48	13.46	25.73	7.35
49	10.80	21.37	5.30
67	5.39	9.83	2.42
81	6.29	7.45	4.35
92	4.46	6.00	2.82
112	1.65	3.03	1.00
136	6.27	5.80	3.61
149	5.57	6.09	2.58
156	10.14	9.71	6.40
173	4.68	6.54	2.95
178	5.14	5.14	5.14

* Values of Parameters are shown in Table 5.5

** Only the Indicated Value is changed, while others remain unchanged as in Table

Table 5.6c. Sensitivity of Chlorophyll "a" Distribution to the Change of Various Parameters.

Chlorophyll ($\mu\text{g}/\ell$)									
Node Number	*Calibrated Result	** $\epsilon_1=800$ $\epsilon_2=56$	$k_4=0.0042$	$k_5=0.018$	$k_7=0.004$	$r_p=0.010$	$k_9=0.14$	$r_c=0.08$	$k_0=16$
2	4.94	4.94	4.94	4.94	4.94	4.94	4.94	4.94	4.94
18	4.83	5.14	4.84	4.83	4.85	4.80	4.83	4.83	4.83
26	5.00	5.58	5.01	5.00	5.05	4.91	5.00	5.00	5.00
47	5.28	6.13	5.28	5.27	5.34	5.12	5.27	5.27	5.27
48	5.21	6.08	5.22	5.21	5.28	5.05	5.21	5.21	5.21
49	5.22	6.10	5.23	5.22	5.30	5.05	5.22	5.22	5.22
67	7.39	8.18	7.40	7.39	7.48	7.18	7.39	7.39	7.39
81	9.52	10.15	9.52	9.52	9.59	9.33	9.52	9.52	9.52
92	7.93	9.27	7.93	7.92	8.01	7.69	7.92	7.92	7.92
112	4.51	5.93	4.51	4.51	4.59	4.29	4.51	4.51	4.51
136	1.55	2.02	1.55	1.55	1.57	1.53	1.55	1.55	1.55
149	1.30	1.65	1.31	1.30	1.33	1.28	1.30	1.30	1.30
156	1.53	1.76	1.53	1.53	1.57	1.50	1.53	1.53	1.53
173	2.40	2.49	2.40	2.40	2.44	2.37	2.40	2.40	2.40
178	3.30	3.30	3.30	3.30	3.30	3.30	3.30	3.30	3.30

* Values of Parameters are shown in Table 5.5

** Only the Indicated Value is changed, while others remain unchanged as in Table 5.5

Table 5.6d. Sensitivity of Organic-N Distribution to the Change of Various Parameters.

Organic N (mg/l)									
Node Number	*Calibrated Result	** $\epsilon_1=800$ $\epsilon_2=56$	$k_4=0.0042$	$k_5=0.018$	$k_7=0.004$	$r_p=0.010$	$k_9=0.14$	$r_c=0.08$	$k_0=16$
2	0.1900	0.1900	0.1900	0.1900	0.1900	0.1900	0.1900	0.1900	0.1900
18	0.2050	0.2065	0.1955	0.2050	0.2050	0.2050	0.2050	0.2050	0.2050
26	0.1968	0.2029	0.1784	0.1968	0.1968	0.1967	0.1968	0.1968	0.1968
47	0.1918	0.2012	0.1667	0.1918	0.1918	0.1918	0.1918	0.1918	0.1918
48	0.1940	0.2032	0.1685	0.1940	0.1940	0.1940	0.1940	0.1940	0.1940
49	0.1938	0.2029	0.1683	0.1938	0.1938	0.1938	0.1939	0.1938	0.1938
67	0.1856	0.1950	0.1613	0.1856	0.1856	0.1856	0.1856	0.1856	0.1856
81	0.1918	0.1970	0.1737	0.1918	0.1918	0.1918	0.1918	0.1918	0.1918
92	0.1827	0.1911	0.1609	0.1827	0.1827	0.1826	0.1827	0.1827	0.1827
112	0.1630	0.1714	0.1354	0.1630	0.1631	0.1630	0.1630	0.1630	0.1630
136	0.1521	0.1557	0.1250	0.1521	0.1521	0.1521	0.1521	0.1521	0.1521
149	0.1576	0.1603	0.1304	0.1576	0.1576	0.1576	0.1576	0.1576	0.1576
156	0.1693	0.1723	0.1427	0.1693	0.1693	0.1693	0.1693	0.1693	0.1693
173	0.2000	0.2024	0.1862	0.2000	0.2000	0.1999	0.2000	0.2000	0.2000
178	0.2200	0.2200	0.2200	0.2200	0.2200	0.2200	0.2200	0.2200	0.2200

* Values of Parameters are shown in Table 5.5

** Only the Indicated Value is changed, while others remain unchanged as in Table 5.5

Table 5.6e. Sensitivity of Ammonia-N Distribution to the Change of Various Parameters.

Ammonia N (mg/l)									
Node Number	*Calibrated Result	** $\epsilon_1=800$ $\epsilon_2=56$	$k_4=0.0042$	$k_5=0.018$	$k_7=0.004$	$r_p=0.010$	$k_9=0.14$	$r_c=0.08$	$k_0=16$
2	0.1900	0.1900	0.1900	0.1900	0.1900	0.1900	0.1900	0.1900	0.1900
18	0.1347	0.1446	0.1419	0.1182	0.1346	0.1347	0.1347	0.1347	0.1347
26	0.1151	0.1307	0.1282	0.0866	0.1150	0.1151	0.1151	0.1151	0.1151
47	0.0987	0.1202	0.1162	0.0632	0.0987	0.0988	0.0987	0.0987	0.0987
48	0.0950	0.1187	0.1127	0.0599	0.0949	0.0951	0.0950	0.0950	0.0950
49	0.0942	0.1166	0.1119	0.0590	0.0941	0.0943	0.0942	0.0942	0.0942
67	0.1137	0.1309	0.1309	0.0742	0.1137	0.1138	0.1137	0.1137	0.1137
81	0.1419	0.1515	0.1551	0.1089	0.1419	0.1419	0.1419	0.1419	0.1419
92	0.1223	0.1401	0.1380	0.0864	0.1223	0.1224	0.1223	0.1223	0.1223
112	0.0791	0.0970	0.0982	0.0444	0.0791	0.0792	0.0791	0.0791	0.0791
136	0.0561	0.0600	0.0751	0.0315	0.0561	0.0561	0.0561	0.0561	0.0561
149	0.0560	0.0593	0.0757	0.0315	0.0560	0.0560	0.0560	0.0560	0.0560
156	0.0631	0.0658	0.0829	0.0371	0.0631	0.0631	0.0631	0.0631	0.0631
173	0.0851	0.0866	0.0967	0.0679	0.0851	0.0851	0.0851	0.0851	0.0851
178	0.1000	0.1000	0.1000	0.1000	0.1000	0.1000	0.1000	0.1000	0.1000

* Values of Parameters are shown in Table 5.5

** Only the Indicated Value is changed, while others remain unchanged as in Table 5.5

Table 5.6f. Sensitivity of Nitrite-Nitrate-N Distribution to the Change of Various Parameters.

Nitrite-Nitrate N (mg/l)									
Node Number	*Calibrated Result	** $\epsilon_1=800$ $\epsilon_2=56$	$k_4=0.0042$	$k_5=0.018$	$k_7=0.004$	$r_p=0.010$	$k_9=0.14$	$r_c=0.08$	$k_0=16$
2	0.0600	0.0600	0.0600	0.0600	0.0600	0.0600	0.0600	0.0600	0.0600
18	0.1088	0.1034	0.1111	0.1244	0.1086	0.1092	0.1088	0.1088	0.1088
26	0.1746	0.1649	0.1797	0.2012	0.1741	0.1756	0.1746	0.1746	0.1746
47	0.2371	0.2303	0.2449	0.2703	0.2363	0.2389	0.2371	0.2371	0.2371
48	0.2259	0.2184	0.2338	0.2587	0.2250	0.2277	0.2259	0.2259	0.2259
49	0.2327	0.2265	0.2407	0.2656	0.2318	0.2346	0.2327	0.2327	0.2327
67	0.4495	0.4303	0.4571	0.4867	0.4485	0.4519	0.4495	0.4495	0.4495
81	0.5897	0.5817	0.5952	0.6214	0.5889	0.5919	0.5897	0.5897	0.5897
92	0.5707	0.5818	0.5780	0.6052	0.5697	0.5737	0.5707	0.5707	0.5707
112	0.4929	0.5183	0.5032	0.5258	0.4918	0.4956	0.4929	0.4929	0.4929
136	0.4118	0.4395	0.4227	0.4357	0.4115	0.4121	0.4118	0.4118	0.4118
149	0.4388	0.4595	0.4499	0.4631	0.4385	0.4392	0.4388	0.4388	0.4388
156	0.5147	0.5131	0.5251	0.5408	0.5141	0.5153	0.5147	0.5147	0.5147
173	0.6129	0.6056	0.6169	0.6307	0.6123	0.6133	0.6129	0.6129	0.6129
178	0.6400	0.6400	0.6400	0.6400	0.6400	0.6400	0.6400	0.6400	0.6400

* Values of Parameters are shown in Table 5.5

** Only the Indicated Value is changed, while others remain unchanged as in Table 5.5

Table 5.6g. Sensitivity of Organic-P Distribution to the Change of Various Parameters.

Organic P (mg/l)									
Node Number	*Calibrated Result	** $\epsilon_1=800$ $\epsilon_2=56$	$k_4=0.0042$	$k_5=0.018$	$k_7=0.004$	$r_p=0.010$	$k_9=0.14$	$r_c=0.08$	$k_0=16$
2	0.0900	0.0900	0.0900	0.0900	0.0900	0.0900	0.0900	0.0900	0.0900
18	0.0900	0.0930	0.0909	0.0909	0.0866	0.0912	0.0909	0.0909	0.0909
26	0.0938	0.0976	0.0938	0.0938	0.0850	0.0945	0.0938	0.0938	0.0938
47	0.0972	0.1033	0.0972	0.0972	0.0846	0.0982	0.0972	0.0972	0.0972
48	0.0963	0.1021	0.0963	0.0963	0.0838	0.0974	0.0963	0.0963	0.0963
49	0.0975	0.1034	0.0975	0.0975	0.0848	0.0986	0.0975	0.0975	0.0975
67	0.1254	0.1300	0.1254	0.1254	0.1105	0.1268	0.1254	0.1254	0.1254
81	0.1526	0.1557	0.1526	0.1526	0.1399	0.1539	0.1526	0.1526	0.1526
92	0.1423	0.1511	0.1423	0.1423	0.1271	0.1438	0.1423	0.1423	0.1423
112	0.1144	0.1261	0.1144	0.1144	0.0961	0.1160	0.1144	0.1144	0.1144
136	0.0996	0.1081	0.0996	0.0996	0.0826	0.1002	0.0996	0.0996	0.0996
149	0.1102	0.1193	0.1102	0.1102	0.0919	0.1108	0.1102	0.1102	0.1102
156	0.1434	0.1473	0.1434	0.1434	0.1221	0.1441	0.1434	0.1434	0.1434
173	0.2088	0.2089	0.2088	0.2088	0.1957	0.2092	0.2088	0.2088	0.2088
178	0.2400	0.2400	0.2400	0.2400	0.2400	0.2400	0.2400	0.2400	0.2400

* Values of Parameters are shown in Table 5.5

** Only the Indicated Value is changed, while others remain unchanged as in Table 5.5

Table 5.6h. Sensitivity of Inorganic-P Distribution to the Change of Various Parameters.

Inorganic P (mg/l)									
Node Number	*Calibrated Result	** $\epsilon_1=800$ $\epsilon_2=56$	$k_4=0.0042$	$k_5=0.018$	$k_7=0.004$	$r_p=0.010$	$k_9=0.14$	$r_c=0.08$	$k_0=16$
2	0.0300	0.0300	0.0300	0.0300	0.0300	0.0300	0.0300	0.0300	0.0300
18	0.0286	0.0286	0.0286	0.0286	0.0326	0.0249	0.0286	0.0286	0.0286
26	0.0309	0.0308	0.0309	0.0309	0.0390	0.0225	0.0309	0.0309	0.0309
47	0.0321	0.0326	0.0320	0.0321	0.0435	0.0193	0.0321	0.0321	0.0321
48	0.0314	0.0325	0.0314	0.0314	0.0428	0.0185	0.0314	0.0314	0.0314
49	0.0311	0.0320	0.0311	0.0311	0.0427	0.0179	0.0311	0.0311	0.0311
67	0.0373	0.0376	0.0373	0.0373	0.0512	0.0203	0.0373	0.0373	0.0373
81	0.0430	0.0433	0.0430	0.0430	0.0550	0.0275	0.0430	0.0430	0.0430
92	0.0424	0.0431	0.0424	0.0424	0.0568	0.0235	0.0424	0.0424	0.0424
112	0.0454	0.0447	0.0454	0.0454	0.0629	0.0243	0.0454	0.0454	0.0454
136	0.0617	0.0580	0.0617	0.0617	0.0786	0.0510	0.0617	0.0617	0.0617
149	0.0606	0.0569	0.0606	0.0606	0.0793	0.0500	0.0606	0.0606	0.0606
156	0.0538	0.0506	0.0538	0.0538	0.0756	0.0430	0.0538	0.0538	0.0538
173	0.0324	0.0315	0.0324	0.0324	0.0459	0.0263	0.0324	0.0324	0.0324
178	0.0200	0.0200	0.0200	0.0200	0.0200	0.0200	0.0200	0.0200	0.0200

* Values of Parameters are shown in Table 5.5

** Only the Indicated Value is changed, while others remain unchanged as in Table 5.5

Table 5.6i. Sensitivity of CBOD Distribution to the Change of Various Parameters.

CBOD (mg/l)									
Node Number	*Calibrated Result	** $\epsilon_1=800$ $\epsilon_2=56$	$k_4=0.0042$	$k_5=0.018$	$k_7=0.004$	$r_p=0.010$	$k_9=0.14$	$r_c=0.08$	$k_0=16$
2	1.6800	1.6800	1.6800	1.6800	1.6800	1.6800	1.6800	1.6800	1.6800
18	1.6220	1.6800	1.6220	1.6224	1.6224	1.6223	1.4939	1.6283	1.6224
26	1.6310	1.7458	1.6310	1.6312	1.6313	1.6310	1.3731	1.6437	1.6312
47	1.6930	1.8526	1.6930	1.6925	1.6928	1.6923	1.3920	1.7119	1.6926
48	1.6980	1.8602	1.6980	1.6980	1.6982	1.6977	1.3336	1.7180	1.6980
49	1.6990	1.8582	1.6990	1.6993	1.6995	1.6990	1.3324	1.7198	1.6993
67	2.0180	2.1866	2.018	2.0807	2.0809	2.0803	1.6619	2.1064	2.0807
81	2.4990	2.5536	2.4990	2.4992	2.4994	2.4989	2.1472	2.5232	2.4997
92	2.3290	2.4594	2.3290	2.3288	2.3290	2.3283	1.9065	2.3573	2.3288
112	1.8700	2.0025	1.8700	1.8695	1.8697	1.8690	1.3706	1.8982	1.8695
136	1.3310	1.4030	1.3310	1.3308	1.3309	1.3307	0.9532	1.3425	1.3308
149	1.2950	1.3457	1.2950	1.2954	1.2955	1.2953	0.9357	1.3069	1.2954
156	1.3240	1.3728	1.3240	1.3239	1.3241	1.3238	0.9864	1.3363	1.3239
173	1.5550	1.5863	1.5550	1.5546	1.5547	1.5545	1.3823	1.5628	1.5546
178	1.7600	1.7600	1.7600	1.7600	1.7600	1.7600	1.7600	1.7600	1.7600

* Values of Parameters are shown in Table 5.5

** Only the Indicated Value is changed, while others remain unchanged as in Table 5.5

Table 5.6j. Sensitivity of DO Deficit Distribution to the Change of Various Parameters.

D.O. Deficit (mg/l)									
Node Number	*Calibrated Result	** $\epsilon_1=800$ $\epsilon_2=56$	$k_4=0.0042$	$k_5=0.018$	$k_7=0.004$	$r_p=0.010$	$k_0=0.14$	$r_c=0.08$	$k_0=16$
2	0.7800	0.7800	0.7800	0.7800	0.7800	0.7800	0.7800	0.7800	0.7800
18	0.9142	0.8492	0.9229	0.9761	0.9110	0.9203	1.0169	0.8103	0.7998
26	1.1030	0.9946	1.1230	1.2051	1.0958	1.1191	1.3031	0.8708	0.8791
47	1.2750	1.1544	1.3050	1.3942	1.2628	1.3024	1.5456	0.9246	0.9475
48	1.2440	1.1351	1.2740	1.3580	1.2320	1.2726	1.5078	0.8983	0.9020
49	1.2470	1.1391	1.2760	1.3600	1.2339	1.2761	1.5108	0.8918	0.8999
67	1.4340	1.3397	1.4640	1.5593	1.4196	1.4725	1.7522	0.9569	1.0650
81	1.4120	1.3946	1.4320	1.5235	1.3996	1.4446	1.6701	0.9993	1.0753
92	1.4670	1.4501	1.4910	1.5801	1.4520	1.5086	1.7599	0.9838	1.0380
112	1.8900	1.7953	1.9300	1.9995	1.8744	1.9314	2.2568	1.3299	1.3411
136	2.0590	2.0405	2.0980	2.1309	2.0548	2.0630	1.3176	1.8244	1.2921
149	1.9380	1.9457	1.9760	2.0039	1.9331	1.9422	2.1669	1.7255	1.1414
156	1.9300	1.8705	1.9670	2.0077	1.9207	1.9367	2.1635	1.6910	1.2065
173	1.5740	1.4880	1.5890	1.6395	1.5662	1.5806	1.7165	1.4206	1.2656
178	1.1000	1.1000	1.1000	1.1000	1.1000	1.1000	1.1000	1.1000	1.1000

* Values of Parameters are shown in Table 5.5

** Only the Indicated Value is changed, while others remain unchanged as in Table 5.5

tables is the average value of the last tidal cycle in an eight-tidal-cycle run, all starting from the same initial conditions. Note also these results are not universal, but depend on the initial condition and the range of parameters used.

Based on these computed results and on the way the mathematical model is built, the general pattern could be stated as follows: The increase of dispersion coefficients, ϵ_x and ϵ_y , tends to smooth water quality distribution throughout the river. The increase of coliform die-off rate, k_2 , tends to decrease coliform bacteria. The effect of other parameters on the water quality distribution is summarized in Table 5.7. This table shows only short-term immediate reactions among the constituents. To determine the long term response which would include feedback effects, one should use the table iteratively.

Note that in Table 5.6a there is low sensitivity of salinity to the dispersion coefficient. This is probably due to the smooth distribution (therefore small gradient) of salinity, making the dispersion effect insignificant.

5.5 Water Quality Discussion

Since numerous physical and biogeochemical parameter constants are involved in the system, the simulation of water quality in a large estuary is difficult, expensive and time-consuming. Furthermore, the calibrated parameter constants might not be unique in the real situation. However, the model is able to reproduce the hydrodynamic and biogeochemical water quality behavior of the lower James River with satisfactory accuracy as shown by comparing model predictions and observed field data (see

Figures 5.6a thru j).

Salinity and fecal coliform bacteria are two somewhat independent sub-systems. Observed depth averaged salinity varies smoothly from 21 ppt at river mouth to 0.17 ppt at the upstream near Sandy Point. This indicates that the river is fresh at upstream end, but farther downstream one sees seawater intrusion and salinity stratification, particularly, near Newport News. At some locations the salinity difference between river bottom and surface is measured as high as 5 ppt. Between storm events observed fecal coliform in the lower James River is generally less than 20 MPN/100 ml. It is far less than the Virginia Water Quality Standard for water supplies and primary contact recreation, a log-mean of 200 MPN/100 ml. In the Elizabeth River and the zone of the James under its influence the coliform count may reach 250 MPN/100 ml. However, following storm events coliform counts may rise several times, particularly at some locations near the Elizabeth River and the Nansemond River. Nevertheless, based on the Virginia Water Quality Standard on coliform counts, much of the lower James River is suitable for primary contact recreation and the propagation of fish and aquatic life.

Observed chlorophyll 'a' concentrations were generally in the range of 1 to 14 $\mu\text{g}/\ell$, well below the algae bloom level of 40 $\mu\text{g}/\ell$, suggested by the Annapolis Field Office of the Environmental Protection Agency (EPA) in a study of the upper Chesapeake Bay. This mild algae growth is limited by the availability of nitrogen and the effect of deep water. Observed nutrients indicate that inorganic nitrogen concentrations were in the range of 0.1 to 0.75 mg/ℓ and inorganic phosphorus concentrations were about 0.05 mg/ℓ throughout the river, compared with the values:

inorganic nitrogen - 0.8 mg/l and inorganic phosphorus - 0.04 mg/l (0.12 mg/l as PO_4), which are the minimum nutrient values to sustain an algae level of 40 μ g/l. The deep water of the river, averaging 5 m, also constrains the growth of phytoplankton, due to attenuation of solar radiation with depth because of turbidity. The river is quite turbid, secchi-disc depth reading averaging 0.98 m and ranging from 0.4 m near the conjunction of the Chickahominy to 1.3 m in the river zone of Newport News. Observed chlorophyll 'a' concentrations also show significant differences between river surface and bottom during daytime.

Dissolved oxygen (DO) concentrations observed in the lower James River are generally satisfactory with average DO level above 5.5 mg/l, even near the river bottom DO values are still above 4.5 mg/l, well above the 4 mg/l water quality standard. Point sources and non-point sources for DO deficit are around 750 to 490 kg/day respectively, being comparatively small amounts for a large estuary like the James River. (DO deficit is defined as saturation DO minus DO; the loads are calculated by multiplying water discharge of point and non-point sources by DO deficit). Observed carbonaceous biochemical oxygen demand (CBOD) concentration averaged around 2 mg/l. This low value is expected for a huge tidal prism, although CBOD loads are of the order of 8,000 kg/day. It appears that present CBOD loads have only little impact on the DO deficits. Similarly, due to the low concentration of chlorophyll 'a', diurnal DO variations subject to photosynthesis in the daytimes and respiration during nights are not significant. Additionally, the DO demand by dead phytoplankton as they decompose is, therefore, also insignificant. High DO concentration may also be aided by meteorological effects on the large river surface and

heavy traffic of marine vehicles, which generally increase reaeration and diffusivity in the river. Large values of reaeration and dispersion coefficients are used in the calibration model study.

In summary, the tidal prism water volume for the James River is of the order of 10^9 m^3 (one billion cubic meter), according to Cronin (1971). As a result, the present wasteloads which are discharged into the river are greatly diluted to low concentration levels by the high tidal flushing. Based on the Virginia Water Quality Standard, except at some locations near the Elizabeth River and the Nansemond River, where fecal coliform counts may occasionally exceed 200 MPN/100ml, each constituent of biogeochemical water quality considered is within satisfactory levels. Therefore, as far as the present situation is concerned, the wasteloads and wastes which have been modeled and studies in this investigation are not likely to have a strong impact on the water quality of the lower James River. However, for future development, a careful management of the James River water quality system is still a necessity.

6. CONCLUSION

A real-time two-dimensional depth-integrated mathematical model for the biogeochemical water quality system has been developed. The model uses Galerkins weighted residual finite element numerical technique. The finite element spatial discretization is found to be superior to other approaches for the flexibility of the grid layout. The model, being capable of simulating the major feature of the water circulation and the water quality in the lower James River, can be considered at present one of the most sophisticated two-dimensional formulations of the biogeochemical water quality system. Possible studies for further improvement are a more precise estimate of the coefficient constants of the water quality and a more complete field data of water circulation and water quality.

REFERENCES

- Brandes, Robert J. and Frank D. Masch. 1975. Estuarine ecologic simulations. Symposium on Modeling Techniques, ASCE.
- Chen, C. W. and G. T. Orlob. 1971. Ecologic simulation for aquatic environments. OWRR Proj. IV.C-2044, Office of Water Resources Research, Dept. of the Interior, Washington, D. C.
- Chen, H. S. 1978. A storm surge model study volume II, a finite element storm surge analysis and its application to a bay-ocean system. Special Report in Applied Marine Science and Ocean Engineering No. 189, Virginia Institute of Marine Science, June.
- Chen, H. S. and C. C. Mei. 1974. Oscillations and wave forces in a man-made harbor in the open sea. Proceedings of 10th Naval Hydrodynamics Symposium, June.
- Connor, J. and J. Wang. 1974. Finite element modelling of hydrodynamic circulation, in Numerical Methods in Fluid Dynamics, ed. by Brebbia and Connor, Pentech Press.
- Cronin, William B. 1971. Volumetric, areal, and tidal statistics of the Chesapeake Bay Institute and its tributaries. Chesapeake Bay Institute, The Johns Hopkins University, Special Report 20, Reference 71-2, March.
- Dugdale, R. C. 1976. Nutrient cycles. The Ecology of the Seas. W. B. Saunders Co.
- Durance, A. 1974. A mathematical model of the residual circulation of the Southern North Sea. Sixth Liège Colloquium on Ocean Hydrodynamics, Mém. Soc. Roy. Sc de Liège.
- Fair, G. M., J. C. Geyer and D. A. Okun. 1968. Water and wastewater engineering, Vol. 2, John Wiley & Sons, Inc., New York.
- Harleman, Donald R. F. 1970. Transport processes in water quality control. A series of notes to accompany lectures in 1.77-water quality control.
- Harleman, Donald R. F. 1977. Real-time models for salinity and water-quality analysis in estuaries. Estuaries, Geophysics, and the Environment. National Academy of Science.
- Heaps, N. S. 1969. A two-dimensional numerical sea model. Royal Society of London, Philosophical Transactions, Ser. A, Vol. 265, No. 1160, October.

- Leendertse, J. J. and S. K. Liu. 1974. A water-quality simulation model for well-mixed estuaries and coastal seas. Vol. VI Simulation, Observation, and State Estimation, New York City Rand Institute, Rep. R-1586-NYC, New York.
- McKinney, R. E. 1962. Microbiology for Sanitary Engineers. McGraw-Hill Book Company, Inc., New York.
- Najarian, Tavit O. and Donald R. F. Harleman. 1975. A real time model of nitrogen-cycle dynamics in an estuary system. Report No. 204, Ralph M. Parsons Laboratory, MIT, July.
- Najarian, Tavit O. and Donald R. F. Harleman. 1976. Model of nitrogen cycle in an estuary. ASCE National Water Resources and Ocean Engineering Convention.
- Nemerow, Nelson Leonard. 1974. Scientific Stream Pollution Analysis. Scripta Book Company.
- Nihoul, J. C. J. 1975. Modelling of Marine Systems. Elsevier Publ. Co. Amsterdam.
- O'Connor, D. J., et al. 1975. Mathematical modeling of natural systems. Summer Institute in Water Pollution Control, Manhattan College.
- Parsons, T. R., Masayuki Takahashi and Barry Hargrave. 1977. Biological Oceanographic Processes. 2nd edition, Pergamon Press.
- Phillips, O. M. 1966. The Dynamics of the Upper Ocean. Cambridge University Press.
- Reid, R. O. and B. R. Bodine. 1968. Numerical model for storm surges in Galveston Bay. Journal of Waterways and Harbors Division, ASCE, Vol. 98, No. WW1.
- Seitz, R. C. 1971. Drainage area statistics for the Chesapeake Bay fresh-water drainage basin. Special Report 19, Reference 71-1, Chesapeake Bay Institute, The Johns Hopkins University, February.
- Strickland, J. D. H. 1960. Measuring the production of marine phytoplankton. Fisheries Research Board of Canada Bulletin No. 122.
- Thomann, Robert V., Dominic M. DiToro, Donald J. O'Connor. 1974. Preliminary model of Potomac Estuary phytoplankton, EE3, ASCE, June.
- Wang, John D. and Jerome J. Connor. 1975. Mathematical modeling of near coastal circulation. MIT, Ralph M. Parsons Laboratory Report No. 200, April.

- VanDorn, William G. 1953. Wind stress on an artificial pond. *Journal of Marine Research*, Vol. 12, No. 3.
- Whitaker, R. E., et al. 1973. Drag coefficients at hurricane wind speeds as deduced from the numerical simulation of dynamical water level changed in Lake Okeechobee. Ref. 73-13-5, Texas A&M, August.
- Wilson, B. W. 1960. Note on surface wind stress over water at low and high wind speeds. *Journal of Geophysical Research*, Vol. 65, No. 10.
- Wu, J. 1969. Wind stress and surface roughness at air-sea interface. *Journal of Geophysical Research*, Vol. 74, No. 2, January.

Appendix A. Summary of Water Quality Data

The water quality data from the intensive field survey during July 15,16,20 and 21, 1976 and two slack water runs on August 23 and 24 were sampled at several depths at each station. This appendix only presents the data near surface and bottom in two slack water runs. Due to voluminous data the presentation of the intensive survey observation is omitted. The reader is referred to the original set of field data stored in the Department of Physical Oceanography & Hydraulics of VIMS for more information.

Table A.1. Biogeochemical Water Quality of Two Slack Water Runs.

(In each space below, the first and the second row present respectively the values near the surface and the bottom of the river. Note that the value with * is sampled near the middle depth. Temp.=Temperature, Sal.=Salinity, SRP=Soluble Reactive Phosphorus, TP=Total Phosphorus, Ammon-N=Ammonia Nitrogen, Ni-N=Nitrite-Nitrogen, Na-N=Nitrate-Nitrogen, TKN=Total Kjeldahl Nitrogen, Chlor=Chlorophyll "a", FC=Fecal Coliform, DO=Dissolved Oxygen and BOD5=5-day Biochemical Oxygen Demand.)

Time Date/Hour	Location	Temp. °C	Sal. ppt	SRP mg/l	TP mg/l	Ammon-N mg/l	Ni-N mg/l	Na-N mg/l	TKN mg/l	Chlor µg/l	FC MPN/100 ml	DO mg/l	BOD5 mg/l
23/8 15.6	J1B	-	21.61*	0.05	0.05	0.09	0.02	0.12	0.47	13.65	9.1*	10.6	4.28
		-		0.05	0.05	0.19	0.01	0.07	0.32	3.99		11.0	4.44
15.7	J1C	-	21.40*	0.07	0.04*	0.15	0.01	0.10	0.25*	13.23	3*	15.0	8.55
		-		0.05	0.25	0.01	0.07	4.20	9.0	4.73			
16.2	J1.1C	-	22.51*	0.04	0.04	0.22	0.01	0.06	0.33	8.40	3.6*	7.2*	0.15*
		-		0.06	0.04	0.08	0.01	0.13	0.40	6.30			
16.3	J1.1A	-	21.42*	0.07	0.05	0.14	0.01	0.10	0.38*	13.65	43.0*	-	-
		-		0.07	0.06	0.15	0.02	0.11	10.82	-		-	
16.6	JE1	-	21.06*	-	0.06	0.08*	-	-	0.39	-	20.0*	-	-
		-		-	0.06	-	-	0.24	-	-			
16.8	J1.15A	-	21.42*	0.06*	0.07	0.31*	0.01*	0.12*	0.38	12.18	9.1*	-	-
		-			0.05			0.52	5.88	-		-	
17.0	J1.15B	-	21.97*	0.05	0.05	0.36	0.01	0.08	0.33*	8.40	3.6*	-	-
		-		0.05	0.06	0.30	0.01	0.08	4.41	-		-	
17.1	J1.2B	-	21.22*	0.06	0.06	0.16	0.01	0.13	0.38	8.82	-	-	-
		-		0.06	0.09	0.25	0.02	0.11	0.32	4.41		-	-

Table A.1. Continue - 1

Time Date/Hour	Location	Temp. °C	Sal. ppt	SRP mg/l	TP mg/l	Ammon-N mg/l	Ni-N mg/l	Na-N mg/l	TKN mg/l	Chlor µg/l	FC MPN/100 ml	DO mg/l	BOD5 mg/l
23/8 17.3	J1.2D	-	21.47*	0.24	0.26	0.84	0.01	0.09	1.07	3.78	-	-	-
		-		0.07	0.11	0.43	0.01	0.09	0.40	4.20	-	-	-
17.4	JN1	-	20.00*	0.05*	0.08*	0.11*	0.01*	0.06*	0.42*	14.91*	-	-	-
17.8	J1.25A	-	20.16*	0.05	0.03	0.17	0.01	0.10	0.34	10.92	230.0	-	-
		-		0.06	0.07	0.27	0.01	0.11	0.35	6.72	230.0	-	-
17.9	J1.25B	-	17.87*	0.04	0.04	0.05	0.01	0.13	0.41	8.61	3.6*	-	-
		-		0.05	0.10	0.16	0.02	0.16	0.41	4.41		-	-
18.1	J2B	-	17.40*	0.04	0.04	0.17	0.01	0.11	0.23	12.39	-	-	-
		-		0.05	0.07	0.19	0.01	0.14	0.33	5.67	-	-	-
18.1	J2D	-	-	0.04	0.04	0.11	0.01	0.12	0.42	5.88	3.6*	-	-
		-		0.05	0.04	0.16	0.01	0.12	0.35	3.78		-	-
18.4	J2.5	-	-	0.04	0.04	0.07	0.01	0.16	0.30	7.14	-	-	-
		-		0.06	0.07	0.15	0.01	0.13	0.38	3.57	-	-	-
18.7	J3B	-	18.28*	0.05	0.05	0.01-	0.00	0.17	0.22	2.94	-	-	-
		-		0.07	0.06	0.02	0.00	0.15	0.26	0.21	-	-	-
18.9	J3.5	-	16.38*	0.04	0.04	0.01	0.00	0.22	0.24	0.21	3.6*	7.0*	-
		-		0.04	0.04	0.16	0.00	0.22	0.20	1.05			-
19.1	J4C	-	14.11*	0.03	0.04*	0.05	0.01	0.33	0.25	5.46	-	7.2	0.37*
		-		0.04		0.10	0.01	0.26	0.42	3.15	-	7.2	
19.5	J4.5	-	10.29*	0.01	0.03	0.07	0.01	0.42	0.29*	3.99	3.6*	5.2	0.15*
		-		0.02	0.11	0.09	0.00	0.35		3.99		6.8	
19.6	J5C	-	6.89*	0.02	0.03	0.08	0.01	0.54	0.39	4.22	-	7.8	0.03*
		-		0.07	0.09	0.01-	0.00	0.49	0.37	0.63	-	7.5	

Table A.1. Continue - 2

Time Date/Hour	Location	Temp. °C	Sal. ppt	SRP mg/l	TP mg/l	Ammon-N mg/l	Ni-N mg/l	Na-N mg/l	TKN mg/l	Chlor µg/l	FC MPN/100 ml	DO mg/l	BOD5 mg/l	
23/8	20.0	J6B	-	4.91*	0.03	0.07	0.16	0.01	0.97	0.37	2.94	-	6.0	0.86*
			-	-	0.03	0.57	0.75	0.01	1.00	1.17	4.62	-	6.3	
20.2	J6	-	2.67*	-	-	-	-	-	-	-	-	6.6	-	
		-	-	-	-	-	-	-	-	-	-	7.0	-	
24/8	09.3	J1C	24.25	-	0.01	0.04*	0.08	0.00	0.06	0.33*	5.76	3.0*	5.5	-
			23.10	-	0.04	0.16	0.01	0.04	0.33*	2.52	-	4.4	-	
09.5	J1B	25.00	-	0.02	0.03*	0.07	0.00	0.03	0.17*	5.46	-	5.5	-	
		24.60	-	0.03	0.40	0.01	0.06	0.17*	4.62	-	5.2	-		
09.8	J1.1C	24.95	22.64	0.02*	0.05	0.18*	0.61*	4.59*	0.50	9.03	-	5.4	-	
		24.95	22.79	0.05	0.05	0.18*	0.61*	4.59*	0.24	5.88	-	5.6	-	
10.0	J1.1A	24.85	22.04	0.04	0.12*	0.18	0.01	0.05	0.32*	3.36	93.0	5.7	3.01*	
		23.70	26.07	0.05	0.50	0.01	0.11	0.32*	5.67	23.0	7.3			
10.3	JE1	25.40	21.10	0.05	0.08	0.25	0.02	0.11	0.31	7.77	23.0	6.8	0.22*	
		24.45	22.14	0.06	0.04	0.13	0.01	0.11	0.32	6.51	9.1	5.2		
10.6	J1.15A	25.00	22.68	0.04*	0.05	0.12*	0.01*	4.99*	0.24	2.42*	3.6	4.6	0.03*	
		24.65	22.68	0.05	0.05	0.12*	0.01*	4.99*	0.32	3.6	3.6	5.9		
10.9	J1.15B	25.00	22.72	0.03	0.05	0.13	0.01	0.06	0.37*	5.67	3.6*	6.3	-	
		24.25	22.88	0.03	0.07	0.14	0.01	0.07	0.37*	5.25	-	5.0	-	
11.1	J1.2D	25.00	21.91	0.05	0.06*	0.15	0.01	0.12	0.40	3.57	-	5.4	-	
		24.85	22.16	0.05	0.24	0.01	0.11	0.35	4.41	-	4.9	-		
11.4	J1.2B	25.68	21.47	0.04	0.07	0.13	0.01	0.12	0.29	4.61	9.1	4.6	-	
		24.85	21.98	0.05	0.09	0.16	0.01	0.10	0.35	5.36	-	5.2	-	
11.6	JN1	26.25	20.02	0.05*	0.11*	0.10*	0.01*	0.08*	0.38*	2.84*	-	4.8	3.57*	
		26.03	19.98	-	-	-	-	-	-	-	-	-		

Table A.1. Continue - 3

Time Date/Hour	Location	Temp. °C	Sal. ppt	SRP mg/l	TP mg/l	Ammon-N mg/l	Ni-N mg/l	Na-N mg/l	TKN mg/l	Chlor µg/l	FC MPN/100 ml	DO mg/l	BOD5 mg/l
24/8 11.8	J1.25A	25.75	20.07	0.04	0.06	0.11	0.01	0.13	0.41	4.41	3.6*	5,6*	-
		25.58	20.09	0.05	0.06	0.11	0.01	0.13	0.33	5.04			-
12.0	J1.25B	25.75	20.73	0.05	0.06	0.17	0.01	0.10	0.25	2.52	-	8.0	1.62*
		24.80	19.85	0.06	0.06	0.16	0.01	0.09	0.35	6.51	-	5.2	
12.3	J2B	25.85	20.10	0.05	0.08	0.16	0.01	0.12	0.20*	5.46	-	6.4	-
		25.10	20.37	0.06	0.08	0.16	0.01	0.12		6.09	-	5.3	-
12.5	J2D	25.80	20.68	0.05	0.08*	0.14	0.01	0.10	0.27*	4.20	7.3	4.7	-
		25.58	17.84	0.06		0.15	0.01	0.12		1.05	3.6	4.5	-
12.7	J2.5	26.40	18.04	0.06	0.06	0.11	0.01	0.13	0.25	3.36	-	4.9	-
		25.15	16.86	0.06	0.08	0.15	0.01	0.13	0.27	5.46	-	4.4	-
13.1	J3B	25.68	16.92	0.04	0.06	0.09	0.01	0.12	0.25	6.09	-	5.5	-
		25.15	11.12	0.05	0.05	0.12	0.01	0.13	0.32	2.94	-	5.6	-
13.3	J3.5	27.00	12.14	0.03	0.06	0.10	0.01	0.22	0.13	3.57	3.6*	5.5*	-
		26.20	8.70	0.04	0.04	0.07	0.01	0.21	0.33	2.31		2.31	-
13.6	J4C	26.80	9.44	0.04*	0.05	0.08*	0.01*	0.26*	0.18	4.62*	-	5.6	0.53*
		26.40	6.18		0.06						0.24	-	
14.0	J4.5	27.20	6.83	0.03	0.04	0.11	0.01	0.58	0.26	2.94	-	7.0	-
		26.95	5.06	0.03	0.05	0.11	0.01	0.31	0.19	2.35	-	7.2	-
14.3	J5C	27.00	5.92	0.02	0.05	0.08	0.06	0.33	0.27	9.87	3.0*	8.8	1.62
		25.75	2.36	0.03	0.05	0.09	0.01	0.33	0.42	3.26		8.0	0.49
14.7	J6B	26.75	2.43	0.02	0.06	0.08	0.01	0.67	0.28	2.73	-	8.3	0.69*
		26.40	1.57	0.02	0.07	0.10	0.01	0.63	0.28	3.36	-	7.6	
14.8	J6	27.10	1.61*	0.03*	0.07*	0.10*	0.01*	0.36*	0.40*	5.88*	-	7.2	-
		27.15									-	7.2	-